UNIVERSITY OF CALIFORNIA, SAN DIEGO

High Energy Processes using Effective Field Theories.

A dissertation submitted in partial satisfaction of the
requirements for the degree
Doctor of Philosophy

in

Physics

by

Randall Scott Kelley

Committee in charge:

Professor Aneesh Manohar, Chair
Professor Benjamin Grinstein
Professor Jeffrey Rabin
Professor Justin Roberts
Professor Vivek Sharma

2009

The dissertation of Randall Scott Kelley is approved, and it is acceptable in quality and form for publication on microfilm:

_____

_____

_____

_____

_____

Chair

University of California, San Diego

2009

DEDICATION

To my friends and family who tolerated me during the writing of this dissertation.

EPIGRAPH

All truths are easy to understand once they are discovered; the point is to discover them.

—Galileo Galilei

TABLE OF CONTENTS

LIST OF FIGURES

LIST OF TABLES

ACKNOWLEDGEMENTS

Thank you to my parents for never asking me “physics...what are you going to do with that?”

Some formalities: Partial text of chapter 1 is extracted from J. y. Chiu, F. Golf, R. Kelley and A. V. Manohar, “Electroweak Corrections in High Energy Processes using Effective Field Theory,” Phys. Rev. D 77, 053004 (2008), and partial text of chapter 2 is extracted from J. y. Chiu, A. Fuhrer, A. H. Hoang, R. Kelley and A. V. Manohar, “Soft-Collinear Factorization and Zero-Bin Subtractions,” Phys. Rev. D 79, 053007 (2009).

VITA

1999	B. S. in Physics, University of Virginia
1999-2004	U.S. Navy
2009	Ph. D. in Physics, University of California, San Diego

PUBLICATIONS

"Electroweak Sudakov corrections using effective field theory.", *Physical Review Letters*, 100, 2008.

"Electroweak corrections to high energy processes using effective field theory.", *Physical Review D*, 77, 2008.

"Electroweak Corrections using Effective Field Theory: Applications to the LHC.", *Physical Review D*, 78, 2008.

"Soft-Collinear Factorization and Zero-Bin Subtractions.", *Physical Review D*, 79, 2009.

ABSTRACT OF THE DISSERTATION

High Energy Processes using Effective Field Theories.

by

Randall Scott Kelley

Doctor of Philosophy in Physics

University of California San Diego, 2009

Professor Aneesh Manohar, Chair

Electroweak Sudakov logarithms at high energy, of the form $(\alpha/\sin^2\theta_W)^n \log^m s/M_{Z,W}^2$, are summed using effective theory methods. The corrections are computed to processes involving two external fermionic or scalar particles, first in a spontaneously broken $SU(2)$ gauge theory and then in the standard model. The results include non-zero particle masses, such as the t-quark mass, electroweak mixing effects which lead to unequal W and Z masses, and radiative Higgs corrections proportional to the Yukawa couplings. We show that the matching at the scale $M_{W,Z}$ has a term at most linear in $\log s/\mu^2$ to all orders. The effective theory formalism is compared with, and extends, previous work based on infrared evolution equations. Finally corrections to processes involving two external gauge bosons are computed in the broken $SU(2)$ theory for both transverse and then longitudinal polarizations. The later will require the calculation of the multiplication factor $\mathcal{E}$, which relates the amplitude for longitudinal gauge boson production to Goldstone boson production at high energy, in R_ξ gauge using the $\overline{MS}$ regularization scheme.

Chapter 1

Electroweak Corrections: Matter fields

The Large Hadron Collider (LHC) has a center-of-mass energy of $\sqrt{s} = 14$ TeV, and will be able to measure collisions with a partonic center-of-mass energy of several TeV, more than an order of magnitude larger than the masses of the electroweak gauge bosons. Radiative corrections to scattering processes depend on the ratio of mass scales, and at high energy this dependence is logarithmic with the form $\log s/M_{W,Z}^2$. In high energy exclusive processes, radiative corrections are enhanced by two powers of a large logarithm for each order in perturbation theory, and the logarithms are often referred to as Sudakov (double) logarithms. Electroweak Sudakov corrections are not small at LHC energies, since $\alpha \log^2(s/M_{W,Z}^2/(4\pi \sin^2\theta_W)) \sim 0.15$ at $\sqrt{s} = 4$ TeV. These Sudakov corrections lead to a breakdown of fixed order perturbation theory, and need to be summed to all orders.

Electroweak corrections at high energy have double logarithms, even for processes which are conventionally called inclusive, such as the total e^+e^- cross-section at large angles, because the colliding particles are not electroweak gauge singlets [1]. There are no electroweak singlet fields in the standard model. A composite particle such as the proton, while a color singlet, is not an electroweak singlet.

There is an extensive literature on electroweak Sudakov effects [2, 3, 4, 5, 6, 7, 8, 9, 10, 11, 12, 13, 14, 15]. The computations use infrared evolution equations [3], based on an analysis of the infrared structure of the perturbation theory amplitude and a factorization theorem for the Sudakov form factor [16]. These summations have been checked against one-loop [8, 9, 10] and two-loop [11, 12, 13, 14, 15] computations.

The Sudakov logarithm $\log(s/M_{W,Z}^2)$ can be thought of as an infrared logarithm in the electroweak theory, since it diverges as $M_{W,Z} \to 0$. By using an effective field theory (EFT), these infrared logarithms in the original theory can be converted to ultraviolet logarithms in the

effective theory, and summed using standard renormalization group techniques. The effective theory needed is soft-collinear effective theory (SCET) [17, 18], which has been used to study high energy processes in QCD [19], and to perform Sudakov resummations arising from radiative gluon corrections.

This chapter studies high energy electroweak Sudakov corrections using SCET, and expands on work of [21]. In Ref. [21], it was shown how to compute $\log s/M_{W,Z}^2$ corrections to the Sudakov form factor for massless fermions using EFT methods. In this chapter, the results are generalized to massive fermions such as the top quark, and include radiative corrections due to Higgs exchange. The corrections are computed without assuming that the Higgs and electroweak gauge bosons are degenerate in mass, as in previous calculations. A new feature of EFT matching, the existence of single logarithmic matching corrections [21], is discussed in detail, and proven to be true to all orders in perturbation theory. This chapter discusses the Sudakov form factor computation in detail. The Sudakov form factor is not of direct relevance to LHC processes, but it allows us to illustrate the EFT method for operators involving two external particles. The computations of the Sudakov form factor can be used to compute electroweak corrections to processes relevant for the LHC, such as dijet production, $t\bar{t}$ production, or squark pair production, which involve operators with four external particles. The results are given in the publication [23], and can be obtained from the computations given in this chapter by summing over all pairs of external particles with the appropriate group theoretic factors.

The outline of the calculation is given in Sec. 1.1. The SCET formalism and the full theory we use for our calculations are described in Sec. 1.2. Known results on the exponentiation of the Sudakov form factor, and a comparison of the infrared evolution equation formalism with the SCET approach is given in Sec. 1.3. Section 1.4 discusses the calculation of Sudakov corrections for massive gauge bosons and massless external particles. Section 1.5 gives the proof that there is at most a single logarithm found in the matching condition to all orders in perturbation theory, and consistency conditions on the matching coefficients and anomalous dimensions are given in Sec. 1.6. The extension to massive external particles is given in Sec. 1.7 for all possible hierarchies of mass-scales, including cases in which particle masses are not widely separated, so that multiple scales have to be integrated out simultaneously. Massive scalar exchange graphs, relevant for Higgs exchange, are computed in Sec. 1.8. Applications of the formalism to electroweak Sudakov corrections in the standard model are given in Sec. 1.9 for light quarks, the top quark, and leptons.

Notation: We use $a(\mu) \equiv \alpha(\mu)/(4\pi)$, and $a_i(\mu) \equiv \alpha_i(\mu)/(4\pi)$ where $i = s, 2, 1$ for the QCD, $SU(2)$ and $U(1)$ couplings in the standard model. Hypercharge is normalized so that $Q = T_3 + Y$. Logarithms are denoted by $\mathsf{L}_A \equiv \log A^2/\mu^2$, for $A = Q, M, m_1, m_2$. C_F and T_F are the Casimir and index for the external particles. We use the subscript F for both fermions and scalars, to avoid rewriting the same expression twice.

1.1 Outline of Calculation

The physical quantity we study is the Sudakov form factor in the Euclidean region, defined as the amplitude $F_E(Q^2) = \langle p_2|\mathcal{O}|p_1\rangle$ for the scattering of on-shell particles $p_i^2 = m_i^2$ by an operator $\mathcal{O}$, with $Q^2 = -(p_2 - p_1)^2 > 0$. The timelike Sudakov form factor is given by analytic continuation, $F(s) = F_E(-s - i0^+)$, so that $\log(Q^2/\mu^2) \to \log(s/\mu^2) - i\pi$.

We will compute $F_E(Q^2)$ for fermion scattering by $\mathcal{O} = \bar\psi\gamma^\mu\psi$, $\bar\psi\psi$, $\bar\psi\sigma^{\mu\nu}\psi$, scalars scattering by $\mathcal{O} = \phi^\dagger\phi$, $i(\phi^\dagger D^\mu\phi - D^\mu\phi^\dagger\phi)$, and fermion to scalar (or vice-versa) scattering by $\mathcal{O} = \bar\psi\phi$. All operators are taken to be gauge singlets so the incoming and outgoing particles have the same gauge quantum numbers, but not necessarily the same mass.

The form factor, $F_E(Q^2)$ is computed using a sequence of effective theories. For the high energy process considered in this chapter, there are several widely separated scales and we must switch to the relevant theory as we move between scales. At scales higher than Q^2, the theory is the original gauge theory, referred to as the full theory in EFT terminology. The precise theory, and the SCET formalism used are given in Sec. 1.2.

As we move to scales below Q^2 we transition to an effective field theory (SCET) where degrees of freedom with offshellness on the order of Q^2 are integrated out. The full and EFT have the same infrared (IR) physics but different ultraviolet (UV) behavior and to ensure that the operators in the respective theories have the same on-shell matrix elements, we must introduce a matching coefficient, $\exp[C(\mu)]$. For later convenience, the matching coefficient is written as an exponential. If the full theory is matched onto SCET at μ_Q then the matching coefficient is chosen so that

$$\langle p_2|\mathcal{O}(\mu_Q)|p_1\rangle \quad = \quad \exp[C(\mu_Q)]\,\langle p_2|\widetilde{\mathcal{O}}(\mu_Q)|p_1\rangle \tag{1.1}$$

where $\tilde{\mathcal{O}}(\mu)$ is the EFT operator corresponding to the full theory operator $\mathcal{O}(\mu)$. The matching coefficient $\exp C(\mu_Q)$ is independent of infrared physics, and can be computed if perturbation theory is valid at μ_Q. In general, a single operator $\mathcal{O}$ can match onto a set of operators $\widetilde{\mathcal{O}}_i$ in the EFT with the same quantum numbers. This occurs, for example, for four-fermion operators in the analysis of high-energy parton scattering, and can be included by treating all the equations below as matrix equations, as is familiar from the well-known analysis of operator mixing. The matching coefficient $C(\mu_Q)$ contains $\log\mu_Q^2/Q^2$ terms, and there are no large logarithms if μ_Q is chosen to be of order Q. We will choose $\mu_Q = Q$, though any value of order Q is acceptable. Any physical observable is independent of the choice for μ_Q. It is conventional to choose $c(\mu)$, the coefficient of $\mathcal{O}$ in the full theory, to equal unity at $\mu = Q$. With this choice, which gives the usual normalization for $F_E(Q^2)$, $c(Q) = \exp C(Q)$ is the coefficient of $\widetilde{\mathcal{O}}$ in SCET at $\mu = Q$. The evolution of $c(\mu)$ between scales is given by the renormalization group equation

$$\mu\frac{dc(\mu)}{d\mu} = \gamma(\mu)c(\mu), \tag{1.2}$$

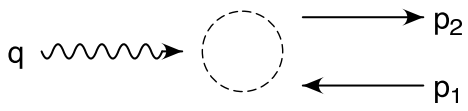

Figure 1.1: Breit frame kinematics.

where $\gamma(\mu)$ is the anomalous dimension of $\widetilde{\mathcal{O}}$ in the EFT.

We must repeat this sequence of matching and renormalization group evolution as various energy scales are crossed, and more and more degrees of freedom are integrated out. An advantage of the EFT approach is that it divides the full multiscale computation into several simpler pieces, each of which depends on a single scale. This allows one to easily identify which quantities are universal, and which ones depend on the specific process. In an EFT calculation, the IR divergences in the theory above a matching scale must match with the UV divergences in the theory below the matching scale. We have checked this explicitly for all the computations in this chapter. In most of the tables, we have given only the finite parts of the graphs.

1.2 SCET Formalism

SCET is an effective theory that describes energetic particles, with energy of order Q, where Q is some large scale which characterizes the scattering process. SCET contains all the modes of the full theory with invariant mass much smaller than Q^2. The SCET fields and Lagrangian depend on two null four-vectors n and $\bar{n}$, with $n = (1, \mathbf{n})$ and $\bar{n} = (1, -\mathbf{n})$, where $\mathbf{n}$ is a unit vector, so that $\bar{n} \cdot n = 2$. In the Sudakov problem, one works in the Breit frame, with n chosen to be along the p_2 direction, so that $\bar{n}$ is along the p_1 direction. The momentum transfer q has no time component, $q^0 = 0$, so that the particle is back-scattered(see Fig. 1.1). The light-cone components of a four-vector p are defined by $p^+ \equiv n \cdot p$, $p^- \equiv \bar{n} \cdot p$, and $p_\perp$, which is orthogonal to n and $\bar{n}$, so that

$$p^\mu = \frac{1}{2} n^\mu (\bar{n} \cdot p) + \frac{1}{2} \bar{n}^\mu (n \cdot p) + p_\perp^\mu . \tag{1.3}$$

In our problem, $p_1^- = p_{1\perp} = p_2^+ = p_{2\perp} = 0$, and $Q^2 = p_1^+ p_2^-$. A fermion moving in a direction close to n is described by the n-collinear SCET field $\xi_{n,p}(x)$, where p is a label momentum, and has components $\bar{n} \cdot p$ and $p_\perp$ [17, 18]. It describes particles (on- or off-shell) with energy $2E \sim \bar{n} \cdot p$, and $p^2 \ll Q^2$. The total momentum of the field $\xi_{n,p}(x)$ is $p + k$, where k is the residual momentum of order $Q\lambda^2$ contained in the Fourier transform of x. Note that the label momentum p only contributes to the minus and $\perp$ components of the total momentum.

The massive gauge fields are represented by several distinct fields in the effective theory: n-collinear fields $A_{n,p}(x)$ and $\bar{n}$-collinear fields $A_{\bar{n},p}(x)$ with labels, and so-called mass-mode fields $A_s(x)$ [20] to which we do not give any label. These labels are analogous to the label conventions

for soft and ultrasoft fields introduced in NRQCD [24]. The n-collinear field contains massive gauge bosons with momentum near the n-direction, and momentum scaling $\bar{n}\cdot p \sim Q$, $n\cdot p \sim Q\lambda^2$, $p_\perp \sim Q\lambda$, and the $\bar{n}$-collinear field contains massive gauge bosons moving near the $\bar{n}$-direction, with momentum scaling $n\cdot p \sim Q$, $\bar{n}\cdot p \sim Q\lambda^2$, $p_\perp \sim Q\lambda$. Here we have $\lambda \sim M/Q$, where $\lambda \ll 1$ is the power counting parameter used for the EFT expansion. The mass-mode field contains massive gauge bosons with all momentum components scaling as $Q\lambda \sim M$. The effective theory discussed here is $\mathrm{SCET_{EW}}$ studied in Refs. [21, 22, 23], and is similar to $\mathrm{SCET_I}$, but with weak-scale mass modes intead of the ultrasoft modes familiar from QCD. If we would consider the broken $SU(2)$ together with QCD, the effective theory would have additional n- and $\bar{n}$-collinear massless gluons and ultrasoft massless gluons, as in $\mathrm{SCET_I}$. The n- and $\bar{n}$-collinear massless gluons would have the momentum scaling of the n- and $\bar{n}$-collinear massive gauge fields of the broken $SU(2)$. The ultrasoft gluon fields would have the momentum scaling $p^\mu \sim Q\lambda^2$ with $p^2 \sim M^4/Q^2$. At $\mu = M$ the n- and $\bar{n}$-collinear massive gauge fields and the mass-modes can be integrated out, leaving a common massless $\mathrm{SCET_I}$ theory for $\mu < M$. Such a situation is realized in the $SU(3)\times SU(2)\times U(1)$ electroweak theory [21, 22].

The interactions of the mass-mode fields with the collinear fields are described by mass-mode S-Wilson lines whose definition is identical to the Y-Wilson lines that arise for massless ultrasoft modes in massless $\mathrm{SCET_I}$ upon the ultrasoft field redefinition. The difference is that the mass-mode Wilson lines contain mass-mode gauge fields rather than ultrasoft massless gauge fields. Thus the effective field theory current for the broken $SU(2)$ has the form[1]

$$J(\omega,\bar{\omega},\mu) = [\bar{\xi}_{n,\omega} W_n S_n^\dagger \Gamma S_{\bar{n}} W_{\bar{n}}^\dagger \xi_{\bar{n},\bar{\omega}}](0)\,, \tag{1.4}$$

where

$$\begin{aligned} S_n^\dagger(x) &= \mathrm{P}\,\exp\Big[ig\int_0^\infty ds\, n\cdot A_s(ns+x)\Big]\,, \\ S_{\bar{n}}(x) &= \overline{\mathrm{P}}\,\exp\Big[-ig\int_0^\infty ds\, \bar{n}\cdot A_s(\bar{n}s+x)\Big]\,. \end{aligned} \tag{1.5}$$

More details can be found in Ref. [20].

The EFT fermion field satisfies the constraint

$$\frac{\not{n}\bar{\not{n}}}{4}\xi_{n,p} = \xi_{n,p}, \tag{1.6}$$

where

$$P_n = \frac{\not{n}\bar{\not{n}}}{4}, \quad P_{\bar{n}} = \frac{\bar{\not{n}}\not{n}}{4}, \quad P_n + P_{\bar{n}} = 1, \tag{1.7}$$

are projection operators. The leading order fermion Lagrangian is [18]

$$\bar{\xi}_{n,p}\frac{\bar{\not{n}}}{2}\left(in\cdot D + \frac{p_\perp^2}{\bar{n}\cdot p}\right)\xi_{n,p} + \dots\,, \tag{1.8}$$

[1] In the presence of additional ultrasoft massless gauge fields the effective theory current would have the form $J(\omega,\bar{\omega},\mu) = [\bar{\xi}_{n,\omega} W_n S_n^\dagger Y_n^\dagger \Gamma Y_{\bar{n}} S_{\bar{n}} W_{\bar{n}}^\dagger \xi_{\bar{n},\bar{\omega}}](0)$, with ultrasoft Y-Wilson lines.

where $iD = i\partial + gA$ is the ultrasoft covariant derivative, and ... denotes terms involving the collinear gauge field. The fermion propagator is

$$\frac{\not{n}\ \bar{n}\cdot p}{2p^2}. \tag{1.9}$$

The effective theory knows about the large momentum scale Q through the labels $\bar{n}\cdot p_2$ and $n\cdot p_1$ on the fields ξ_{n,p_2} and $\xi_{\bar{n},p_1}$ for the outgoing and incoming particles. As a result, SCET anomalous dimensions can depend on Q. However, there are no modes in SCET which couple $\bar{n}\cdot p_2$ to $n\cdot p_1$, so that SCET does not contain modes with off-shellness of order Q^2, which are present in the full theory.

We will also need to introduce SCET fields to describe energetic scalar particles, such as the Higgs boson. We will use $\Phi_{n,p}$ as the n-collinear field for a scalar particle moving in a direction close to n, analogous to $\xi_{n,p}$ for fermions. The field $\Phi_{n,p}$ is normalized the same way as the full-theory field ϕ, and produces scalar particles with amplitude unity. The scalar kinetic energy term becomes

$$D_\mu\phi^\dagger D^\mu\phi \to \Phi^\dagger_{n,p}\left[(\bar{n}\cdot p)\,(in\cdot D) + p_\perp^2\right]\Phi_{n,p} \tag{1.10}$$

in the effective theory. It is also convenient to use a redefined scalar field,

$$\phi_{n,p} = \sqrt{(\bar{n}\cdot p)}\,\Phi_{n,p}, \tag{1.11}$$

in terms of which the kinetic term becomes

$$L \;=\; \phi^\dagger_{n,p}\left(in\cdot D + \frac{p_\perp^2}{\bar{n}\cdot p}\right)\phi_{n,p} \tag{1.12}$$

and has the same normalization as the fermion Lagrangian Eq. (1.8). The rescaled scalar propagator is now

$$\frac{1}{p^2} \;\to\; \frac{\bar{n}\cdot p}{p^2}. \tag{1.13}$$

$\phi_{n,p}$ produces scalar particles moving in the n-direction with amplitude $\sqrt{(\bar{n}\cdot p)}$.

The theory we consider is a $SU(2)$ spontaneously broken gauge theory, with a Higgs in the fundamental representation, where all gauge bosons have a common mass, M. This is the theory used in many previous computations [4, 5, 6, 7, 15], and allows us to compare with previous results. A detailed description of this theory is given Appendices A and B including Feynman rules and the choice of gauge. It is convenient, as in Ref. [15], to write the group theory factors using C_F, C_A, T_F and n_F, where n_F is defined to be the number of weak doublets Weyl fermions.[2] We will consider this theory with fermionic and scalar matter fields in arbitrary gauge representations, with the fermions assumed to be vector-like if they are massive. These fields

[2]Note that the results only hold for $C_A = 2$, since for an $SU(N)$ group with $N > 2$, a fundamental Higgs does not break the gauge symmetry completely.

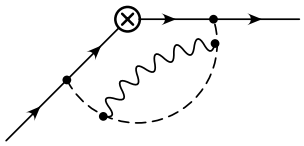

Figure 1.2: Graphs in the standard model involving both Yukawa and gauge couplings which have no analog in the toy example.

are the external particles in the operators $\mathcal{O}$. We will also need to consider graphs which are analogous to Higgs exchange graphs in the standard model. For this purpose, we will add a gauge singlet scalar field χ, which couples to the fermions and scalars via gauge-invariant interactions,

$$L_{\rm int} \;=\; -h_{\psi,i}\chi\bar{\psi}_i\psi_i - h_{\phi,i}\chi\phi_i^\dagger\phi_i, \tag{1.14}$$

where $h_{\psi,i}$ is dimensionless, and $h_{\phi,i}$ has dimensions of mass. We will assume that $h_{\phi,i}$ is independent of Q for power counting purposes. In our toy example, χ is a gauge singlet field, and does not break the gauge symmetry. The fermion masses are independent of the Yukawa couplings of χ. The toy example Higgs field is a doublet, and breaks the gauge symmetry, but does not couple to the matter fields. In the standard model, the Higgs field breaks the gauge symmetry, and also has Yukawa couplings which generate fermion masses.

The computations are extended to the $SU(3) \times SU(2)_L \times U(1)_Y$ standard model in Sec. 1.9, including Higgs exchange corrections and unequal gauge boson masses. Our results are given to leading order in the EFT power counting, i.e. we neglect power corrections of the form m_i^2/Q^2, and M^2/Q^2, while retaining all logarithmic corrections $\log m_i^2/Q^2$ and $\log M^2/Q^2$. The gauge boson exchange graphs can be obtained from those of the toy model. In the standard model, the Higgs field breaks the gauge symmetry, and also has Yukawa couplings to the chiral fermions. At one-loop, we can obtain the Higgs exchange corrections from the χ-exchange graphs in our toy example. Graphs with Higgs bosons coupling to both the fermions and the gauge bosons start at two-loops (see Fig. 1.2).

1.3 Exponentiation

We start by summarizing some known properties of the Sudakov form-factor [25] for the vector current. We will see later how the same expressions can be rederived using renormalization group methods in SCET. The Euclidean form-factor $F_E(Q^2)$ has the expansion ($\mathsf{L} = \log(Q^2/M^2)$)

$$\begin{aligned} F_E \;=\;& 1 + \alpha\left(k_{12}\mathsf{L}^2 + k_{11}\mathsf{L} + k_{10}\right) \\ & + \alpha^2\left(k_{24}\mathsf{L}^4 + k_{23}\mathsf{L}^3 + k_{22}\mathsf{L}^2 + k_{21}\mathsf{L} + k_{20}\right) \\ & + \alpha^3\left(k_{36}\mathsf{L}^6 + \ldots\right) + \ldots\,, \end{aligned} \tag{1.15}$$

with the α^n term having powers of L up to L^{2n}. In the literature, the highest power of L is called the $\mathrm{LL_F}$ term, the next power is called the $\mathrm{NLL_F}$ term, etc. We have included the subscript F (for the form-factor) to distinguish it from the renormalization group counting described below.

The series for $\log F_E(Q^2)$ takes a simpler form

$$\begin{aligned}\log F_E &= \alpha\left(\tilde{k}_{12}\mathsf{L}^2+\tilde{k}_{11}\mathsf{L}+\tilde{k}_{10}\right)\\ &\quad+\alpha^2\left(\tilde{k}_{23}\mathsf{L}^3+\tilde{k}_{22}\mathsf{L}^2+\tilde{k}_{21}\mathsf{L}+\tilde{k}_{20}\right)\\ &\quad+\alpha^3\left(\tilde{k}_{34}\mathsf{L}^4+\ldots\right)+\ldots\,,\end{aligned} \tag{1.16}$$

with the α^n term having powers of L up to L^{n+1}, and the expansion begins at order α. Note that Eq. (1.16) implies non-trivial relations among the coefficients k_{nm} in Eq. (1.15). At order n, there are $2n+1$ coefficients k_{nm}, $0\le m\le 2n$ in Eq. (1.15), but only $n+2$ coefficients $\tilde{k}_{nm}$, $0\le m\le n+1$ in Eq. (1.16).

The right-hand-side (rhs) of Eq. (1.16) can be written in terms of the LL series $\mathsf{L}f_0(\alpha\mathsf{L})=\tilde{k}_{12}\alpha\mathsf{L}^2+\tilde{k}_{23}\alpha^2\mathsf{L}^3+\ldots$, the NLL series $f_1(\alpha\mathsf{L})=\tilde{k}_{11}\alpha\mathsf{L}+\tilde{k}_{22}\alpha^2\mathsf{L}^2+\ldots$, the NNLL series $\alpha f_2(\alpha\mathsf{L})=\tilde{k}_{10}\alpha+\tilde{k}_{21}\alpha^2\mathsf{L}+\ldots$ etc. as

$$\log F_E = \mathsf{L}f_0(\alpha\mathsf{L})+f_1(\alpha\mathsf{L})+\alpha f_2(\alpha\mathsf{L})+\ldots\,. \tag{1.17}$$

f_0 and f_1 begin at order α, and the remaining f_n begin at order one.

In this chapter, LL, NLL, etc. (with no subscripts) will refer to the counting for $\log F_E$. This is also the counting appropriate for a renormalization group improved computation, and is different from the conventional counting discussed above. If one looks at the order α^2 terms, for example, the conventional counting is that the L^4 term is $\mathrm{LL_F}$, the L^3 term is $\mathrm{NLL_F}$, the L^2 term is $\mathrm{N^2LL_F}$, the L term is $\mathrm{N^3LL_F}$, and the L^0 term is $\mathrm{N^4LL_F}$. Using our counting, the terms are given by exponentiating $\log F_E$ to LL, NLL, $\mathrm{N^2LL}$, $\mathrm{N^2LL}$, and $\mathrm{N^3LL}$, respectively. At higher orders, the mismatch in powers of N between the two counting methods increases.

For precision electroweak studies, the first few orders are sufficient. Typical loop corrections are suppressed by $\alpha/(4\pi)$. There can be large coefficients in the perturbation expansion. For example, there are large coefficients in the cusp anomalous dimension (see Eqs. (1.53,1.57)). In this chapter we have computed corrections to the Sudakov form factor; for dijet production and processes involving four-particle operators, the anomalous dimensions are at least twice as large as for the Sudakov problem. For these reasons, we use the estimate α instead of $\alpha/(4\pi)$ for the size of loop corrections. For QCD, $\alpha\sim 0.1$, and for electroweak corrections, $\alpha\to\alpha_{\rm em}/\sin^2\theta_W\sim 0.03$. $\log s/M_Z^2\sim 8$ for $s\sim 4$ TeV, so $\alpha\mathsf{L}\sim 1$ for QCD and ~ 0.2 for electroweak corrections. The NLL series is of order ten percent for QCD corrections, and a few percent for electroweak corrections. The NNLL series is of order a percent for QCD, and sub-percent for electroweak corrections.

1.3.1 Infrared Evolution Equations

An expression for the Sudakov form-factor in the limit $M/Q \ll 1$ with onshell massless fermions, $p_2^2 = p_1^2 = 0$, obtained using the evolution equations is [26, 25, 27, 15]

$$\log F_E(Q^2) = \log F_0(a(M)) + \int_{M^2}^{Q^2} \frac{\mathrm{d}\mu^2}{\mu^2} \left[\zeta(a(\mu)) + \xi(a(M)) + \int_{M^2}^{\mu^2} \frac{\mathrm{d}\mu'^2}{\mu'^2} \Gamma(a(\mu')) \right] \tag{1.18}$$

in terms of functions F_0, ζ, ξ and Γ of the coupling constant, which have the expansions

$$\begin{aligned} F_0(a) &= 1 + F_0^{(1)} a + F_0^{(2)} a^2 + \dots , \\ \Gamma(a) &= \Gamma^{(1)} a + \Gamma^{(2)} a^2 + \dots , \\ \zeta(a) &= \zeta^{(1)} a + \zeta^{(2)} a^2 + \dots , \\ \xi(a) &= \xi^{(1)} a + \xi^{(2)} a^2 + \dots . \end{aligned} \tag{1.19}$$

The superscript gives the loop-order of the Feynman graphs which contribute. Γ is known as the cusp anomalous dimension.

The gauge coupling constant g satisfies the renormalization group evolution equation

$$\begin{aligned} \mu \frac{\mathrm{d}g}{\mathrm{d}\mu} &= \beta_g(g) \\ &= -b_0 \frac{g^3}{16\pi^2} - b_1 \frac{g^5}{(16\pi^2)^2} - b_2 \frac{g^7}{(16\pi^2)^3} + \dots , \end{aligned} \tag{1.20}$$

or equivalently,

$$\begin{aligned} \mu \frac{\mathrm{d}a}{\mathrm{d}\mu} &= \beta_a(a) \\ &= -2a \left(b_0 a + b_1 a^2 + b_2 a^3 + \dots \right) . \end{aligned} \tag{1.21}$$

The one-loop coefficient is

$$b_0 = \frac{11}{3} C_A - \frac{4}{3} T_F n_F - \frac{1}{3} T_F n_S \tag{1.22}$$

where n_S is the number of complex scalars, and $2n_F$ is the number of fermion weak doublets, in the convention of Ref. [15].

After combining Eqs. (1.18–1.21) and expanding to order $a(M)^3$, the form factor takes

the following form:

$$\begin{aligned}
&\log F_E(Q^2) = \\
&\left[F_0^{(1)} + \left(\zeta^{(1)} + \xi^{(1)}\right)\mathsf{L} + \frac{1}{2}\Gamma^{(1)}\mathsf{L}^2\right] a(M) + \left[-\frac{1}{2}\left(F_0^{(1)}\right)^2 + F_0^{(2)} + \left(\zeta^{(2)} + \xi^{(2)}\right)\mathsf{L}\right. \\
&+ \frac{1}{2}\left(\Gamma^{(2)} - b_0\zeta^{(1)}\right)\mathsf{L}^2 - \frac{1}{6}\left(b_0\Gamma^{(1)}\right)\mathsf{L}^3\Big] a(M)^2 + \left[\frac{1}{3}\left(F_0^{(1)}\right)^3 - F_0^{(1)}F_0^{(2)} + F_0^{(3)}\right. \\
&+ \left(\zeta^{(3)} + \xi^{(3)}\right)\mathsf{L} + \frac{1}{2}\left(\Gamma^{(3)} - b_1\zeta^{(1)} - 2b_0\zeta^{(2)}\right)\mathsf{L}^2 + \frac{1}{6}\left(-b_1\Gamma^{(1)} + 2b_0\left(b_0\zeta^{(1)} - \Gamma^{(2)}\right)\right)\mathsf{L}^3 \\
&\left.+\frac{1}{12}b_0^2\Gamma^{(1)}\mathsf{L}^4\right] a(M)^3 + \dots\,. \qquad (1.23)
\end{aligned}$$

A comparison of this expansion with Eq. (1.17) shows that f_0 is determined by $\Gamma^{(1)}$ and b_0, f_1 by $\Gamma^{(1,2)}, \zeta^{(1)}, \xi^{(1)}, b_{0,1}$, and f_2 by $F_0^{(1)}, \Gamma^{(1,2,3)}, \zeta^{(1,2)}, \xi^{(2)}, b_{0,1,2}$. In general f_n is determined by $\xi^{(n)}$ and terms up to $F_0^{(n-1)}, \Gamma^{(n+1)}, \zeta^{(n)}, b_n$.

The expression Eq. (1.18) is not unique. The identity

$$\frac{1}{2}\int_{y^2}^{z^2}\frac{\mathrm{d}\mu^2}{\mu^2}\frac{\partial G(a(\mu))}{\partial a(\mu)}\beta_a(a(\mu)) \;=\; G(a(z)) - G(a(y)) \qquad (1.24)$$

can be used to show that Eq. (1.18) is invariant under the transformation

$$\begin{aligned}
\Gamma(a(\mu')) &\to \Gamma(a(\mu')) + \frac{\partial G(a(\mu'))}{\partial a}\beta_a(a(\mu'))\,,\\
\zeta(a(\mu)) &\to \zeta(a(\mu)) - 2G(a(\mu))\,,\\
\xi(a(M)) &\to \xi(a(M)) + 2G(a(M))\,. \qquad (1.25)
\end{aligned}$$

As a result, Γ, ζ and ξ are not uniquely determined from $F_E(Q^2)$ by Eq. (1.18).

1.3.2 Renormalization Group Evolution Equations

The corresponding expression for $F_E(Q^2)$ in the EFT formalism, as will be derived in Sec. 1.4, is

$$\begin{aligned}
\log F_E(Q^2) = C(a(Q)) + D_0(a(M)) + D_1(a(M))\log\frac{Q^2}{M^2}\\
-\int_M^Q\frac{\mathrm{d}\mu}{\mu}\left[A(a(\mu))\log\frac{\mu^2}{Q^2} + B(a(\mu))\right], \qquad (1.26)
\end{aligned}$$

where $\exp C(a(Q))$ is the multiplicative matching coefficient at Q^2, $\gamma(\mu) = A(a(\mu))\log(\mu^2/Q^2) + B(a(\mu))$ is the SCET anomalous dimension between Q and M, and $\exp D(a(M))$, $D(a(M)) = D_0(a(M)) + D_1(a(M))\log Q^2/M^2$ is the multiplicative matching coefficient at M. The matching coefficient C and the SCET anomalous dimension γ are independent of physics at the low scale M, and so do not depend on the gauge boson and Higgs masses. The new feature of the massive gauge boson calculation is the existence of a single-log term, $D_1(a(M))$ in the matching at M.

That there are no higher powers of $\log Q^2/M^2$ in the matching is proved to hold to all orders in Sec. 1.5. $A, B, C, D_{0,1}$ have loop expansions analogous to Eq. (1.19). The $\mathrm{N}^n\mathrm{LL}$ series for $\log F_E$ requires $A^{(n+1)}$, $B^{(n)}$, $D_0^{(n-1)}$, and $C^{(n-1)}$. $D_1^{(n)}$ contributes *only* to the $\alpha^n \mathsf{L}$ term in f_n.

The identity Eq. (1.24) and

$$\int_{M^2}^{Q^2} \frac{\mathrm{d}\mu^2}{\mu^2} \int_{M^2}^{\mu^2} \frac{\mathrm{d}\mu'^2}{\mu'^2} \Gamma(a(\mu')) \;=\; \int_{M^2}^{Q^2} \frac{\mathrm{d}\mu^2}{\mu^2} \Gamma(a(\mu)) \log \frac{Q^2}{\mu^2} \tag{1.27}$$

can be used to show that Eq. (1.26) is unchanged by the redefinitions

$$\begin{aligned}
A(a(\mu)) &\to A(a(\mu)) + \frac{\partial \tilde{G}(a(\mu))}{\partial a} \beta_a(a(\mu)) \,, \\
B(a(\mu)) &\to B(a(\mu)) + \frac{\partial \tilde{H}(a(\mu))}{\partial a} \beta_a(a(\mu)) \\
&\quad + 2\tilde{G}(a(\mu)) \,, \\
C(a(Q)) &\to C(a(Q)) + \tilde{H}(a(Q)) \,, \\
D_0(a(M)) &\to D_0(a(M)) - \tilde{H}(a(M)) \,, \\
D_1(a(M)) &\to D_1(a(M)) + \tilde{G}(a(M)) \,.
\end{aligned} \tag{1.28}$$

Transformations such as these can arise from a change of scheme in the computation of the SCET matching coefficients and anomalous dimensions.

We can now demonstrate the equivalence of the Sudakov form-factor in Eq. (1.26) and the form-factor given in Eq. (1.18). Taking $G(a) = -\xi(a)/2$ in Eq. (1.25), $\tilde{H}(a) = -C(a)$ and $\tilde{G}(a) = -D_1(a)$ in Eq. (1.28), brings Eq. (1.18) with Eq. (1.26) to a common form, and gives the identifications:

$$\begin{aligned}
\frac{1}{2} A(a(\mu)) - \frac{1}{2} \frac{\partial D_1(a(\mu))}{\partial a} \beta_a(a(\mu)) &= \Gamma(a(\mu)) - \frac{1}{2} \frac{\partial \xi(a(\mu))}{\partial a} \beta_a(a(\mu)) \,, \\
-\frac{1}{2} B(a(\mu)) + \frac{1}{2} \frac{\partial C(a(\mu))}{\partial a} \beta_a(a(\mu)) + D_1(a(\mu) &= \zeta(a(\mu)) + \xi(a(\mu)) \,,
\end{aligned}$$

$$C(a(M)) + D_0(a(M)) \;=\; \log F_0(a(M)). \tag{1.29}$$

The lhs of Eq. (1.29) is invariant under Eq. (1.28), and the rhs under Eq. (1.25). The computations of the SCET anomalous dimension and the cusp anomalous dimension in the literature use the same scheme, so that $\Gamma = A/2$, and

$$\begin{aligned}
\frac{1}{2} A(a) &= \Gamma(a) \,, \\
D_1(a) &= \xi(a) \,, \\
-\frac{1}{2} B(a) + \frac{1}{2} \frac{\partial C(a)}{\partial a} \beta_a(a) &= \zeta(a) \,, \\
C(a) + D_0(a) &= \log F_0(a) \,.
\end{aligned} \tag{1.30}$$

Table 1.1: One-loop corrections to the Sudakov form-factor. γ_F is the full theory anomalous dimension, C is the matching coefficient at $\mu \sim Q$, γ_1 is the SCET anomalous dimension, and D is the matching coefficient at $\mu \sim M$. $\gamma_F^{(1)}$, $C^{(1)}$, $\gamma_1^{(1)}$ and $D^{(1)}$ are the coefficients of $a \equiv \alpha/(4\pi)$ in the one-loop corrections, and $\mathsf{L}_Q \equiv \log Q^2/\mu^2$, $\mathsf{L}_M \equiv \log M^2/\mu^2$.

$\mathcal{O}$	$\gamma_F^{(1)}/C_F$	$C^{(1)}(\mu)/C_F$	$\gamma_1^{(1)}(\mu)/C_F$	$D^{(1)}(\mu)/C_F$
$\bar\psi\psi$	-6	$-\mathsf{L}_Q^2 + \frac{\pi^2}{6} - 2$	$4\mathsf{L}_Q - 6$	$-\mathsf{L}_M^2 + 2\mathsf{L}_M\mathsf{L}_Q - 3\mathsf{L}_M + \frac{9}{2} - \frac{5\pi^2}{6}$
$\bar\psi\gamma^\mu\psi$	0	$-\mathsf{L}_Q^2 + 3\mathsf{L}_Q + \frac{\pi^2}{6} - 8$	$4\mathsf{L}_Q - 6$	$-\mathsf{L}_M^2 + 2\mathsf{L}_M\mathsf{L}_Q - 3\mathsf{L}_M + \frac{9}{2} - \frac{5\pi^2}{6}$
$\bar\psi\sigma^{\mu\nu}\psi$	2	$-\mathsf{L}_Q^2 + 4\mathsf{L}_Q + \frac{\pi^2}{6} - 8$	$4\mathsf{L}_Q - 6$	$-\mathsf{L}_M^2 + 2\mathsf{L}_M\mathsf{L}_Q - 3\mathsf{L}_M + \frac{9}{2} - \frac{5\pi^2}{6}$
$\phi^\dagger\phi$	-6	$-\mathsf{L}_Q^2 + \mathsf{L}_Q + \frac{\pi^2}{6} - 2$	$4\mathsf{L}_Q - 8$	$-\mathsf{L}_M^2 + 2\mathsf{L}_M\mathsf{L}_Q - 4\mathsf{L}_M + \frac{7}{2} - \frac{5\pi^2}{6}$
$i\phi^\dagger \overleftrightarrow{D^\mu} \phi$	0	$-\mathsf{L}_Q^2 + 4\mathsf{L}_Q + \frac{\pi^2}{6} - 8$	$4\mathsf{L}_Q - 8$	$-\mathsf{L}_M^2 + 2\mathsf{L}_M\mathsf{L}_Q - 4\mathsf{L}_M + \frac{7}{2} - \frac{5\pi^2}{6}$
$\bar\psi\phi, \phi^\dagger\psi$	-3	$-\mathsf{L}_Q^2 + 2\mathsf{L}_Q + \frac{\pi^2}{6} - 4$	$4\mathsf{L}_Q - 7$	$-\mathsf{L}_M^2 + 2\mathsf{L}_M\mathsf{L}_Q - \frac{7}{2}\mathsf{L}_M + 4 - \frac{5\pi^2}{6}$

The expansion of $\log F_E(Q^2)$ to order $a(M)^3$ using the SCET form is:

$$\begin{aligned}
\log F_E(Q^2) = &\left[C^{(1)} + D_0^{(1)} + \left(-\frac{1}{2}B^{(1)} + D_1^{(1)}\right)\mathsf{L} + \frac{1}{4}A^{(1)}\mathsf{L}^2\right] a(M) \\
&+ \left[C^{(2)} + D_0^{(2)} + \left(-\frac{1}{2}B^{(2)} - b_0 C^{(1)} + D_1^{(2)}\right)\mathsf{L} + \frac{1}{4}\left(A^{(2)} + b_0 B^{(1)}\right)\mathsf{L}^2 \right. \\
&\left. - \frac{1}{12}\left(b_0 A^{(1)}\right)\mathsf{L}^3\right] a(M)^2 + \left[C^{(3)} + D_0^{(3)} + \left(-\frac{1}{2}B^{(3)} - b_1 C^{(1)} - 2b_0 C^{(2)} + D_1^{(3)}\right)\mathsf{L}\right. \\
&+ \frac{1}{4}\left(A^{(3)} + b_1 B^{(1)} + 2b_0\left(B^{(2)} + 2b_0 C^{(1)}\right)\right)\mathsf{L}^2 - \frac{1}{12}\left(b_1 A^{(1)}\right. \\
&\left. \left. + 2b_0^2 B^{(1)} + 2b_0 A^{(2)}\right)\mathsf{L}^3 + \frac{1}{24}b_0^2 A^{(1)}\mathsf{L}^4\right] a(M)^3 \,. \qquad (1.31)
\end{aligned}$$

1.4 Massless External Particles

In this section we calculate the form-factor $\log F_E(Q^2)$ for the case $Q^2 \gg M^2 \gg m_1^2, m_2^2$. At scales $\mu > Q$ we use the full theory, and the renormalization group evolution of $c(\mu)$ is given by

$$\mu\frac{\mathrm{d}c(\mu)}{\mathrm{d}\mu} \;=\; \gamma_F(a(\mu))\; c(\mu)\,, \qquad (1.32)$$

where $\gamma_F(a) = \gamma_F^{(1)}a + \gamma_F^{(2)}a^2 + \ldots$ is the full theory anomalous dimension for $\mathcal{O}$. The one-loop values $\gamma_F^{(1)}$ are given in Table 1.1. The general form for F_E given in Sec. 1.3 is for the vector current, where $\gamma_F = 0$, and $c(\mu > Q)$ is chosen to be unity. It also holds for the other operators with $c(\mu = Q) = 1$ in the full theory.

The full theory is matched onto SCET at a scale μ of order Q. The effective theory

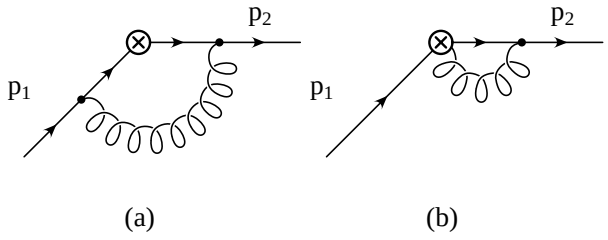

Figure 1.3: Graphs contributing to the matching condition $C(\alpha(Q))$. The solid line can be either a fermion or scalar. The second graph only exists for the scalar case $\mathcal{O} = i(\phi^\dagger D^\mu \phi - D^\mu \phi^\dagger \phi)$.

has modes with off-shellness of order Q integrated out, so the matching coefficient depends on $\log Q^2/\mu^2$, and these logarithms are not large if $\mu \sim Q$.

The operator $\mathcal{O}$ in the full theory matches to the operator $\widetilde{\mathcal{O}}$ in SCET:

$$\begin{aligned}
\bar\psi\Gamma\psi &\to \exp C(\mu)\,[\bar\xi_{n,p_2} W_n]\Gamma[W_{\bar n}^\dagger \xi_{\bar n,p_1}]\,,\\
\phi^\dagger\phi &\to \exp C(\mu)\,[\Phi_{n,p_2}^\dagger W_n][W_{\bar n}^\dagger \Phi_{\bar n,p_1}]\,,\\
i\phi^\dagger \overleftrightarrow{D}^\mu \phi &\to \exp C(\mu)\,[\Phi_{n,p_2}^\dagger W_n](i\mathcal{D}_1 + i\mathcal{D}_2)^\mu[W_{\bar n}^\dagger \Phi_{\bar n,p_1}]\,,\\
\bar\psi\phi &\to \exp C(\mu)\,[\bar\xi_{n,p_2} W_n][W_{\bar n}^\dagger \Phi_{\bar n,p_1}]\,,
\end{aligned} \tag{1.33}$$

where $i\mathcal{D}_1 = \mathcal{P} - g(n\cdot A_{\bar n,q})\frac{\bar n}{2}$, $i\mathcal{D}_2 = \mathcal{P}^\dagger - g(\bar n\cdot A_{n,-q})\frac{n}{2}$ and $\mathcal{P}$ are the SCET label operators introduced in Bauer *et al.* [18]. Collinear gauge invariance requires that, in the matching of gauge invariant operators at leading order in the power counting, the fields occur in the combination $W_n^\dagger \xi_{n,p}$, $W_n^\dagger \Phi_{n,p}$, where W_n is a Wilson line containing n-collinear gauge fields obtained by integrating over a path in the $\bar n$-direction [18].

$C(\mu)$ depends on the operator being matched (i.e. the C's in Eq. (1.33) have different values, and C can depend on Γ) and, for convenience, we have written the multiplicative matching coefficient as $\exp C(\mu)$ rather than $C(\mu)$. As is well-known, the matching coefficient can be computed as the finite part of the full theory matrix element, evaluated on-shell, with all infrared scales such as the gauge boson mass set to zero (see e.g. [29, 30, 28]). The full theory graphs to be evaluated at one-loop are those in Fig. 1.3, and when combined with the wavefunction and tree-level graphs, give the value of the full theory matrix element $\langle p_2|\mathcal{O}|p_1\rangle$. The graphs for the EFT vertex correction are shown in Fig. 1.4, and when combined with the tree-level and wavefunction graphs, give the EFT matrix element $\langle p_2|\widetilde{\mathcal{O}}|p_1\rangle$. The gauge boson and fermion masses are infrared scales and can be set to zero in the matching computation thus leading to scaleless integrals for the one-loop EFT and wavefunction graphs. Since these scaleless integrals are set to zero in dimensional regularization, the EFT matrix element is equal to its tree-level value. The full theory and EFT operators $\mathcal{O}$ and $\widetilde{\mathcal{O}}$ are normalized to have the same tree-level value, so $\exp[C(\mu)] = \langle p_2|\mathcal{O}|p_1\rangle \,/\, \langle p_2|\mathcal{O}|p_1\rangle_{\rm tree}$, i.e. the matching condition $\exp C$ is given by the

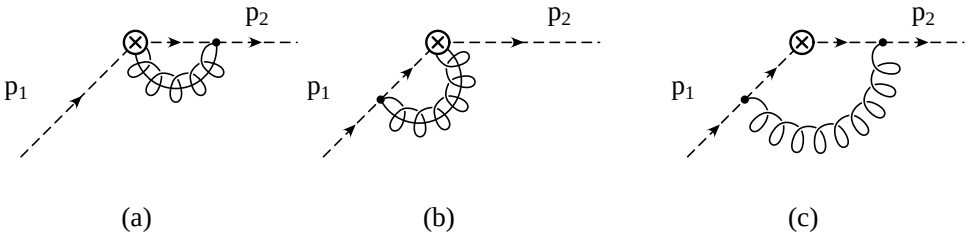

Figure 1.4: SCET graphs for the matrix element of $\widetilde{\mathcal{O}}$. The dotted lines are SCET propagators, and represent either fermions or scalars. The upper graphs are the n-collinear and $\bar{n}$-collinear graphs, and the lower graph is the ultrasoft graph. There are also wavefunction graphs. For $i\phi^\dagger \overleftrightarrow{D}^\mu \phi$, graph (a) also has a contribution where the gauge boson field at $\otimes$ arises from the covariant derivative.

on-shell full theory matrix element normalized to its tree-level value (see e.g. Ref. [29] for more details).

The computation of the SCET one loop graphs for $\mathcal{O} = \bar{\psi}\gamma^\mu\psi$ is identical to that for DIS [28]. Particle masses, such as the gauge boson mass, are all much smaller than Q, and only contribute M^2/Q^2 power corrections at the scale Q, which are being neglected. The one-loop values of $C(\mu)$ for the other cases are computed similarly, and are given in Table 1.1, where $C(\mu) = C^{(1)}\alpha(\mu)/(4\pi)$ defines the one-loop correction $C^{(1)}$. There are no large logarithms in this matching correction if the matching scale μ is chosen to be of order Q. We will choose the matching at the high scale to be at $\mu = Q$, and $C(\mu = Q)$ is given by the third column in Table 1.1 with $\mathsf{L}_Q \to 0$.

The renormalization group evolution of $c(\mu)$ in the effective theory is given by the anomalous dimension of $\widetilde{\mathcal{O}}$ in SCET. The anomalous dimension γ_1 is used to evolve $c(\mu)$ from $\mu = Q$ down to the low scale $\mu = M$. The one-loop anomalous dimension is given by the ultraviolet counterterms for the SCET graphs in Fig. 1.4 (after zero-bin subtraction, see Ref [31]). As noted earlier, anomalous dimensions in SCET can depend on Q. Ultraviolet divergences do not depend on the infrared properties of the theory, such as a gauge boson mass, so the anomalous dimension for $\mathcal{O} = \bar{\psi}\gamma^\mu\psi$ is identical to the DIS result [28]. The same argument as that given in Ref. [28] for deep inelastic scattering shows that $\gamma_1(\mu)$ is linear in $\log \mu^2/Q^2$ to all orders [28, 32], so γ_1 is written as

$$\gamma_1(\mu) \quad = \quad A(\alpha(\mu)) \log \frac{\mu^2}{Q^2} + B(\alpha(\mu))\,, \tag{1.34}$$

which defines A and B. The anomalous dimension has the expansion $\gamma_1 = \gamma_1^{(1)} a + \gamma_1^{(2)} a^2 + \ldots$, $A = A^{(1)} a + A^{(2)} a^2 + \ldots$, $B = B^{(1)} a + B^{(2)} a^2 + \ldots$ The computations for the other cases are similar, and the results are given in Table 1.1. Note that the anomalous dimension depends only on the external fields for the operators, and is equal for the three different fermion operators,

and for the two different scalar operators. The reason is that the EFT anomalous dimension depends on the IR divergence of the full theory graph, and the IR divergence is independent of the vertex factors. The anomalous dimension for $\bar{\psi}\phi$ is the average of the anomalous dimensions for the fermionic and scalar operators.

The next step in the EFT computation is the matching condition at the low scale $\mu \sim M$. At this scale, the massive gauge boson is integrated out, and one matches to an effective theory which is SCET without the massive gauge boson. In our toy example, this effective theory contains no gauge particles, and is a free theory. There is no need to introduce any propagating gauge modes below M [33]. The matching at $\mu \sim M$ is given by evaluating the graphs in Fig. 1.4, and the wavefunction graphs. The gauge boson mass can no longer be set to zero, since it is of the same order as the matching scale, and the one loop SCET graphs are non-zero. The matching computation is discussed in detail here for the fermion vector current. The other cases are treated similarly.

One matches the operator $c(\mu)[\bar{\xi}_{n,p_2} W_n]\gamma^\mu [W_{\bar{n}}^\dagger \xi_{\bar{n},p_1}]$ in SCET with gauge particles (the theory above M) onto the operator $[\exp D(\mu)]\, c(\mu)\bar{\xi}_{n,p_2}\gamma^\mu \xi_{\bar{n},p_1}$ in SCET without gauge particles (the theory below M). The n-collinear graph in Fig. 1.4 gives

$$\begin{aligned} I_n &= -ig^2\mu^{2\epsilon} C_F c(\mu) \int \frac{\mathrm{d}^d k}{(2\pi)^d} \frac{1}{k^2 - M^2} \frac{\bar{n}\!\!\!/}{2} n^\alpha \frac{n\!\!\!/}{2} \frac{\bar{n}\cdot(p_2 - k)}{(p_2 - k)^2} \gamma^\mu \frac{1}{-\bar{n}\cdot k} \bar{n}_\alpha \\ &= -2ig^2 C_F \gamma^\mu \mu^{2\epsilon} \int \frac{\mathrm{d}^d k}{(2\pi)^d} \frac{\bar{n}\cdot(p_2 - k)}{[(p_2 - k)^2 + i0^+][-\bar{n}\cdot k + i0^+][k^2 - M^2 + i0^+]}. \end{aligned} \tag{1.35}$$

This integral is divergent, even in $4 - 2\epsilon$ dimensions with an off-shellness, unlike the previously studied examples where the gauge boson was massless. A related divergence was encountered by Beneke and Feldman in their study of the $B \to \pi\ell\nu$ form-factor. Beneke and Feldman used an analytic regulator [34, 35] to evaluate their integrals, and we use an extension of their method. A similar procedure was used by Jantzen *et al.* [7] in their study of two-loop electroweak Sudakov corrections. The p_i propagator denominator $(p_i - k)^2$ in the full theory is analytically continued to

$$\frac{1}{(p_i - k)^2} \quad \to \quad \frac{(-\nu_i^2)^{\delta_i}}{[(p_i - k)^2]^{1+\delta_i}}\,. \tag{1.36}$$

where ν_i and δ_i are new parameters. The $(p_2 - k)^2$ denominator in Eq. (1.35) arises from the collinear p_2 propagator, and so gets modified as in Eq. (1.36). The $-\bar{n}\cdot k$ propagator in Eq. (1.35) arises from the $(p_1 - k)^2$ propagator when k becomes n-collinear. In this limit

$$\frac{1}{(p_1 - k)^2} \quad \to \quad \frac{(-\nu_1^2)^{\delta_1}}{[(n\cdot p_1)(-\bar{n}\cdot k)]^{1+\delta_1}}\,. \tag{1.37}$$

We will therefore analytically continue the $-\bar{n}\cdot k$ propagator in Eq. (1.35), which arises from the

W_n Wilson line in $\mathcal{O}$ using

$$\frac{1}{-\bar{n}\cdot k} \quad \to \quad \frac{(-\nu_1^-)^{\delta_1}}{(-\bar{n}\cdot k)^{1+\delta_1}}\,, \tag{1.38}$$

where $\nu_1^- \equiv \nu_1^2/p_1^+$. We will see below that it is important that ν_1^- is related to ν_1^2 in this way. Note that under boosts, ν_1^- transforms like the minus component of a four-vector. With this choice, Eq. (1.35) gives

$$\begin{aligned} I_n &= -2\frac{\alpha}{4\pi}C_F c(\mu)\gamma^\mu \left(\frac{\mu^2}{M^2}\right)^\epsilon \left(\frac{\nu_2^2}{M^2}\right)^{\delta_2} \left(\frac{\nu_1^-}{p_2^-}\right)^{\delta_1} \\ &\quad \times \frac{\Gamma(\epsilon+\delta_2)}{\Gamma(1+\delta_2)}\frac{\Gamma(2-\epsilon-\delta_2)\Gamma(\delta_2-\delta_1)}{\Gamma(2-\epsilon-\delta_1)}\,. \end{aligned} \tag{1.39}$$

The regulated value of I_n is given by setting $\delta_i = r_i\delta$ and taking the limit $\delta \to 0$ first, followed by $\epsilon \to 0$ [34, 35],

$$\begin{aligned} I_n &= \frac{\alpha}{4\pi}C_F c(\mu)\gamma^\mu \Bigg[\frac{2}{r_1-r_2}\frac{1}{\delta\epsilon} + \frac{2}{r_1-r_2}\frac{1}{\delta}\log\frac{\mu^2}{M^2} - \frac{2r_2}{r_1-r_2}\frac{1}{\epsilon^2} \\ &\quad + \frac{1}{\epsilon}\left(2 + \frac{2r_1}{r_1-r_2}\log\frac{\nu_1^-}{p_2^-} + \frac{2r_2}{r_1-r_2}\log\frac{\nu_2^2}{\mu^2}\right) + 2 + 2\log\frac{\mu^2}{M^2} \\ &\quad + \frac{2r_2}{r_1-r_2}\log\frac{\mu^2}{M^2}\log\frac{\nu_2^2}{\mu^2} + \frac{2r_1}{r_1-r_2}\log\frac{\mu^2}{M^2}\log\frac{\nu_1^-}{p_2^-} \\ &\quad + \frac{r_2}{r_1-r_2}\log^2\frac{\mu^2}{M^2} + \frac{r_2\pi^2}{2(r_1-r_2)} - \frac{r_1\pi^2}{3(r_1-r_2)}\Bigg], \end{aligned} \tag{1.40}$$

which is a boost invariant expression, since ν_1^-/p_2^- is boost invariant. Equation (1.40) is valid away from the symmetric point $r_1 = r_2$.

The $\bar{n}$-collinear graph is given by Eq. (1.40) with the replacements $\delta_1 \leftrightarrow \delta_2$, $\nu_2 \to \nu_1$, $\nu_1^- \to \nu_2^+$, $p_2^- \to p_1^+$, with $\nu_2^+ \equiv \nu_2^2/p_2^-$,

$$\begin{aligned} I_{\bar{n}} &= -2\frac{\alpha}{4\pi}C_F c(\mu)\gamma^\mu \left(\frac{\mu^2}{M^2}\right)^\epsilon \left(\frac{\nu_1^2}{M^2}\right)^{\delta_1} \left(\frac{\nu_2^+}{p_1^+}\right)^{\delta_2} \\ &\quad \times \frac{\Gamma(\epsilon+\delta_1)}{\Gamma(1+\delta_1)}\frac{\Gamma(2-\epsilon-\delta_1)\Gamma(\delta_1-\delta_2)}{\Gamma(2-\epsilon-\delta_2)}\,. \end{aligned} \tag{1.41}$$

The parameters ν_2^+ and ν_1^- play the same role as $\mu^\pm$ in the rapidity regularization method of Ref. [31].

The ultrasoft graph in Fig. 1.4 is regulated by the same method. The p_2 propagator $(p_2-k)^2$ is multipole expanded in the effective theory, and becomes $-p_2^- k^+$, where p_2^- is a label momentum. Using Eq. (1.36) for the fermion propagators, we see that after multipole expansion, they are regulated in the same way as the Wilson line propagators. The ultrasoft graph gives

$$\begin{aligned} I_{\rm us} &= -ig^2 C_F c(\mu)\gamma^\mu \int \frac{\mathrm{d}^d k}{(2\pi)^d}\frac{1}{k^2-M^2} \\ &\quad n^\alpha \frac{(-\nu_2^+)^{\delta_2}}{[n\cdot(p_2-k)]^{1+\delta_2}}\gamma^\mu \frac{(-\nu_1^-)^{\delta_1}}{[\bar{n}\cdot(p_1-k)]^{1+\delta_1}}\bar{n}_\alpha\,, \end{aligned} \tag{1.42}$$

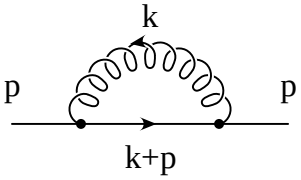

Figure 1.5: One-loop correction to the fermion propagator.

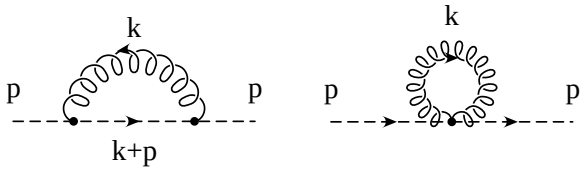

Figure 1.6: One-loop correction to the scalar propagator.

and vanishes on-shell, since $p_2^+ = p_1^- = 0$.

The total SCET contribution is given by the sum of the n-collinear, $\bar{n}$-collinear and ultrasoft graphs, as well as the wavefunction renormalization correction. The collinear correction to the particle propagator is the same as in the full theory [18], and the ultrasoft correction vanishes, so the wavefunction corrections are the same as in the full theory. The fermion graph, Fig. 1.5, gives

$$C_F \frac{\alpha}{4\pi}\, i\not{p} \left[\frac{1}{\epsilon_{\rm UV}} - \frac{1}{2} - \ln\frac{M^2}{\mu^2}\right] , \tag{1.43}$$

and so contributes a wavefunction correction

$$\delta z = C_F \frac{\alpha}{4\pi} \left[\frac{1}{\epsilon_{\rm UV}} - \frac{1}{2} - \mathsf{L}_M\right] . \tag{1.44}$$

Our normalization convention is such that the on-shell matrix element gets a contribution $-\delta z/2$ for each external particle. The wavefunction corrections for the various cases we need are tabulated in Table 1.2. In the table, we have distinguished between UV and IR divergences by the subscript on the $1/\epsilon$ terms. The scalar operators require the scalar propagator correction, Fig. 1.6, which gives

$$ip^2 \frac{\alpha_s}{4\pi} C_F \left[-\frac{2}{\epsilon_{\rm UV}} - \frac{3}{2} + 2\ln\frac{M^2}{\mu^2}\right] - iM^2 \frac{\alpha_s}{4\pi} C_F \left[-\frac{3}{\epsilon_{\rm UV}} - 1 + 3\ln\frac{M^2}{\mu^2}\right] . \tag{1.45}$$

The first term gives the wavefunction correction, and the second is the mass-shift of the scalar proportional to the gauge boson mass. The scalar mass-shift is canceled by the bare mass term in

Table 1.2: One-loop gauge boson contribution to on-shell wavefunction renormalization. The gauge boson mass is M and the particle (fermion or scalar) mass is m. $h_{F,S}$ are given in Appendix C.

Field	m	M	
ψ	0	0	$\frac{1}{\epsilon_{\rm UV}} - \frac{1}{\epsilon_{\rm IR}}$
ψ	0	$\neq 0$	$\frac{1}{\epsilon_{\rm UV}} - \frac{1}{2} - \mathsf{L}_M$
ψ	$\neq 0$	0	$\frac{1}{\epsilon_{\rm UV}} + \frac{2}{\epsilon_{\rm IR}} + 4 - 3\mathsf{L}_m$
ψ	$\neq 0$	$\neq 0$	$\frac{1}{\epsilon_{\rm UV}} - \frac{1}{2} - \mathsf{L}_M + h_F(m^2/M^2)$
ϕ	0	0	$-\frac{2}{\epsilon_{\rm UV}} + \frac{2}{\epsilon_{\rm IR}}$
ϕ	0	$\neq 0$	$-\frac{2}{\epsilon_{\rm UV}} - \frac{3}{2} + 2\mathsf{L}_M$
ϕ	$\neq 0$	0	$-\frac{2}{\epsilon_{\rm UV}} + \frac{2}{\epsilon_{\rm IR}}$
ϕ	$\neq 0$	$\neq 0$	$-\frac{2}{\epsilon_{\rm UV}} - \frac{3}{2} + 2\mathsf{L}_M + h_S(m^2/M^2)$
h_v	∞	0	$-\frac{2}{\epsilon_{\rm UV}} + \frac{2}{\epsilon_{\rm IR}}$
h_v	∞	$\neq 0$	$-\frac{2}{\epsilon_{\rm UV}} + 2\mathsf{L}_M$

the scalar Lagrangian, which is adjusted to keep the physical scalar massless. This cancellation is an example of fine-tuning required to have light scalars.

The total on-shell amplitude $I_n + I_{\bar{n}} + I_s - 2(\delta z/2)$ is

$$\frac{\alpha}{4\pi} C_F c(\mu) \gamma^\mu \left[\frac{2}{\epsilon^2} + \frac{1}{\epsilon}\left(3 - 2\mathsf{L}_Q\right) + 2\mathsf{L}_M \mathsf{L}_Q - \mathsf{L}_M^2 - 3\mathsf{L}_M + \frac{9}{2} - \frac{5\pi^2}{6} \right]. \tag{1.46}$$

The total amplitude Eq. (1.46) is independent of δ, r_1 and r_2 introduced by the analytic regulator, and depends only on ϵ of dimensional regularization. In evaluating Eq. (1.46), we have used $\nu_1^- = \nu_1^2/p_1^+$, $\nu_2^+ = \nu_2^2/p_2^-$ and $Q^2 = p_1^+ p_2^-$. The $1/\epsilon$ and $1/\epsilon^2$ poles are ultraviolet divergences, and are canceled by the renormalization counterterms in the effective theory. The IR divergences in the EFT are regulated by the gauge boson mass, so the $1/\epsilon$ divergences in Eq. (1.46) are UV divergences. The $1/\epsilon$ term multiplied by -2 gives the SCET anomalous dimension listed in Table 1.1, and is a non-trivial check on the analytic regulator computation. The SCET anomalous dimension was computed in Ref. [28] using an off-shell regulator, and the analytic regulator gives the same result. While the total anomalous dimension is the same, the contribution of individual diagrams to the anomalous dimension depends on the regulator. For example, in Ref. [28], the ultrasoft graph had a $1/\epsilon$ divergence which contributed to the anomalous dimension, whereas the ultrasoft graph vanishes on-shell when evaluated using the analytic regulator method. Contributions can be moved between the collinear and ultrasoft diagrams, depending on the

choice of regulator.

The EFT below the matching scale $\mu \sim M$ is SCET without gauge particles; thus there are no one loop diagrams to consider in the theory below M. The finite part of Eq. (1.46) gives the multiplicative matching coefficient $\exp D(\mu)$ at the low scale μ of order M. The coefficient of $\widetilde{\mathcal{O}}$ in the effective theory after integrating out the gauge bosons is given by $c(\mu - 0^+) = [\exp D(\mu)]\, c(\mu + 0^+)$, where $c(\mu \pm 0^+)$ are the coefficients before and after integrating out the gauge bosons, respectively. The coefficient $D(\mu)$ has the usual expansion $D = D^{(1)}a + D^{(2)}a^2 + \ldots$, and at one-loop order is

$$D^{(1)} \;=\; C_F \left[-\mathsf{L}_M^2 + 2\mathsf{L}_M \mathsf{L}_Q - 3\mathsf{L}_M + \frac{9}{2} - \frac{5\pi^2}{6} \right]. \tag{1.47}$$

for the fermion vector current. The other cases are computed similarly, and are given in Table 1.1. The matching at M is independent of the vertex structure, and depends only on whether the particles are fermions or scalars. The $\bar{\psi}\phi$ matching is the average of the results for two fermions and two scalars. This is a new feature of the effective theory, which follows because the graphs factorize into contributions from the individual particles. The matching at Q from the full theory does not have this property.

Note that $D(\mu)$ is a function of both L_M and L_Q, and is linear in L_Q. The matching condition depends on both scales Q and M. The dependence of the matching on the high scale Q is a new feature of SCET with massive gauge bosons, and has not occurred in previous computations in SCET, or other EFTs. We noted earlier that SCET graphs know about the scale Q through the labels $\bar{n}\cdot p_2$ and $n\cdot p_1$ since $Q^2 = \bar{n}\cdot p_2\, n\cdot p_1$. Nevertheless, in previous computations such as DIS, the matching condition at the jet scale $M_J^2 \ll Q^2$ depended on $\log M_J^2/\mu^2$, and there was no $\log Q^2/\mu^2$ dependence. It is easy to see why there must in general be L_Q terms in the matching condition in our case. If D is the matching condition at μ, and $\gamma_{h,l}$ are the anomalous dimension in the theories above and below μ,

$$\mu \frac{\mathrm{d}D}{\mathrm{d}\mu} = \gamma_l(\mu) - \gamma_h(\mu). \tag{1.48}$$

In our example, $\gamma_l = 0$ since the theory below M is a free theory. Since γ_h has the form Eq. (1.34) with a L_Q term, such terms must also be present in D. Let us contrast this with DIS. For moments M_N of the deep inelastic scattering structure function with $N \gg 1$, the jet scale is $M_J^2 = Q^2/N$. The theory above the jet scale has an anomalous dimension γ_h which depends on L_Q, and the theory below the jet scale has Altarelli-Parisi evolution with anomalous dimension γ_l which depends on $\log N$. The two anomalous dimensions are related in such a way that $\gamma_l - \gamma_h \propto \log Q^2/N$, the logarithm of the jet scale. The matching D also depends only on the jet scale Q^2/N, and there are no large logarithms in D if μ is chosen to be of order the jet scale [28].

The L_Q term in Eq. (1.47) is multiplied by L_M, and so there is no L_Q term in D if the matching scale is chosen to be exactly equal to M. This is accidental, and does not happen at

higher orders. One can show explicitly that at two-loops, there is a non-zero L_Q contribution to D even if $\mu = M$. In the standard model, it is convenient to integrate the weak gauge bosons out at a single scale $\mu = M_Z$, and one has one-loop terms in the matching condition of the form $(\log Q^2/M_Z^2)(\log M_W^2/M_Z^2)$.

Renormalization group improved perturbation theory is used to sum logarithms in an EFT. This would not be possible if there were arbitrary powers of L_Q in the matching condition. We will prove in Sec. 1.5 that to all orders in perturbation theory, the matching condition D is *linear* in L_Q. Thus renormalization group summation can be used to obtain all logarithms except the first, so that in the Sudakov problem at order α^n, the $2n-1$ terms $\alpha^n\mathsf{L}^{2n}, \ldots, \alpha^n\mathsf{L}^2$ can be obtained by renormalization group evolution, but not the single log term $\alpha^n\mathsf{L}$, which gets a matching contribution from D. The general form for $D(\mu)$ is

$$D(\mu) \;=\; D_0(a(\mu), \mathsf{L}_M) + D_1(a(\mu), \mathsf{L}_M)\mathsf{L}_Q \,, \tag{1.49}$$

which defines $D_{0,1}$. At one-loop, Eq. (1.47) gives

$$\begin{aligned} D_0^{(1)} &= C_F\left[-\mathsf{L}_M^2 - 3\mathsf{L}_M + \frac{9}{2} - \frac{5\pi^2}{6}\right], \\ D_1^{(1)} &= 2C_F\mathsf{L}_M \,. \end{aligned} \tag{1.50}$$

Choosing $\mu = M$ gives the matching coefficient

$$D(\mu = M) \;=\; D_0(a(M), 0) + D_1(a(M), 0)\log\frac{Q^2}{M^2} \,. \tag{1.51}$$

In our example, $D_1(a(M), 0) = 0$, so there is no $\log Q^2/M^2$ term in the one-loop matching coefficient. One expects that $D_1(a(M), 0) \neq 0$ at higher orders, so there can be a single large logarithm in the matching coefficient.

The final step in the computation is to compute the on-shell matrix element of $\widetilde{\mathcal{O}}$ in the theory below M. Since the gauge bosons have been integrated out, this theory is a free theory, and the matrix element is trivial, being given by its free field value. The Sudakov form-factor is defined as the ratio of the scattering amplitude to its value in the free theory, so the low-energy matrix element contribution to the Sudakov form-factor is unity.

The contributions to the Sudkakov form-factor are:

1. The coefficient $c(\mu)$ in the full theory just above the matching scale $\mu = Q$, which is chosen to be unity.

2. The multiplicative matching coefficient $\exp C(\mu)$ for the matching between the full theory and SCET at the scale $\mu = Q$.

3. The integral of the SCET anomalous dimension between $\mu = Q$ and $\mu = M$.

4. The multiplicative matching coefficient $\exp D(\mu)$ for the matching at the scale $\mu = Q$ between SCET, and SCET with the gauge bosons integrated out.

5. The low-energy matrix element, which gives unity, using the conventional normalization for the form-factor.

Combining these contributions gives Eq. (1.26) for the Sudakov form-factor given earlier. The terms are represented schematically as:

$$\begin{array}{ccc} C & \gamma_1 & D \\ Q & \longrightarrow & M \end{array} \tag{1.52}$$

The expression Eq. (1.26) for the Sudakov form-factor, with the one-loop coefficients given in Table 1.1, can be compared with known fixed order results in the case of the fermion vector current by expanding this in a power series expansion in $\alpha(M)$ as shown in Eq. (1.31). The result correctly reproduces the known $\alpha\mathsf{L}$, $\alpha^2\mathsf{L}^4$ and $\alpha^2\mathsf{L}^3$ terms ($\mathsf{L} = \log Q^2/M^2$).

Comparison with the two-loop results of Ref. [7, 15] allows us to extract values for the two-loop cusp anomalous dimension,

$$A^{(2)} = \left(-\frac{268}{9} + \frac{4}{3}\pi^2\right) C_F C_A + \frac{80}{9} C_F T_F n_F + \frac{32}{9} C_F T_F n_S \,. \tag{1.53}$$

The non-log part of the anomalous dimension is

$$\begin{aligned} B^{(2)} &= \left(4\pi^2 - 3 - 48\zeta(3)\right) C_F^2 + \left(-\frac{961}{27} - \frac{11\pi^2}{3} + 52\zeta(3)\right) C_F C_A \\ &\quad + \left(\frac{260}{27} + \frac{4\pi^2}{3}\right) C_F T_F n_F + \left(\frac{167}{27} + \frac{\pi^2}{3}\right) C_F T_F n_S \,. \end{aligned} \tag{1.54}$$

The log part of the matching at M for equal Higgs and gauge boson masses is

$$D_1^{(2)} = \left[\frac{112}{27} + \frac{4}{9}\pi^2\right] C_F T_F n_F + \left[-\frac{782}{27} - \frac{20}{3}\zeta(3) + 5\sqrt{3}\pi + \frac{26}{\sqrt{3}}\mathrm{Cl}_2\left(\frac{\pi}{3}\right)\right] C_F \,. \tag{1.55}$$

where the Clausen function is

$$\mathrm{Cl}_2(x) = \sum_1^\infty \frac{\sin nx}{n^2} \,. \tag{1.56}$$

The anomalous dimension for $Q > \mu > M$ is independent of infrared physics, such as spontaneous symmetry breaking and the gauge boson mass, and so can be written in terms of group invariants such as C_F and C_A. The expressions for $A^{(2)}$ and $B^{(2)}$ hold in a gauge theory with fermion and scalar fields in arbitrary representations.

The matching $D_1^{(2)}$ depends on the gauge boson masses, and is only valid in a $SU(2)$ gauge theory with scalars in the fundamental representation. The expression Eq. (1.55) has a $C_F T_F n_F$ term from fermion loop corrections to the gauge boson propagator, and a C_F term. The C_F term arises from scalar loop corrections to the gauge boson propagator, as well as graphs such as Fig. 1.7 which arise due to spontaneous symmetry breaking. The group theory invariant for Fig. 1.7 depends on the pattern of symmetry breaking, and cannot be written in terms of $SU(2) \times U(1)$ invariants. Jantzen and Smirnov [15] have therefore explicitly used the group

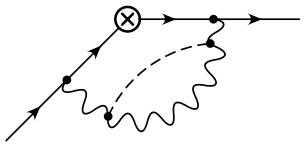

Figure 1.7: A graph whose group-theoretic factor cannot be written in terms of invariants such as C_F and C_A.

theory factors for a broken $SU(2)$ theory in evaluating these contributions, and we follow their convention here. Furthermore, Ref. [15] computed the two-loop graphs only for $M_H = M_W$, and so Eq. (1.55) is only valid for equal Higgs and gauge boson masses.

The three-loop cusp anomalous dimension is known in a theory without scalar fields [36]

$$\begin{aligned}\Gamma^{(3)} &= C_F\left[\left(-\frac{245}{3}+\frac{268}{27}\pi^2-\frac{44}{3}\zeta(3)-\frac{22}{45}\pi^4\right)C_A^2\right.\\ &\quad+\left(\frac{836}{27}-\frac{80}{27}\pi^2+\frac{112}{3}\zeta(3)\right)C_A T_F n_F\\ &\quad\left.+\left(\frac{110}{3}-32\zeta(3)\right)C_F T_F n_F+\frac{32}{27}(T_F n_F)^2\right].\end{aligned} \tag{1.57}$$

so $A^{(3)} = 2\Gamma^{(3)}$ is known, neglecting scalar contributions. These missing scalar contributions are expected to make small corrections to $\Gamma^{(3)}$. The scalar term contributes 7% to the two-loop cusp anomalous dimension $A^{(2)}$.

Our one-loop computation combined with the known two-loop cusp anomalous dimension sums the LL and NLL series for the Sudakov form factor. The NNLL series requires $A^{(3)}$ which is known excluding Higgs contributions, $B^{(2)}$ which is known (Eq. (1.54)), $D_1^{(2)}$ which is known for $M_H = M$, and $C^{(1)}, D_0^{(1)}$ which are known (Table 1.1). For electroweak applications, the LL and NLL are more than adequate for precision studies.

1.5 Proof that D is linear in L_Q

The general functional form of the n-collinear graphs is $\exp F(a(\mu), \mathsf{L}_M, \mathsf{L}_2, \mathsf{L}_-)$, where $\mathsf{L}_M = \log M^2/\mu^2$, $\mathsf{L}_2 = \log \nu_2^2/\mu^2$ and $\mathsf{L}_- = \log \nu_1^-/p_2^-$. Using $\nu_1^- = \nu_1^2/p_1^+$ and $Q^2 = p_1^+ p_2^-$, this can be rewritten as $\exp F(a(\mu), \mathsf{L}_M, \mathsf{L}_2, \mathsf{L}_1 - \mathsf{L}_Q)$, where $\mathsf{L}_Q = \log Q^2/\mu^2$. Similarly, the $\bar{n}$-collinear graphs have the functional form $\exp G(a(\mu), \mathsf{L}_M, \mathsf{L}_1, \mathsf{L}_2 - \mathsf{L}_Q)$. The sum of all the collinear graphs is the product $\exp(F+G)$, because the n and $\bar{n}$-collinear graphs factor. These graphs give the matching coefficient $\exp D$, since the ultrasoft graphs vanish on-shell, so that D has the additive form

$$D(a(\mu), \mathsf{L}_M, \mathsf{L}_Q) = F(a(\mu), \mathsf{L}_M, \mathsf{L}_2, \mathsf{L}_1 - \mathsf{L}_Q) + G(a(\mu), \mathsf{L}_M, \mathsf{L}_1, \mathsf{L}_2 - \mathsf{L}_Q)\,. \tag{1.58}$$

The $\mathsf{L}_1, \mathsf{L}_2$ dependence cancels, since D is independent of $\nu_{1,2}$.[3]

Equation (1.58) implies that $D(a(\mu), \mathsf{L}_M, \mathsf{L}_Q)$ is linear in L_Q. The proof is as follows: Differentiating Eq. (1.58) with respect to L_1 and L_Q, with respect to L_2 and L_Q, and with respect to L_1 and L_2 give

$$\begin{aligned} 0 &= \partial_1\partial_1 F + \partial_2\partial_1 G\,, \\ 0 &= \partial_1\partial_2 F + \partial_2\partial_2 G\,, \\ 0 &= \partial_2\partial_1 F + \partial_2\partial_1 G\,, \end{aligned} \tag{1.59}$$

where $\partial_{1,2}$ is the derivative with respect to $\mathsf{L}_{1,2}$. The second derivative of D with respect to L_Q is

$$\begin{aligned} \frac{\partial D}{\partial \mathsf{L}_Q^2} &= \partial_1\partial_1 F + \partial_2\partial_2 G \\ &= -\partial_2\partial_1 G - \partial_1\partial_2 F \\ &= -\partial_1\partial_2 \left(F + G\right) \\ &= -\partial_1\partial_2 D = 0\,, \end{aligned} \tag{1.60}$$

using Eq. (1.59) and the commutation of partial derivatives, $\partial_3\partial_2 = \partial_2\partial_3$. Thus D can be at most linear in L_Q. Equation (1.58) is D before the addition of renormalization counterterms. The finite part shows that the matching correction is linear in L_Q, justifying the form Eq. (1.49) used earlier. The infinite part shows that the SCET anomalous dimension is linear in L_Q, and so gives another proof of this known result [28, 32].

1.6 Consistency Conditions

There are consistency conditions on matching coefficients and anomalous dimensions which follow from the structure of the effective theory. Consider the matching of an operator between a high energy theory and a low energy theory at some scale μ. The operator coefficients are $c_{h,l}(\mu)$, with anomalous dimensions $\gamma_{h,l}(\mu)$ in the two theories, $\mu \mathrm{d}c_{h,l}/\mathrm{d}\mu = \gamma_{h,l} c_{h,l}$. Assume that there is a multiplicative matching coefficient $X(\mu)$ between the two theories, so that $c_l(\mu) = X(\mu) c_h(\mu)$. The matching scale μ is arbitrary, so one gets the constraint

$$\mu \frac{\mathrm{d}}{\mathrm{d}\mu} \log c_l = \mu \frac{\mathrm{d}}{\mathrm{d}\mu} \log X + \mu \frac{\mathrm{d}}{\mathrm{d}\mu} \log c_h\,, \tag{1.61}$$

which gives the relation

$$\gamma_l - \gamma_h = \mu \frac{\mathrm{d}}{\mathrm{d}\mu} \log X\,, \tag{1.62}$$

[3] There are also wavefunction contributions to D. These are independent of Q.

between the matching coefficient and the anomalous dimensions in the two theories. In the Sudakov problem, applying Eq. (1.62) to the matching between the full theory and SCET gives

$$\gamma - \gamma_F = \mu \frac{\mathrm{d}}{\mathrm{d}\mu} C \,, \tag{1.63}$$

and applying it to the matching when the gauge boson is integrated out gives

$$0 - \gamma = \mu \frac{\mathrm{d}}{\mathrm{d}\mu} D \,, \tag{1.64}$$

since the theory below M is a free theory, and so has zero anomalous dimension.

The anomalous dimension in the full theory and SCET have the form $\gamma_F(a(\mu))$ and $\gamma = -A(a(\mu))\mathsf{L}_Q + B(a(\mu))$, respectively, where we have used the result that γ is linear in L_Q to all orders [28]. The matching coefficient C at the high scale Q is independent of the low-energy scales such as M, and has the form $C(a(\mu), \mathsf{L}_Q)$. The matching coefficient D at $\mu \sim M$ can depend on both Q and M, since the SCET field labels depend on Q. As a result, D has the form $D(a(\mu), \mathsf{L}_M, \mathsf{L}_Q)$. Any dependence on Q^2/M^2 can be converted into dependence on L_M and L_Q using $Q^2/M^2 = \exp(\mathsf{L}_Q - \mathsf{L}_M)$.

Equation (1.63) gives

$$A(a(\mu))\mathsf{L}_Q - B(a(\mu)) + \gamma_F(a(\mu)) = 2\frac{\partial C}{\partial \mathsf{L}_Q} - \frac{\partial C}{\partial a}\beta_a(a) \,. \tag{1.65}$$

Writing C as an expansion in L_Q

$$C(a(\mu), \mathsf{L}_Q) = \sum_{n=0}^{\infty} C_n(a(\mu))\mathsf{L}_Q^n \,, \tag{1.66}$$

gives the consistency conditions

$$\begin{aligned} \gamma_F(a) - B(a) &= 2C_1(a) - \frac{\partial C_0}{\partial a}\beta_a(a) \,, \\ A(a) &= 4C_2(a) - \frac{\partial C_1}{\partial a}\beta_a(a) \,, \\ 2nC_n(a) &= \frac{\partial C_{n-1}}{\partial a}\beta_a(a) \,, \qquad n \geq 3 \,, \end{aligned} \tag{1.67}$$

which determine C_n, $n > 0$ in terms of C_0, A, B and γ_F, and are satisfied by the one-loop values in Table 1.1. The matching coefficient at $\mu = Q$ is $C_0(a(Q))$.

Equation (1.64) applied to the matching at M, gives

$$A(a(\mu))\mathsf{L}_Q - B(a(\mu)) = \frac{\partial D}{\partial a}\beta_a(a) - 2\frac{\partial D}{\partial \mathsf{L}_Q} - 2\frac{\partial D}{\partial \mathsf{L}_M} \,. \tag{1.68}$$

Using Eq. (1.49), and equating powers of L_Q gives

$$\begin{aligned} -B(a(\mu)) &= \frac{\partial D_0}{\partial a}\beta_a(a) - 2D_1 - 2\frac{\partial D_0}{\partial \mathsf{L}_M} \,, \\ A(a(\mu)) &= \frac{\partial D_1}{\partial a}\beta_a(a) - 2\frac{\partial D_1}{\partial \mathsf{L}_M} \,. \end{aligned} \tag{1.69}$$

Writing D_i, $i = 0, 1$ as an expansion in L_M

$$D_i(a(\mu), \mathsf{L}_M) = \sum_{n=0}^{\infty} D_{i,n}(a(\mu))\mathsf{L}_M^n \,, \tag{1.70}$$

gives the consistency conditions

$$\begin{aligned}
-B &= \frac{\partial D_{0,0}}{\partial a}\beta_a - 2D_{1,0} - 2D_{0,1} \,, \\
2nD_{0,n} &= \frac{\partial D_{0,n-1}}{\partial a}\beta_a - 2D_{1,n-1} \,, \qquad n \geq 2 \,, \\
A &= \frac{\partial D_{1,0}}{\partial a}\beta_a - 2D_{1,1} \,, \\
2nD_{1,n}(a) &= \frac{\partial D_{1,n-1}}{\partial a}\beta_a \,, \qquad n \geq 2 \,,
\end{aligned} \tag{1.71}$$

which determine $D_{i,n}$, $n > 0$ in terms of $D_{i,0}$, A and B, and are satisfied by the one-loop values in Table 1.1. The matching coefficient at $\mu = M$ is $D_{0,0}(a(M)) + D_{1,0}(a(M)) \log Q^2/M^2$.

1.7 Massive Particles

The calculations so far have been performed for external particles with masses $m_{1,2}$ much smaller than the gauge boson mass. In this section, we extend the results to massive external particles. For fermions, we will assume that the theory is vectorlike, so that the fermion mass arises from a gauge invariant mass term $-m\bar{\psi}\psi$. The standard model, a chiral gauge theory, where masses arise from Higgs couplings due to spontaneous symmetry breaking, is discussed in Sec. 1.9.

1.7.1 $Q \gg m_2 \gg M \gg m_1$

Consider first the case where one particle has mass m_2, with $Q \gg m_2 \gg M$, and the other particle has mass m_1 much smaller than M. For definiteness, the outgoing particle is taken to be heavier than M, and the incoming one lighter than M, but the results are symmetric under $1 \leftrightarrow 2$. The Sudakov form-factor can be computed using a sequence of effective field theories.

One first matches from the full theory to SCET with a massive particle at $\mu \sim Q$ and uses the same set of operators listed in Eq. (1.33) except ξ_{n,p_2} is now a n-collinear SCET field with mass m_2 as in Ref. [37, 38]. This matching is independent of scales much smaller than Q, such as m_1, m_2 and M, and thus remains the same as in Table 1.1. The second step is to run the operator in the effective theory from Q to m_2. The anomalous dimension γ is also independent of low mass scales and again gives the same result as the massless case. At the scale m_2, one switches from SCET to a new effective theory in which the massive particle is described by a heavy quark effective theory (HQET) field h_{v_2}, with a velocity v_2, with $v_2^2 = 1$ [39]. The other (massless) particle is still described by a SCET field. The fermion vector current, for example,

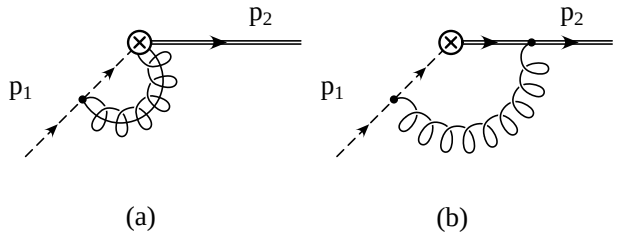

Figure 1.8: SCET graphs for the matrix element of $\widetilde{\mathcal{O}}$. The dotted lines are SCET propagators, and represent either fermions or scalars. The double lines are HQET propagators.

is now given by $\bar{h}_{v_2}\gamma^\mu W_{\bar{n}}^\dagger \xi_{\bar{n},p_1}$, instead of Eq. (1.33), and similarly for the other operators. The HQET field, h_{v_2}, does not transform under collinear gauge transformations; therefore, there is no factor analogous to the $W_{\bar{n}}^\dagger$ Wilson line that goes along with the $\xi_{\bar{n}}$ field. h_v still couples to ultrasoft gluons. One can make an additional field redefinition which eliminates the ultrasoft gluon coupling to h_v and introduces a Wilson line in the v_2 direction [20]. Both methods give the same on-shell matrix elements.

The matching condition at m_2 is given by the difference between the vertex graphs in Fig. 1.4 and Fig. 1.8, and the wavefunction graphs, evaluated at $\mu = m_2$, i.e. between graphs where ξ_{n,p_2} and h_{v_2} are used for particle 2. Note that there are three vertex graphs in the theory above m_2, and only two graphs in the theory below m_2, because there is no collinear Wilson line associated with h_{v_2}. The graphs in the theory above m_2 are evaluated with the gauge boson mass set to zero (since $m_2 \gg M$) at the on-shell point $p_2^2 = m_2^2$. The graphs in the effective theory are evaluated with $M \to 0$ at the onshell point $k_2 \cdot v_2 = 0$, where k_2 is the residual momentum of particle 2. Graphs Fig. 1.4b and Fig. 1.8a are equal, since the $\bar{n}$ collinear interactions do not depend on whether the other field at the vertex is $\bar{h}_v$ or $\bar{\xi}_{n,p_2}$. They cancel in the matching computation. The ultrasoft graphs Fig. 1.4c and Fig. 1.8b, the $\xi_{\bar{n},p_1}$ wavefunction graph, and the HQET wavefunction graph all vanish on-shell, so the matching computation is given by Fig. 1.4a and the on-shell wavefunction graph for ξ_{n,p_2}. The vertex graph Fig. 1.4a does not need an analytic regulator, and gives (for $\mathcal{O} = \bar{\psi}\gamma^\mu\psi$)

$$\begin{aligned} I_n &= aC_F\gamma^\mu\left[\frac{1}{\epsilon^2} + \frac{1}{\epsilon}\left(2 - \log\frac{m_2^2}{\mu^2}\right)\right. \\ &\quad \left. + \frac{1}{2}\log^2\frac{m_2^2}{\mu^2} - 2\log\frac{m_2^2}{\mu^2} + \frac{\pi^2}{12} + 4\right]. \end{aligned} \tag{1.72}$$

The wavefunction correction for a massive fermion is

$$\delta z = aC_F\left[\frac{1}{\epsilon_{\rm UV}} + \frac{2}{\epsilon_{\rm IR}} + 4 - 3\log\frac{m_2^2}{\mu^2}\right]. \tag{1.73}$$

Combining Eq. (1.72) and Eq. (1.73) gives the multiplicative matching condition $\exp R$, $R =$

Table 1.3: One-loop results for $Q > m_2 > M > m_1$. R is the matching coefficient at $\mu \sim m_2$, γ_2 is the anomalous dimension between m_2 and M, and S is the matching coefficient at $\mu \sim M$. The results only depend on whether the light particle is a fermion or scalar.

$\mathcal{O}$	$R^{(1)}/C_F$	$\gamma_2^{(1)}/C_F$	$S^{(1)}/C_F$
$\bar\psi_2\Gamma\psi_1$	$\frac{1}{2}\mathsf{L}_{m_2}^2 - \frac{1}{2}\mathsf{L}_{m_2} + \frac{\pi^2}{12} + 2$	$-5 - 2\mathsf{L}_{m_2} + 4\mathsf{L}_Q$	$-\frac{5}{2}\mathsf{L}_M + \frac{9}{4} - \frac{5\pi^2}{12} - \frac{1}{2}\mathsf{L}_M^2 + \mathsf{L}_M\mathsf{L}_{Q^2/m_2^2}$
$\phi_2^\dagger\phi_1, \cdots$	$\frac{1}{2}\mathsf{L}_{m_2}^2 - \mathsf{L}_{m_2} + \frac{\pi^2}{12} + 2$	$-6 - 2\mathsf{L}_{m_2} + 4\mathsf{L}_Q$	$-3\mathsf{L}_M + \frac{7}{4} - \frac{5\pi^2}{12} - \frac{1}{2}\mathsf{L}_M^2 + \mathsf{L}_M\mathsf{L}_{Q^2/m_2^2}$
$\bar\psi_2\phi_1$	$\frac{1}{2}\mathsf{L}_{m_2}^2 - \frac{1}{2}\mathsf{L}_{m_2} + \frac{\pi^2}{12} + 2$	$-6 - 2\mathsf{L}_{m_2} + 4\mathsf{L}_Q$	$-3\mathsf{L}_M + \frac{7}{4} - \frac{5\pi^2}{12} - \frac{1}{2}\mathsf{L}_M^2 + \mathsf{L}_M\mathsf{L}_{Q^2/m_2^2}$
$\phi_2^\dagger\psi_1$	$\frac{1}{2}\mathsf{L}_{m_2}^2 - \mathsf{L}_{m_2} + \frac{\pi^2}{12} + 2$	$-5 - 2\mathsf{L}_{m_2} + 4\mathsf{L}_Q$	$-\frac{5}{2}\mathsf{L}_M + \frac{9}{4} - \frac{5\pi^2}{12} - \frac{1}{2}\mathsf{L}_M^2 + \mathsf{L}_M\mathsf{L}_{Q^2/m_2^2}$

$R^{(1)}a + \ldots$, at μ of order m_2,

$$R = aC_F\left[\frac{1}{2}\mathsf{L}_{m_2}^2 - \frac{1}{2}\mathsf{L}_{m_2} + \frac{\pi^2}{12} + 2\right], \tag{1.74}$$

where $\mathsf{L}_{m_2} \equiv \log m_2^2/\mu^2$. The other cases are evaluated in a similar manner, and the results are summarized in Table 1.3. The wavefunction correction for a massive scalar, which is needed for the last three rows, is

$$\delta z = aC_F\left[-\frac{2}{\epsilon_{\rm UV}} + \frac{2}{\epsilon_{\rm IR}}\right]. \tag{1.75}$$

The remaining steps are the evaluation of the anomalous dimension in the region $M < \mu < m_2$, and the matching condition $\exp S$ at the scale M. These can be computed by evaluating the graphs in Fig. 1.8 and the wavefunction corrections, at the on-shell point $k_2 = 0$, $p_1^2 = 0$, and keeping the gauge boson mass non-zero. The graphs need to be regulated using an analytic regulator. The $\xi_{\bar n, p_1}$ is regulated as in Eq. (1.36) for the collinear propagator. The Wilson line in Fig. 1.8a is regulated using Eq. (1.37), as is the massless particle propagator in Fig. 1.8b. The new feature is the HQET propagator for particle 2, which is regulated using

$$\frac{1}{k_2\cdot v_2} \to \frac{(-\nu_{2H})^{\delta_2}}{[k_2\cdot v_2]^{1+\delta_2}}. \tag{1.76}$$

Taking the HQET limit of the particle 2 propagator,

$$\frac{(-\nu_2^2)^{\delta_2}}{[(m_2 v_2 + k_2)^2 - m_2^2]^{1+\delta_2}} \to \frac{(-\nu_2^2)^{\delta_2}}{[2m_2 k_2\cdot v_2]^{1+\delta_2}}. \tag{1.77}$$

and comparing Eq. (1.76) with Eq. (1.36), we see that $\nu_{2H} = \nu_2^2/(2m_2)$. Figure 1.8a is given by the $\bar n$-collinear graph evaluated earlier, Eq. (1.41). Figure 1.8b is

$$\begin{aligned} &-aC_F\gamma^\mu\left(\frac{2\nu_H}{M}\right)^{\delta_2}\left(\frac{\nu_1^-}{M}\right)^{\delta_1}\left(\frac{\mu^2}{M^2}\right)^{\epsilon} \\ &\times\frac{\Gamma(\delta_2/2-\delta_1/2)\Gamma(\epsilon+\delta_1/2+\delta_2/2)}{\Gamma(1+\delta_2)}. \end{aligned} \tag{1.78}$$

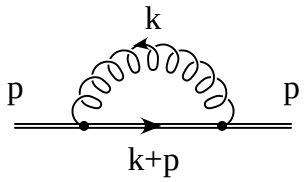

Figure 1.9: HQET propagator correction

The $\bar{n}$-collinear wavefunction graph is Eq. (1.43), and the HQET propagator correction, Fig. 1.9 is

$$aC_F\left[2M\pi + (k_2\cdot v_2)\left(-\frac{2}{\epsilon} + 2\log\frac{M^2}{\mu^2}\right)\right]. \tag{1.79}$$

Eq. (1.79) gives a contribution to the heavy quark residual mass term, $\delta m = -2aC_F M\pi$, and a wavefunction contribution listed in Table 1.2. The shift in the heavy quark mass is non-analytic in the gauge boson mass-squared. Such non-analytic contributions occur in mass corrections to particles with $k\cdot v$ propagators [40, 41]. They arise from loop integrals which diverge as an odd power of k. Such integrals are finite, but non-analytic, in dimensional regularization.

Adding Eqs. (1.41) and Eq. (1.78), expanding in δ_i, and subtracting the wavefunction corrections due to the heavy fermion, Eq. (1.79), and the collinear fermion, Eq. (1.43), gives

$$\begin{aligned} aC_F\Bigg[&\frac{1}{\epsilon^2} + \frac{1}{\epsilon}\left(\frac{5}{2} + 2\log\frac{\mu m_2}{Q^2}\right) + \frac{5}{2}\log\frac{\mu^2}{M^2} \\ &+\frac{9}{4} - \frac{5\pi^2}{12} - \frac{1}{2}\log^2\frac{\mu^2}{M^2} + 2\log\frac{\mu^2}{M^2}\log\frac{\mu m_2}{Q^2}\Bigg]. \end{aligned} \tag{1.80}$$

To obtain Eq. (1.80) we have used $\nu_{2H} = \nu_2^2/(2m_2)$, $\nu_1^- = \nu_1^2/p_1^+$, $\nu_2^+ = \nu_2^2/p_2^-$, and $Q^2 = m_2 p_1^+$. The $1/\epsilon$ coefficient multiplied by -2 gives the anomalous dimension

$$\gamma_2 \;=\; aC_F\left(-5 - 2\mathsf{L}_{m_2} + 4\mathsf{L}_Q\right), \tag{1.81}$$

and the finite part gives the matching correction

$$\begin{aligned} S \;=\; aC_F\Bigg[&-\frac{5}{2}\mathsf{L}_M + \frac{9}{4} - \frac{5\pi^2}{12} \\ &-\frac{1}{2}\mathsf{L}_M^2 - \mathsf{L}_M\left(\mathsf{L}_{m_2} - 2\mathsf{L}_Q\right)\Bigg]. \end{aligned} \tag{1.82}$$

The other cases are computed similarly, and are given in Table 1.3.

The terms which contribute to the final result are summarized schematically as:

$$\begin{array}{ccccc} C & \gamma_1 & R & \gamma_2 & S \\ Q & \longrightarrow & m_2 & \longrightarrow & M \end{array} \tag{1.83}$$

Table 1.4: One-loop results for $Q > m_2 > m_1 > M$. T is the matching at m_1, γ_3 is the anomalous dimension between m_1 and M, and U is the matching at M. T only depends on whether the light particle is a scalar or a fermion

$\mathcal{O}$	$T^{(1)}/C_F$	$\gamma_3^{(1)}/C_F$	$U^{(1)}/C_F$
$\bar{\psi}_2\Gamma\psi_1$	$\frac{1}{2}\mathsf{L}_{m_1}^2 - \frac{1}{2}\mathsf{L}_{m_1} + \frac{\pi^2}{12} + 2$	$4\,[wr(w)-1]$	$2\,[wr(w)-1]\,\mathsf{L}_M$
$\phi_2^\dagger\phi_1, i(\phi_2^\dagger D^\mu\phi_1 - D^\mu\phi_2^\dagger\phi_1)$	$\frac{1}{2}\mathsf{L}_{m_1}^2 - \mathsf{L}_{m_1} + \frac{\pi^2}{12} + 2$	$4\,[wr(w)-1]$	$2\,[wr(w)-1]\,\mathsf{L}_M$
$\bar{\psi}_2\phi_1$	$\frac{1}{2}\mathsf{L}_{m_1}^2 - \mathsf{L}_{m_1} + \frac{\pi^2}{12} + 2$	$4\,[wr(w)-1]$	$2\,[wr(w)-1]\,\mathsf{L}_M$
$\phi_2^\dagger\psi_1$	$\frac{1}{2}\mathsf{L}_{m_1}^2 - \frac{1}{2}\mathsf{L}_{m_1} + \frac{\pi^2}{12} + 2$	$4\,[wr(w)-1]$	$2\,[wr(w)-1]\,\mathsf{L}_M$

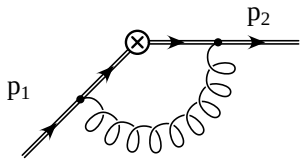

Figure 1.10: Vertex correction in the theory below $m_{1,2}$.

1.7.2 $Q \gg m_2 \gg m_1 \gg M$

The second case we consider is where both particles have mass between Q and M. For definiteness, we choose $m_2 > m_1$. The Sudakov form-factor can be computed using a sequence of matching and running steps. The matching $\exp C$ at Q, the anomalous dimension γ_1 between Q and m_2, the matching $\exp R$ at m_2, and the anomalous dimension γ_2 between m_2 and m_1 are all independent of the lower scales m_1 and M, and have the same values as in Tables 1.1, 1.3.

The new feature is the matching condition $\exp T$ at the lower particle mass m_1. The graphs in the theory above m_1 are shown in Fig. 1.8. In the theory below m_1, the SCET field $\xi_{\bar{n},p_1}$ for particle 1 is replaced by the HQET field h_{v_1}. The fermion vector current, for example, is now given by $\bar{h}_{v_2}\gamma^\mu h_{v_1}$ instead of $\bar{h}_{v_2}\gamma^\mu W_{\bar{n}}^\dagger\xi_{\bar{n},p_1}$. The vertex correction in the theory below m_1 is shown in Fig. 1.10. There is only one vertex graph instead of two, because there is no collinear Wilson line A associated with the HQET field h_{v_1}. The matching condition is given by computing the difference of graphs Fig. 1.8 and Fig. 1.10 on-shell, and setting all scales less than m_1 to zero. The only non-zero contribution is from Fig. 1.8a and the $\bar{n}$-collinear wavefunction renormalization graph. These are the same graphs that contribute to the matching condition at m_2, so T is given by R with $m_2 \to m_1$,[4] and is tabulated in Table 1.4.

The remaining quantities needed are the anomalous dimension γ_3 between m_1 and M,

[4] T depends on whether the particle being integrated out is a fermion or a scalar.

and the matching condition $\exp U$ at M. These can be computed from the graph in Fig. 1.10 evaluated on-shell, but now with the gauge boson mass M included. The graph gives

$$a\, wr(w) \left[-\frac{2}{\epsilon} + 2 \log \frac{M^2}{\mu^2} \right] , \tag{1.84}$$

where $w = v_2 \cdot v_1$ and

$$r(w) \;=\; \frac{\log\left(w + \sqrt{w^2-1}\right)}{\sqrt{w^2-1}} , \tag{1.85}$$

is the factor which occurs in the velocity-dependent anomalous dimension in HQET [39]. Including the heavy quark wavefunction correction, Eq. (1.79), gives the anomalous dimensions and matching coefficient listed in Table 1.4. In the high energy limit $Q^2 \sim 2 m_1 m_2 w$,

$$wr(w) \sim \log(2w) . \tag{1.86}$$

The terms which contribute to the final result are:

$$\begin{array}{ccccccc} C & \gamma_1 & R & \gamma_2 & T & \gamma_3 & U \\ Q & \longrightarrow & m_2 & \longrightarrow & m_1 & \longrightarrow & M \end{array} \tag{1.87}$$

1.7.3 $Q \gg m_2 = m_1 \gg M$

The third case we consider is where the two particles are degenerate, with $m_2 = m_1 = m$, and $Q \gg m \gg M$. This can be computed using the results already derived. The matching $\exp C$ at Q and the running γ_1 between Q and m is the same as in Table 1.1. The matching at m is given by switching both particles from SCET to HQET simultaneously. This is just the sum of the matching coefficients at m_2 and m_1 computed previously, so the matching condition is $\exp[R+T]$, with $m_1 = m_2 = m$, where R and T are given in Tables 1.3 and 1.4, respectively. The anomalous dimension between m and M, and the matching at M are given by γ_3 and U in Table 1.4.

The terms which contribute to the final result are:

$$\begin{array}{ccccc} C & \gamma_1 & R+T & \gamma_3 & U \\ Q & \longrightarrow & m_2 = m_1 & \longrightarrow & M \end{array} \tag{1.88}$$

1.7.4 $Q \gg m_2 \sim M \gg m_1$

It is also useful to derive results where the particle masses and gauge boson masses are not widely separated from each other. In this case, it is more important to include the full m/M dependence, rather than sum high order $\alpha \log m/M$ terms, which are no longer very large. In the standard model, this situation arises for the A, Z and t, which have masses which are not sufficiently widely separated that electroweak logarithms need to be summed. If two (or more) particle masses are not widely separated, one can make a transition to a new EFT by integrating

out both particles at a common scale μ, rather than integrating them out sequentially. The results for the various cases are summarized in this and the following subsections. The difference from previous results is that one has to include all the relevant masses in the particle propagators. For example, for the case studied in this subsection, $m_2 \sim M$, one also includes m_2 in the denominator of Eq. (1.35). The integrals now depend on a dimensionless parameter, the ratio of particle masses m_2^2/M^2.

If $Q \gg m_2 \sim M \gg m_1$, then the matching at Q and the running between Q and $m_2 \sim M$, remain unchanged, and are given by C and γ_1 in Table 1.1. At the scale μ of order $m_2 \sim M$, one integrates out the gauge boson, and switches to a theory in which particle 2 is described by a HQET field. In this matching, the n-collinear graph Eq. (1.35) with the analytic regulator is now

$$\begin{aligned} I_n &= -ig^2\mu^{2\epsilon} C_F c(\mu) \int \frac{\mathrm{d}^d k}{(2\pi)^d} \frac{1}{k^2 - M^2} \frac{\bar{n}\!\!\!/}{2} n^\alpha \\ &\times \frac{\bar{n}\!\!\!/}{2} \frac{(-\nu_2^2)^{\delta_2} \bar{n}\cdot(p_2 - k)}{\left[(p_2-k)^2 - m_2^2\right]^{1+\delta_2}} \gamma^\mu \frac{(-\nu_1^-)^{\delta_1}}{\left[-\bar{n}\cdot k\right]^{1+\delta_1}} \bar{n}_\alpha \ , \end{aligned} \tag{1.89}$$

and is evaluated at the on-shell point $p_2^2 = m_2^2$. The $\bar{n}$-collinear and ultrasoft integrals remain unchanged. We saw in Sec. 1.7.1 that the δ and ν dependence canceled between all the diagrams for the massless case. The cancellation must still hold when I_n is evaluated with $m_2 \neq 0$, so that $aC_F f_F(z) = I_n(m_2) - I_n(m_2 = 0)$, $z = m_2^2/M^2$ has a finite limit independent of the analytic regulator, as can be verified by explicit computation. The result for $f_F(z) = f_F(z, z)$ is given in Eq. (C.3). The wavefunction renormalization is also modified, and the shift $h_F(z)$ is given in Eq. (C.5). The matching condition D is given by $D(m_2) = D(m_2 = 0) + aC_F\left(f_F(z) - h_F(z)/2\right)$ if the particle integrated out is a heavy fermion, where the massless value $D(m_2 = 0)$ is given in Table 1.1. Similarly, if the particle integrated out is a heavy scalar, the matching D is $D(m_2) = D(m_2 = 0) + aC_F\left(f_S(z) - h_S(z)/2\right)$ where the scalar functions are given in Eqs. (C.14,C.16).

The theory below $m_2 \sim M$ is a theory in which particle 2 is described using a HQET field, and particle 1 by an SCET, with the massive gauge boson integrated out. In our toy example, this is a free theory.

Schematically, the terms are ($z = m_2^2/M^2$):

$$\begin{array}{cccc} C & \gamma_1 & D + aC_F(f(z) - h(z)/2) \\ Q & \longrightarrow & m_2 \sim M \end{array} \tag{1.90}$$

1.7.5 $Q \gg m_2 \gg M \sim m_1$

If $Q \gg m_2 \gg M \sim m_1$, the matching and running down to $M \sim m_1$ remains the same as in Sec. 1.7.1. In the theory at $M \sim m_1$, particle 2 is described by an HQET field, and particle 1 by a $\bar{n}$ collinear field. The matching condition at $M \sim m_1$ would be given by S if

$m_1 \to 0$. By the same arguments as above, the effect of m_1 is to modify the $\bar{n}$-collinear integral by a finite amount, so the matching is now $S + aC_F(f(z) - h(z)/2)$, with $z = m_1^2/M^2$, where f, h are the fermion or scalar values Eqs. (C.3,C.12) or Eqs. (C.14,C.16), depending on the type of particle 1.

Schematically, the terms are ($z = m_1^2/M^2$):

$$\begin{array}{cccccc} C & \gamma_1 & R & \gamma_2 & S + aC_F(f(z) - h(z)/2) \\ Q & \longrightarrow & m_2 & \longrightarrow & m_1 \sim M \end{array} \tag{1.91}$$

1.7.6 $Q \gg m_1 \sim m_2 \gg M$

The situation is similar to $Q \gg m_1 = m_2 \gg M$ considered in Sec. 1.7.3. The evolution down to $m_1 \sim m_2$ is the same as for $m_i = 0$. The n and $\bar{n}$ collinear graphs at the scale $m_1 \sim m_2$ are independent of each other, so the matching is given by $R(m_2) + T(m_1)$ given in Tables 1.3, 1.4. Below $m_1 \sim m_2$, the computation reduces to that in Sec. 1.7.3.

Schematically, the terms are:

$$\begin{array}{ccccccc} C & \gamma_1 & R + T & \gamma_3 & U \\ Q & \longrightarrow & m_1 \sim m_2 & \longrightarrow & M \end{array} \tag{1.92}$$

1.7.7 $Q \gg m_1 \sim m_2 \sim M$

The evolution to $\mu \sim m_1 \sim m_2 \sim M$ is the same as for the massless case. The matching at μ involves massive collinear propagators, each of which modifies the massless matching condition, so the matching is given by

$$\begin{aligned} D(m_1, m_2) &= D(m_1 = m_2 = 0) + aC_F\left(f_2(z_2) - h_2(z_2)/2\right) \\ &\quad + aC_F\left(f_1(z_1) - h_1(z_1)/2\right) \end{aligned} \tag{1.93}$$

where $z_i = m_i^2/M^2$, and $f_{1,2}$, $h_{1,2}$ are chosen to be $f_{F,S}$ and $h_{F,S}$ depending on whether the corresponding particle is a fermion or scalar. The massless value $D(m_1 = m_2 = 0)$ is given in Table 1.1.

Schematically, the terms are ($z_i = m_i^2/M^2$):

$$\begin{array}{cccc} C & \gamma_1 & D + aC_F(f(z_1) - h(z_1)/2) + aC_F(f(z_2) - h(z_2)/2) \\ Q & \longrightarrow & m_1 \sim m_2 \sim M \end{array} \tag{1.94}$$

1.8 Scalar corrections

In this section, we compute the scalar exchange corrections to the Sudakov form-factor. The graphs are the same as those for gauge exchange, with the gauge boson replaced by the scalar χ, with mass M_χ. As for gauge bosons, one needs to include both collinear and ultrasoft fields for χ to represent collinear and ultrasoft χ particles. In the gauge boson results we removed

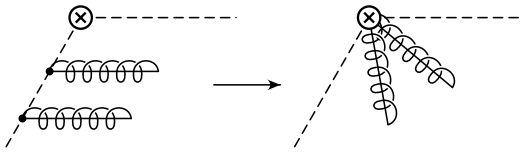

Figure 1.11: Graphs in which n-collinear gauge bosons couple to the $\bar{n}$-collinear line generate the Wilson line W_n.

an overall factor of $a = g^2/(16\pi^2)$. In the χ-exchange graphs, we remove a factor of $h_1 h_2/(16\pi^2)$, where $h_{1,2}$ are the Yukawa couplings at the two vertices. Note that the coupling of χ to scalars $h_{\phi,i}$ has dimensions of mass, so the factor removed for operators such as $\phi^\dagger\phi$ is dimensionful. Unlike for gauge interactions, the wavefunction and vertex corrections can have different coupling constants.

Collinear gauge bosons and matter fields in the operator $\mathcal{O}$ occur in the combination $W_n^\dagger \xi_{n,p}$ or $W_n^\dagger \Phi_{n,p}$. They arise from full theory graphs in which the gauge fields couple to the *other* particle, which moves in the $\bar{n}$-direction. The intermediate propagators are off-shell by order Q^2, and can be shrunk to a point, as shown in Fig. 1.11. Single gauge boson emission gives the vertex $g\bar{n}^\mu/(-\bar{n}\cdot k)$. At higher orders, multiple gauge boson emission from the $\bar{n}$ particle line combined with the non-Abelian multi-gluon interaction give the Wilson line operator W_n. Multi-gluon emission is related to single gluon emission by gauge invariance, and this relation holds even in the presence of loop-corrections. The Wilson line structure of the vertex W_n is required by collinear gauge invariance [18].

One has a similar construction for multiple n-collinear χ fields emitted from the $\bar{n}$ particle. At the level of single χ emission, the χ vertex is $h_{\psi,\phi}/(-\bar{n}\cdot k)$ instead of the gauge vertex $g\bar{n}^\mu/(-\bar{n}\cdot k)$. This is all we require for our computation. It would be interesting to work out the structure of the scalar vertex at higher orders, including radiative corrections. Multi-scalar emission is not related to the single scalar vertex by gauge invariance.

Most of the scalar corrections vanish. In SCET, the fermion Yukawa vertex vanishes, because Eq. (1.6) implies that

$$\bar{\xi}_{n,p}\xi_{n,p} \quad = \quad \bar{\xi}_{n,p}\frac{\bar{\not{n}}\not{n}}{4}\frac{\not{n}\bar{\not{n}}}{4}\xi_{n,p} = 0 \tag{1.95}$$

using $\not{n}\not{n} = n^2 = 0$. The tri-scalar couplings $\chi\phi^\dagger\phi$ have dimensions of mass, and χ exchange corrections to the scalar operators are suppressed by powers of h_ϕ/Q, which is subleading in the EFT power counting given our assumption that h_ϕ does not grow with Q. The easiest way to see this is to use the rescaled fields $\phi_{n,p}$, which have a propagator of the same form as that for fermions. The Yukawa coupling becomes

$$h_\phi\,\chi\phi^\dagger\phi \quad = \quad h_\phi\,\chi\Phi_{n,p}^\dagger\Phi_{n,p} = \frac{h_\phi}{\bar{n}\cdot p}\,\chi\phi_{n,p}^\dagger\phi_{n,p}\,, \tag{1.96}$$

Table 1.5: One-loop scalar exchange contribution to on-shell wavefunction renormalization. The exchanged scalar mass is M_χ, $\mathsf{L}_\chi = \log M_\chi^2/\mu^2$, and the particle (fermion or scalar) mass is m. $\tilde{h}_{F,S}$ are given in Appendix C. An overall factor of $h_1 h_2/(16\pi^2)$ is omitted.

Field	m	M_χ	
ψ	$m=0$	$M_\chi=0$	$\frac{1}{2\epsilon_{\rm UV}} - \frac{1}{2\epsilon_{\rm IR}}$
ψ	$m=0$	$M_\chi\neq 0$	$\frac{1}{2\epsilon_{\rm UV}} + \frac{1}{4} - \frac{1}{2}\mathsf{L}_\chi$
ψ	$m\neq 0$	$M_\chi=0$	$\frac{1}{2\epsilon_{\rm UV}} - \frac{2}{\epsilon_{\rm IR}} - \frac{7}{2} + \frac{3}{2}\mathsf{L}_m$
ψ	$m\neq 0$	$M_\chi\neq 0$	$\frac{1}{2\epsilon_{\rm UV}} + \frac{1}{4} - \frac{1}{2}\mathsf{L}_\chi + \tilde{h}_F(m^2/M_\chi^2)$
ϕ	$m=0$	$M_\chi=0$	0
ϕ	$m=0$	$M_\chi\neq 0$	$\frac{1}{2M_\chi^2}$
ϕ	$m\neq 0$	$M_\chi=0$	$\frac{1}{m^2}\left[-\frac{1}{2\epsilon_{\rm IR}} - 1 + \frac{1}{2}\mathsf{L}_m\right]$
ϕ	$m\neq 0$	$M_\chi\neq 0$	$\frac{1}{2M_\chi^2} + \frac{1}{M_\chi^2}\tilde{h}_S(m^2/M_\chi^2)$
h_v		$M_\chi=0$	$\frac{2}{\epsilon_{\rm UV}} - \frac{2}{\epsilon_{\rm IR}}$
h_v		$M_\chi\neq 0$	$\frac{2}{\epsilon_{\rm UV}} - 2\mathsf{L}_\chi$

which is order $1/Q$ since $\bar{n}\cdot p$ is order Q, and gives an explicit $1/Q$ suppression to the graph at each tri-scalar vertex.

One interesting point is the decoupling of scalars below m_1 and m_2, so that particles 1 and 2 can be treated as HQET fields. If one directly matches from the full theory onto HQET, then $h_\psi \chi \bar{\psi}\psi \to h_\psi \chi \bar{h}_v h_v$, which is non-zero. If instead, one first goes through SCET, then $h_\psi \chi \bar{\psi}\psi \to h_\psi \chi \bar{\xi}_{n,p}\xi_{n,p} = 0$, so we have an apparent contradiction. However, the two results are not in disagreement. The scalar HQET vertex graph (Fig. 1.10 with the gauge boson replaced by a scalar) is equal to $-1/w$ times the corresponding gauge graphs, rescaled by the ratio of the Yukawa couplings to the gauge couplings. In the Sudakov limit, $w \sim Q^2/(m_1 m_2)$, and $1/w$ is a power suppression which can be neglected, so both ways of matching agree, since power corrections are neglected.

The only scalar graphs which remain are the matching at Q, which are full theory graphs, and scalar contributions to wavefunction renormalization in the effective theories. The wavefunction contributions are summarized in Table 1.5, where $\mathsf{L}_\chi = \log M_\chi^2/\mu^2$. The full theory wavefunction renormalization vanishes for both fermions and scalars, so the entire matching correction at Q given in Eq. (1.97) arises from the vertex correction. The EFT matching and running can be computed from the scalar wavefunction graphs in Table 1.5. The EFT matrix elements are given by taking $-1/2$ times the entries in the table for each particle, multiplying

by $h^2/(16\pi^2)$, and then adding the contributions from the two particles. The finite part gives the matching correction, and (-2) times the coefficient of the $1/\epsilon_{\rm UV}$ term gives the anomalous dimension. Since only wavefunction graphs contribute, there are no L_Q terms which can only arise from vertex graphs.

The computation of scalar contributions to the anomalous dimension and matching for the various cases considered in Sec. 1.7 parallels the gauge boson discussion. The matching coefficients for $m_{1,2} \neq 0$ are given by a formula analogous to Eq. (1.93), with the gauge boson functions $f_{F,S}$ and $h_{F,S}$ replaced by the corresponding χ-exchange functions $f_{F,S} \to 0$, since there are no vertex corrections in the effective theory, and $h_{F,S} \to \tilde{h}_{F,S}$. The expression for these integrals is given in Eqs. (C.12) and (C.18)

We have divided the scalar exchange contributions into vertex and wavefunction pieces, rather than giving the total contribution as in the gauge case. The reason is that the standard model is a chiral gauge theory, and the Yukawa couplings connect one matter representation to another. Thus, vertex corrections can mix left-handed currents with right-handed currents, whereas wavefunction corrections do not mix different $SU(2) \times U(1)$ representations. Keeping the two contributions separate allows us to compute Higgs radiative corrections in the standard model using the the results given in this section.

The matching corrections C at Q can be computed as for the gauge boson case. The matching corrections for external scalar particles due to scalar χ exchange are power suppressed, and vanish to leading order. For fermions, the χ exchange corrections give

$$\begin{aligned}
\bar{\psi}\psi &\to \exp\left[a_Y\left(-2+\mathsf{L}_Q\right)\right][\bar{\xi}_{n,p_2}W_n][W_{\bar{n}}^\dagger\xi_{\bar{n},p_1}] \\
\bar{\psi}\gamma^\mu\psi &\to \exp\left[a_Y\left(\frac{1}{2}-\frac{1}{2}\mathsf{L}_Q\right)\right][\bar{\xi}_{n,p_2}W_n]\gamma^\mu[W_{\bar{n}}^\dagger\xi_{\bar{n},p_1}] \\
\bar{\psi}\sigma^{\mu\nu}\psi &\to \exp\left[a_Y\right]\Big\{[\bar{\xi}_{n,p_2}W_n]\sigma^{\mu\nu}[W_{\bar{n}}^\dagger\xi_{\bar{n},p_1}] \\
&\qquad -\frac{i}{2}\left(n^\mu\bar{n}^\nu-n^\nu\bar{n}^\mu\right)[\bar{\xi}_{n,p_2}W_n][W_{\bar{n}}^\dagger\xi_{\bar{n},p_1}]\Big\} \\
a_Y &= \frac{h_{\psi,1}h_{\psi,2}}{16\pi^2}
\end{aligned} \tag{1.97}$$

which have to be combined with the gauge boson matching conditions in Table 1.1. The vertex graph contributes $2a_Y$, $-a_Y$ and 0, respectively, to the anomalous dimensions of the three operators in the full theory. The wavefunction graphs contribute an additional a_Y to all three operators.

1.9 Application to the Standard Model

The results we have obtained for the toy theory can now be used to compute results for the standard model. One has to be careful in using the correct coupling constants, since the standard model is a chiral gauge theory, and the toy model is vector-like.

For the LHC, one is interested in processes such as dijet production. The SCET operators at the high scale Q involve more than two SCET fields. E.g. in $q\bar{q} \to q\bar{q}$, the EFT operator has four fields, two for the incoming particle and two for the outgoing ones. One can obtain results for more than two external particles by combining the two-particle results computed in this chapter with the appropriate gauge theory factors such as C_A and C_F. There are several interesting features of the analysis which are independent of the calculations presented in this chapter, so we defer the discussion of experimentally relevant examples to a subsequent publication [23]. Here we show how our results can be used to compute the radiative corrections to quark production by a gauge invariant current $\bar{Q}_i \gamma^\mu P_L Q_i$, where Q_i is the quark doublet[5] for generation $i = u, c, t$, and to charged lepton production by $\bar{L}\gamma^\mu P_L L$. We will do the computations for light quarks in Sec. 1.9.1, for leptons in Sec. 1.9.2, and for top quarks in Sec. 1.9.3. All fermion masses other than the top quark mass are neglected.

1.9.1 Light Quarks

The first generation quark doublet is

$$Q_u \;=\; \begin{pmatrix} u \\ d' \end{pmatrix} = \begin{pmatrix} u \\ V_{ud} d + V_{us} s + V_{ub} b \end{pmatrix}, \tag{1.98}$$

using the mass eigenstate basis. At the scale $Q \gg m_q$ the coefficient of the operator in the full electroweak theory is assumed to be unity. For the first generation, all quark masses and Yukawa couplings can be neglected, and so the answer is given by combining the gauge boson contributions computed earlier.

The operator in SCET at the scale Q is

$$\bar{Q}_u \gamma^\mu P_L Q_u \;\to\; c(Q) [\bar{\xi}^{(Q_u)}_{n,p_2} W_n] \gamma^\mu P_L [W^\dagger_{\bar{n}} \xi^{(Q_u)}_{\bar{n},p_1}], \tag{1.99}$$

where $\xi^{(Q_u)}$represents the left-handed electroweak u-quark doublet Eq. (1.98) in SCET, and we have suppressed gauge indices. The matching condition is

$$\log c(Q) \;=\; \left[\frac{\alpha_s(Q)}{4\pi}\frac{4}{3} + \frac{\alpha_2(Q)}{4\pi}\frac{3}{4} + \frac{\alpha_1(Q)}{4\pi}\frac{1}{36}\right]\left[\frac{\pi^2}{6} - 8\right], \tag{1.100}$$

using the third column of Table 1.1 with $\mathsf{L}_Q = 0$ at the scale $\mu = Q$. The gauge couplings have been multiplied by the corresponding C_F values: 4/3 for an $SU(3)$ triplet, 3/4 for an $SU(2)$ doublet, and 1/36 for $Y = 1/6$. The electroweak couplings renormalized at $\mu = M_Z$ are

$$\begin{aligned} \alpha_2(M_Z) &= \frac{\alpha_{\rm em}(M_Z)}{\sin^2\theta_W(M_Z)}, \\ \alpha_1(M_Z) &= \frac{\alpha_{\rm em}(M_Z)}{\cos^2\theta_W(M_Z)}, \end{aligned} \tag{1.101}$$

and their values at Q are obtained by the usual β-functions of the standard model.

[5] Not to be confused with Q, the momentum transfer.

The theory below Q is SCET with an $SU(3) \times SU(2) \times U(1)$ gauge symmetry. In this regime, the SCET current in Eq. (1.99) is multiplicatively renormalized with anomalous dimension (from the fourth column in Table 1.1)

$$\gamma(\mu) \;=\; \left[\frac{\alpha_s(\mu)}{4\pi}\frac{4}{3} + \frac{\alpha_2(\mu)}{4\pi}\frac{3}{4} + \frac{\alpha_1(\mu)}{4\pi}\frac{1}{36}\right][4\mathsf{L}_Q - 6] \;. \tag{1.102}$$

The anomalous dimension γ is used to run c down to a scale of order the gauge boson mass. One can integrate out the weak gauge bosons sequentially, by first integrating out the Z boson at $\mu = M_Z$, followed by the A at $\mu = M_W$. This sums $\left(\alpha \log^2 M_W/M_Z\right)^n$, $n > 1$ terms, while neglecting $\alpha\,(M_W/M_Z)^n$, $n > 0$ power corrections. This is not a good choice to use for the standard model, since M_W/M_Z is not very small, and summing powers of M_W/M_Z is more important than summing $\alpha \log^2 M_W/M_Z$ terms. Instead, we integrate out the A and Z at a common scale, chosen to be $\mu = M_Z$. In this way, we match directly from an $SU(3)\times SU(2)\times U(1)$ gauge theory onto a $SU(3) \times U(1)_{\rm em}$ gauge theory of gluons and photons, and there are no complications of an intermediate stage of broken electroweak symmetry where the Z is integrated out, but not the A.

At the scale $\mu = M_Z$, integrating out the A and Z bosons give a matching correction to the SCET operator,

$$\begin{aligned}[\bar{\xi}^{(Q_u)}_{n,p_2} W_n]\gamma^\mu P_L [W^\dagger_{\bar{n}} \xi^{(Q_u)}_{\bar{n},p_1}] \quad &\to \quad a^{(u)} [\bar{\xi}^{(u)}_{n,p_2} W_n]\gamma^\mu P_L [W^\dagger_{\bar{n}} \xi^{(u)}_{\bar{n},p_1}] \\ &+ a^{(d')} [\bar{\xi}^{(d')}_{n,p_2} W_n]\gamma^\mu P_L [W^\dagger_{\bar{n}} \xi^{(d')}_{\bar{n},p_1}] \,. \end{aligned} \tag{1.103}$$

Since the electroweak symmetry is broken, the u and d' parts of the operator get different matching corrections. The corrections a_i are obtained using the last column of Table 1.1:

$$\begin{aligned}
\log a^{(u)}(M_Z) \;&=\; \frac{\alpha_{\rm em}}{4\pi \sin^2\theta_W \cos^2\theta_W}\left(\frac{1}{2} - \frac{2}{3}\sin^2\theta_W\right)^2 \left[\frac{9}{2} - \frac{5\pi^2}{6}\right] \\
&\quad + \frac{\alpha_{\rm em}}{4\pi \sin^2\theta_W}\left(\frac{1}{2}\right)\left[-\log^2\frac{M_W^2}{M_Z^2} + 2\log\frac{M_W^2}{M_Z^2}\log\frac{Q^2}{M_Z^2} - 3\log\frac{M_W^2}{M_Z^2} + \frac{9}{2} - \frac{5\pi^2}{6}\right], \\
\log a^{(d')}(M_Z) \;&=\; \frac{\alpha_{\rm em}}{4\pi \sin^2\theta_W \cos^2\theta_W}\left(-\frac{1}{2} + \frac{1}{3}\sin^2\theta_W\right)^2 \left[\frac{9}{2} - \frac{5\pi^2}{6}\right] \\
&\quad + \frac{\alpha_{\rm em}}{4\pi \sin^2\theta_W}\left(\frac{1}{2}\right)\left[-\log^2\frac{M_W^2}{M_Z^2} + 2\log\frac{M_W^2}{M_Z^2}\log\frac{Q^2}{M_Z^2} - 3\log\frac{M_W^2}{M_Z^2} + \frac{9}{2} - \frac{5\pi^2}{6}\right].
\end{aligned} \tag{1.104}$$

The first term for $\log a^{(u,d')}$ is the Z contribution, the second term is the A contribution, and the coupling constants are renormalized at M_Z.

Below M_Z, the operators in Eq. (1.103) are multiplicatively renormalized, with anoma-

lous dimensions

$$\begin{aligned}\gamma^{(u)} &= \left[\frac{\alpha_s(\mu)}{4\pi}\frac{4}{3}+\frac{\alpha_{\rm em}(\mu)}{4\pi}\frac{4}{9}\right][4\mathsf{L}_Q-6]\,,\\ \gamma^{(d')} &= \left[\frac{\alpha_s(\mu)}{4\pi}\frac{4}{3}+\frac{\alpha_{\rm em}(\mu)}{4\pi}\frac{1}{9}\right][4\mathsf{L}_Q-6]\,,\end{aligned} \tag{1.105}$$

for the u and d' terms.

The final result for the operator at a low scale is

$$\begin{aligned}\bar{Q}_u\gamma^\mu P_L Q_u \;&\to\; c^{(u)}[\bar{\xi}^{(u)}_{n,p_2}W_n]\gamma^\mu P_L[W_{\bar{n}}^\dagger\xi^{(u)}_{\bar{n},p_1}]\\ &+c^{(d')}[\bar{\xi}^{(d')}_{n,p_2}W_n]\gamma^\mu P_L[W_{\bar{n}}^\dagger\xi^{(d')}_{\bar{n},p_1}]\,,\end{aligned} \tag{1.106}$$

with

$$\begin{aligned}\log c^{(u)}(\mu) &= \log c(Q)+\int_Q^{M_Z}\frac{\mathrm{d}\mu}{\mu}\gamma(\mu)+\log a^{(u)}+\int_{M_Z}^{\mu}\frac{\mathrm{d}\mu}{\mu}\gamma^{(u)}(\mu)\,,\\ \log c^{(d')}(\mu) &= \log c(Q)+\int_Q^{M_Z}\frac{\mathrm{d}\mu}{\mu}\gamma(\mu)+\log a^{(d')}+\int_{M_Z}^{\mu}\frac{\mathrm{d}\mu}{\mu}\gamma^{(d')}(\mu)\,,\end{aligned} \tag{1.107}$$

where the various pieces are given in Eqs. (1.100,1.102,1.104,1.105). The EFT operator Eq. (1.106) can then be used to compute processes such as dijet production using SCET [42]. For jet production, the scale μ would be chosen to be of order the jet invariant mass, around 30 GeV for jets at the LHC.

1.9.2 Leptons

The computation for the radiative corrections to the lepton current $\bar{L}\gamma^\mu P_L L$, where L is the lepton doublet

$$L = \begin{pmatrix}\nu\\ \ell\end{pmatrix}, \tag{1.108}$$

is similar to that for the quark doublet, and we summarize the final result. The full theory operator at the low scale μ is

$$\bar{L}\gamma^\mu P_L L \;\to\; c^{(\nu)}[\bar{\xi}^{(\nu)}_{n,p_2}W_n]\gamma^\mu P_L[W_{\bar{n}}^\dagger\xi^{(\nu)}_{\bar{n},p_1}]+c^{(\ell)}[\bar{\xi}^{(\ell)}_{n,p_2}W_n]\gamma^\mu P_L[W_{\bar{n}}^\dagger\xi^{(\ell)}_{\bar{n},p_1}]\,, \tag{1.109}$$

with the coefficients given by Eq. (1.107) with $u\to\nu$, $d'\to\ell$, where the terms on the rhs of Eq. (1.107) for leptons are:

$$\begin{aligned}\log c(Q) &= \left[\frac{\alpha_2(Q)}{4\pi}\frac{3}{4}+\frac{\alpha_1(Q)}{4\pi}\frac{1}{4}\right]\left[\frac{\pi^2}{6}-8\right],\\ \gamma(\mu) &= \left[\frac{\alpha_2(\mu)}{4\pi}\frac{3}{4}+\frac{\alpha_1(\mu)}{4\pi}\frac{1}{4}\right][4\mathsf{L}_Q-6]\,,\\ \gamma^{(\nu)} &= 0\,,\\ \gamma^{(\ell)} &= \frac{\alpha_{\rm em}(\mu)}{4\pi}[4\mathsf{L}_Q-6]\,,\end{aligned} \tag{1.110}$$

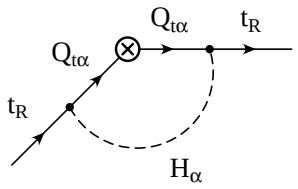

Figure 1.12: Higgs correction which causes $\bar{Q}_t\gamma^\mu P_L Q_t$ to mix with $\bar{t}_R\gamma^\mu P_R t$. The index α is an $SU(2)$ index, and is summed over.

$$\begin{aligned}
\log a^{(\nu)}(M_Z) &= \frac{\alpha_{\rm em}}{4\pi\sin^2\theta_W\cos^2\theta_W}\left(\frac{1}{2}\right)^2\left[\frac{9}{2}-\frac{5\pi^2}{6}\right] \\
&\quad+\frac{\alpha_{\rm em}}{4\pi\sin^2\theta_W}\left(\frac{1}{2}\right)\left[-\log^2\frac{M_W^2}{M_Z^2}+2\log\frac{M_W^2}{M_Z^2}\log\frac{Q^2}{M_Z^2}-3\log\frac{M_W^2}{M_Z^2}+\frac{9}{2}-\frac{5\pi^2}{6}\right], \\
\log a^{(\ell)}(M_Z) &= \frac{\alpha_{\rm em}}{4\pi\sin^2\theta_W\cos^2\theta_W}\left(-\frac{1}{2}+\sin^2\theta_W\right)^2\left[\frac{9}{2}-\frac{5\pi^2}{6}\right] \\
&\quad+\frac{\alpha_{\rm em}}{4\pi\sin^2\theta_W}\left(\frac{1}{2}\right)\left[-\log^2\frac{M_W^2}{M_Z^2}+2\log\frac{M_W^2}{M_Z^2}\log\frac{Q^2}{M_Z^2}-3\log\frac{M_W^2}{M_Z^2}+\frac{9}{2}-\frac{5\pi^2}{6}\right].
\end{aligned} \tag{1.111}$$

1.9.3 Top Quarks

In this subsection, we show how our results can be used to compute the radiative corrections to $t\bar{t}$ production by a gauge invariant vector current $\bar{Q}_t\gamma^\mu P_L Q_t$, where Q_t is the left-handed quark doublet in the standard model,

$$Q_t \;=\; \begin{pmatrix} t \\ b' \end{pmatrix} = \begin{pmatrix} t \\ V_{td}d+V_{ts}s+V_{tb}b \end{pmatrix}, \tag{1.112}$$

and $b' = V_{td}d+V_{ts}s+V_{tb}b$ using the mass eigenstate basis. We will neglect all quark masses other than m_t. This example illustrates how to use the fermion mass and Higgs exchange contributions computed in the toy example.

The operator in SCET at the scale Q is

$$\bar{Q}_t\gamma^\mu P_L Q_t \;\;\to\;\; c_1(Q)[\bar{\xi}^{(Q_t)}_{n,p_2}W_n]\gamma^\mu P_L[W^\dagger_{\bar{n}}\xi^{(Q_t)}_{\bar{n},p_1}] + c_2(Q)[\bar{\xi}^{(t)}_{n,p_2}W_n]\gamma^\mu P_R[W^\dagger_{\bar{n}}\xi^{(t)}_{\bar{n},p_1}], \tag{1.113}$$

where $\xi^{(Q_t)}$ and $\xi^{(t)}$ represent the left-handed electroweak t-quark doublet Eq. (1.112) and the right-handed t-quark singlet t_R in SCET and we have suppressed gauge indices. The t_R terms arise from Higgs exchange graphs Fig. 1.12.

The matching condition is

$$\begin{aligned} \log c_1(Q) &= \left[\frac{\alpha_s(Q)}{4\pi}\frac{4}{3} + \frac{\alpha_2(Q)}{4\pi}\frac{3}{4} + \frac{\alpha_1(Q)}{4\pi}\frac{1}{36}\right]\left[\frac{\pi^2}{6} - 8\right], \\ c_2(Q) &= \left[2\frac{g_t^2(Q)}{16\pi^2}\right]\left[\frac{1}{2}\right], \end{aligned} \tag{1.114}$$

using Tables 1.1 and Eq. (1.97) with $\mathsf{L}_Q = 0$ at the scale $\mu = Q$. The gauge couplings have been multiplied by the corresponding C_F values, 4/3 for an $SU(3)$ triplet, 3/4 for an $SU(2)$ doublet, and 1/36 for $Y = 1/6$. The top quark Yukawa coupling is normalized so that $g_t = \sqrt{2}m_t/v$, with $v \sim 247$ GeV. The Higgs exchange graph in the chiral standard model has been computed using the toy-model value Eq. (1.97) for a vector-like theory, combined with the result that a Yukawa vertex flips the fermion chirality. The factor of 2 in front of $g_t^2/(16\pi^2)$ arises from summing over a closed $SU(2)$ index loop, i.e. because the Higgs and Q are $SU(2)$ doublets (the sum on α in Fig. 1.12). The factor of 1/2 in square brackets is the coefficient of a_Y in the second line of Eq. (1.97), with $\mathsf{L}_Q \to 0$ at $\mu = Q$. The Higgs exchange vertex correction mixes the Q_L operator with the t_R operator. Higgs exchange corrections do not contribute to the diagonal coefficient c_1, since the first row of Table 1.5 shows that the full theory wavefunction renormalization has no finite part.

The theory below Q is SCET with an $SU(3) \times SU(2) \times U(1)$ gauge symmetry. In this regime, the two operators in Eq. (1.113) are multiplicatively renormalized with anomalous dimensions

$$\begin{aligned} \mu\frac{\mathrm{d}c_1}{\mathrm{d}\mu} &= \left\{\left[\frac{\alpha_s(\mu)}{4\pi}\frac{4}{3} + \frac{\alpha_2(\mu)}{4\pi}\frac{3}{4} + \frac{\alpha_1(\mu)}{4\pi}\frac{1}{36}\right][4\mathsf{L}_Q - 6] + \frac{g_t^2(Q)}{16\pi^2}\right\}c_1\,, \\ \mu\frac{\mathrm{d}c_2}{\mathrm{d}\mu} &= \left\{\left[\frac{\alpha_s(\mu)}{4\pi}\frac{4}{3} + \frac{\alpha_1(\mu)}{4\pi}\frac{4}{9}\right][4\mathsf{L}_Q - 6] + 2\frac{g_t^2(Q)}{16\pi^2}\right\}c_2\,. \end{aligned} \tag{1.115}$$

The t_L wavefunction factor due to Higgs exchange does not have the factor of two from the $SU(2)$ index summation that is present for t_R. The Higgs vertex graph, which causes $c_1 - c_2$ mixing, is $1/Q^2$ suppressed.

The anomalous dimension γ is used to run $c_{1,2}$ down to a scale of order m_t. At this scale there are several different methods one can use. As for massless quarks, one can integrate out the scales m_t, M_W, M_Z and M_H in various ways, e.g. one can integrate out each particle at a scale μ equal to its mass, or integrate out one or more particles simultaneously at some common value of μ. Integrating out the top quark leads to a complicated effective theory with dynamical A and Z bosons which is no longer $SU(2) \times U(1)$ invariant, since the b' quark is in the theory but not t. Luckily, the best method for experimentally relevant computations is also the simplest to use: since m_t, M_W, M_Z, and presumably M_H are not widely separated, one can integrate them all out together. In this way, one goes directly from an $SU(3) \times SU(2) \times U(1)$ invariant theory to a $SU(3) \times U(1)_{\mathrm{em}}$ gauge theory, with broken $SU(2) \times U(1)$ symmetry and no electroweak gauge bosons. This procedure keeps the entire mass dependence on the four mass scales.

At the scale $\mu = m_t$ the t-quark SCET field is replaced by the heavy quark field t_v, whereas the b' quark SCET field in the doublet $\xi^{(Q_t)}$ remains an SCET field $\xi^{(b')}$. The operator matching is

$$\begin{aligned}
[\bar{\xi}^{(Q_t)}_{n,p_2} W_n]\gamma^\mu P_L [W^\dagger_{\bar{n}} \xi^{(Q_t)}_{\bar{n},p_1}] &\to \frac{1}{2} a_1 \bar{t}_{v_2} t_{v_1} + a_2 [\bar{\xi}^{(b')}_{n,p_2} W_n]\gamma^\mu P_L [W^\dagger_{\bar{n}} \xi^{(b')}_{\bar{n},p_1}]\,, \\
[\bar{\xi}^{(t)}_{n,p_2} W_n]\gamma^\mu P_R [W^\dagger_{\bar{n}} \xi^{(t)}_{\bar{n},p_1}] &\to \frac{1}{2} a_3 \bar{t}_{v_2} t_{v_1}\,,
\end{aligned} \tag{1.116}$$

where the matching coefficients are denoted $a_{1,2,3}$. Using the result of Sec. 1.7.7 for the gauge boson exchange graphs, and Sec. 1.8 for the Higgs exchange graphs gives

$$\begin{aligned}
F_g(Q,M,m) &= -\log^2\frac{M^2}{m^2} + 2\log\frac{M^2}{m^2}\log\frac{Q^2}{m^2} - 3\log\frac{M^2}{m^2} + \frac{9}{2} - \frac{5\pi^2}{6} \\
F_h(M^2,\mu^2) &= \frac{1}{4} - \frac{1}{2}\mathsf{L}_M
\end{aligned} \tag{1.117}$$

$$\begin{aligned}
\log a_1(m_t) &= \frac{\alpha_{\rm em}}{4\pi\sin^2\theta_W\cos^2\theta_W}\big[g^2_{Lt}F_g(Q,M_Z,m_t) + 2U_1\big] \\
&\quad + \frac{\alpha_{\rm em}}{4\pi\sin^2\theta_W}\left(\frac{1}{2}\right)[F_g(Q,M_W,m_t) + 2W_1] \\
&\quad + \left(\frac{\alpha_s}{4\pi}\frac{4}{3} + \frac{\alpha_{\rm em}}{4\pi}\frac{4}{9}\right)\left(\frac{\pi^2}{6} + 4\right) + 2H(t_L), \\
\log a_2(m_t) &= \frac{\alpha_{\rm em}}{4\pi\sin^2\theta_W\cos^2\theta_W} g^2_{Lb} F_g(Q,M_Z,m_t) \\
&\quad + \frac{\alpha_{\rm em}}{4\pi\sin^2\theta_W}\left(\frac{1}{2}\right)[F_g(Q,M_W,m_t) + 2W_2] + 2H(b'_L), \\
\log a_3(m_t) &= \frac{\alpha_{\rm em}}{4\pi\sin^2\theta_W\cos^2\theta_W}\big[g^2_{Rt}F_g(Q,M_Z,m_t) \\
&\quad + 2U_2\big] + \frac{\alpha_{\rm em}}{4\pi\sin^2\theta_W}\left(\frac{1}{2}\right)[-c(w_t,0)] \\
&\quad + \left(\frac{\alpha_s}{4\pi}\frac{4}{3} + \frac{\alpha_{\rm em}}{4\pi}\frac{4}{9}\right)\left(\frac{\pi^2}{6} + 4\right) + 2H(t_R),
\end{aligned} \tag{1.118}$$

where,

$$\begin{aligned}
H(t_L) &= -\frac{1}{2}\frac{y_t^2}{16\pi^2}\big[\frac{1}{2}F_h(M_H^2,m_t^2) + \frac{1}{2}F_h(M_Z^2,m_t^2) \\
&\quad + \frac{1}{2}\tilde{a}(h_t,h_t) + \frac{1}{2}\tilde{a}(z_t,z_t) + \tilde{c}(h_t,h_t) + \tilde{c}(z_t,z_t) \\
&\quad + \tilde{c}(w_t,0) - \tilde{b}(h_t,h_t) + \tilde{b}(z_t,z_t)\big], \\
H(t_R) &= H(t_L) - \frac{1}{2}\frac{y_t^2}{16\pi^2}\left(F_h(M_W^2,m_t^2) + \tilde{a}(w_t,0)\right), \\
H(b'_L) &= -\frac{1}{2}\frac{y_t^2}{16\pi^2}\big[F_h(M_W^2,m_t^2) + \tilde{a}(0,w_t)\big], \\
h_t &= \frac{m_t^2}{M_H^2},\ w_t = \frac{m_t^2}{M_W^2},\ z_t = \frac{m_t^2}{M_Z^2}
\end{aligned} \tag{1.119}$$

and

$$\begin{aligned}
W_1 &= f_F(w_t,0) - \frac{1}{2}a(w_t,0) - \frac{1}{2}c(w_t,0), \\
W_2 &= f_F(0,w_t) - \frac{1}{2}a(0,w_t), \\
U_1 &= g_{Lt}^2 f_F(z_t,z_t) - \frac{1}{2}g_{Lt}^2 a(z_t,z_t), \\
&\quad -\frac{1}{2}\left(g_{Lt}^2+g_{Rt}^2\right)c(z_t,z_t) + g_{Lt}g_{Rt}b(z_t,z_t) \\
U_2 &= g_{Rt}^2 f_F(z_t,z_t) - \frac{1}{2}g_{Rt}^2 a(z_t,z_t), \\
&\quad -\frac{1}{2}\left(g_{Lt}^2+g_{Rt}^2\right)c(z_t,z_t) + g_{Lt}g_{Rt}b(z_t,z_t).
\end{aligned} \tag{1.120}$$

The functions f_F, a, b and c are tabulated in Appendix C.

All running couplings are renormalized at $\mu = m_t$. The expressions are given by adding the contributions due to the Z ($F_g(Q,M_Z,m_t)$ term), A ($F_g(Q,M_W,m_t)$ term), gluon, γ, H ($F_h(M_H,m_t)$ term), h^0 ($F_h(M_Z,m_t)$ term) and h^+ ($F_h(M_W,m_t)$ term), where h^0, h^+ are the unphysical Higgs scalars present in $R_{\xi=1}$ gauge. The gluon and photon corrections arise because one is making a transition from a theory in which the top quark is represented by a SCET field to one in which it is represented by an HQET field (see Sec. 1.7.3).

Below $\mu = m_t$, the $\bar{t}_{v_2}t_{v_1}$ operator has anomalous dimension (from the third column of Table 1.4)

$$\gamma_3 = \left[\frac{\alpha_s}{4\pi}\frac{4}{3} + \frac{\alpha_{\rm em}}{4\pi}\frac{4}{9}\right]4\left[wr(w)-1\right] \tag{1.121}$$

where $w = v_2\cdot v_1 = 1 + Q^2/(2m_t^2)$.

The radiative corrections to the $\bar{t}t$ operator can then be combined with known methods to obtain t-quark decay distributions [20]. The QCD corrections (the α_s terms) have already been included in the analysis of Ref. [20]. The new results in this chapter are the additional electroweak radiative corrections, including Higgs effects.

1.10 Numerics and Final Remarks

We have shown how SCET methods can be used to compute the radiative corrections to electroweak processes. We discussed the results for massless external particles given in Ref. [21] in more detail, and derived the result that there is at most a single power of L_Q in the matching at M to all orders in perturbation theory. The existence of L_Q terms in the matching at M is a new feature of SCET with massive gauge bosons. The results of Ref. [21] have been extended to include external particle masses and radiative Higgs exchange corrections proportional to the Yukawa couplings.

Most of the chapter used the vector-like $SU(2)$ gauge theory. Section 1.9 explained in detail how the results for the vector-like theory could be used to compute radiative corrections in the standard model, which is a chiral gauge theory. In this chapter, we have computed radiative corrections to operators with two external particles. These can be used to compute the production rate for two external particles by a gauge invariant bilinear source. This could be applied to the decay rate of a (hypothetical) gauge singlet particle into two fermions. SCET methods can also be used to compute the radiative corrections to the dominant high-energy processes observable at the LHC, such as dijet production from quark-quark scattering. For a partonic process such as $qq \to qq$, the EFT operator is a four-quark operator, and the radiative corrections can be obtained by using the results of this chapter, summed over all pairs of particles. The anomalous dimensions are about twice as big as the ones for the two-quark operators considered here. This discussion is given in a subsequent publication [23].

We conclude by giving some plots which show the typical size of the radiative corrections. The LHC center of mass energy is $\sqrt{s} = 14$ TeV. The partonic center of mass energy $\sqrt{\hat{s}}$ is much lower, because a proton with energy E has partons with energy fraction $x \leq 1$, given by a parton distribution $f(x)$ which vanishes as $x \to 1$. The bulk of the dijet cross-section is at low $\hat{s}$, but the LHC has sufficient luminosity to be able to observe the dijet cross-section up to $\sqrt{\hat{s}}$ of order several TeV. We plot the Sudakov form factor for electron production via $\bar{L}\gamma^\mu P_L L$, u-quark production via $\bar{Q}_u \gamma^\mu P_L Q_u$ and t-quark production via $\bar{Q}_t \gamma^\mu P_L Q_t$, which are the results given in Sec. 1.9, for $\sqrt{\hat{s}}$ between 0.25 and 8 TeV. Figure 1.13 gives the results for $F_E(Q^2)$ for the three cases, stopping the evolution at $\mu = M_Z$. In Fig. 1.14, the EFT operators have been evolved all the way down to $\mu = 30$ GeV, the typical invariant mass used to define a jet at the LHC. In both these figures, the quark form-factors also include QCD radiative corrections. Figure 1.15 shows the electroweak contributions to the three form-factors as a percentage change relative to the form factor including only the QCD radiative corrections. We have used a Higgs mass of 200 GeV in the plots. Varying the Higgs mass between 150 GeV and 500 GeV makes a difference of less than 0.5%. F_E is normalized to unity in the absence of radiative corrections. Radiative corrections for electrons are about 7% at 2 TeV, and $\mu = M_Z$, increasing to about 8% for $\mu = 30$ GeV due to the QED running below M_Z. The corrections for quarks are much larger, 15% for the t-quark, and 30% for the u-quark at $\mu = M_Z$, increasing to 40% and 50%, respectively, at $\mu = 30$ GeV. There is also a significant difference between the results for t- and u-quarks, arising from power corrections which depend on $m_t/M_{W,Z}$ and Higgs corrections which depend on the Yukawa coupling g_t. The bulk of the difference is due to the power corrections, the g_t terms are less than 1%.[6] The corrections for the four-quark operators needed for realistic processes are bigger, with corrections even to color singlet processes being greater than 20%. The radiative corrections are large enough that resummation is necessary to get an accurate prediction for the partonic cross-sections. We have shown how one can perform the resummation using EFT methods. Previous

[6] Note that the Higgs corrections do not have the L_Q enhancement that is present for the gauge bosons.

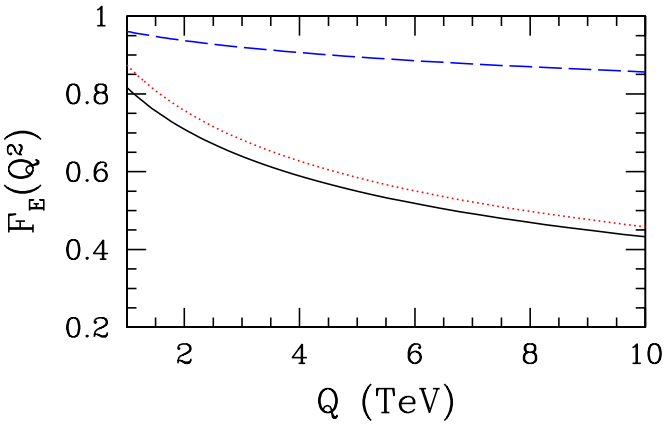

Figure 1.13: The Sudakov form-factor for u-quarks (solid black), t-quarks (dotted red) and electrons (dashed blue) at $\mu = M_Z$ for $m_H = 200$ GeV. Note that the quark form-factors include QCD corrections.

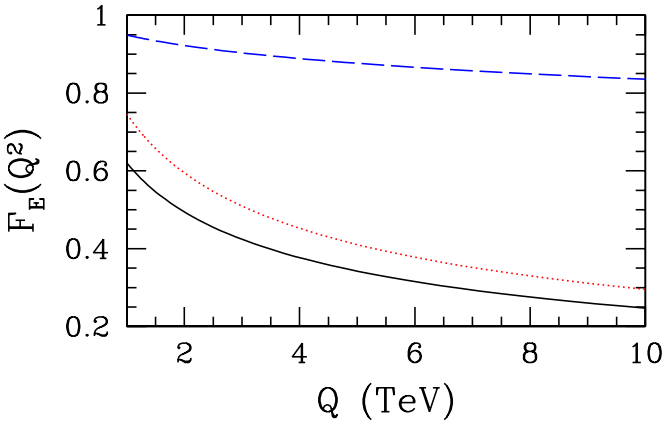

Figure 1.14: The Sudakov form-factor for u-quarks (solid black), t-quarks (dotted red) and electrons (dashed blue) at $\mu = 30$ GeV for $m_H = 200$ GeV. Note that the quark form-factors include QCD corrections.

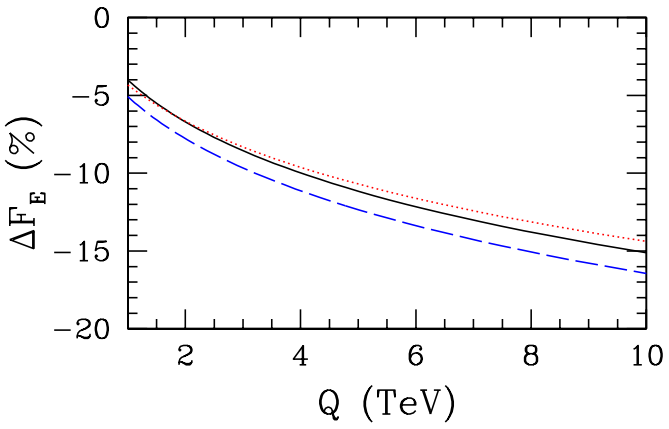

Figure 1.15: The electroweak contribution to the Sudakov form-factor (as a percentage change) for u-quarks (solid black), t-quarks (dotted red) and electrons (dashed blue) at $\mu = 30$ GeV for $m_H = 200$ GeV.

computations [2, 3, 4, 5, 6, 7, 8, 9, 10, 11, 12, 13, 14, 15] have done the resummation using infrared evolution equations [3]. The EFT method allows one to include mass effects as well as Higgs corrections in a systematic way, which have not been included previously. It also handles the cross-over between the $SU(3) \times SU(2) \times U(1)$ and the $SU(3) \times U(1)$ gauge theories above and below the weak interaction symmetry breaking scale, including the effects of unequal A and Z masses. The infrared evolution method uses a conjectured form for this cross-over with equal A and Z masses. The extension of previous results to massive external particles is currently being studied by other groups using a method-of-regions analysis [43].

Partial text of chapter 1 is extracted from J. y. Chiu, F. Golf, R. Kelley and A. V. Manohar, "Electroweak Corrections in High Energy Processes using Effective Field Theory," Phys. Rev. D 77, 053004 (2008).

Chapter 2

The role of zero-bin subtractions.

Applications of SCET to electroweak processes require evaluating collinear and soft Feynman graphs with massive gauge bosons. These graphs are not well defined, even in dimensional regularization with an off-shellness, and require additional regularization. In the first chapter and in Refs. [21, 22, 23], the graphs were evaluated with an analytic regulator [34, 35]; the individual diagrams depend on the analytic regulator parameters, but the total amplitude is regulator independent. The analytic regulator has some unpleasant properties with regards to gauge invariance and factorization, two essential ingredients of SCET. In this chapter we introduce a convenient new regulator, called the Δ-regulator, which can be implemented directly on the level of the SCET Lagrangian without the need to define further prescriptions for computing diagrams. This regulator is similar to using a mass, and unlike off-shellness, it regulates diagrams with massive gauge bosons.

The Δ-regulator is used in this chapter to compute the Sudakov form factor using SCET for a spontaneously broken $SU(2)$ gauge theory with a common gauge boson mass M. We discuss the factorization structure of the effective theory using the Δ-regulator. As noted previously [25, 44] in the framework of QCD, the amplitudes only factorize when the collinear sectors are defined including zero-bin subtractions, to avoid double-counting the soft momentum region. We show in the broken $SU(2)$ gauge theory that the usual construction of collinear gauge interactions into collinear Wilson lines, while true at tree level, is valid at the loop-level only when the collinear sector is defined with zero-bin subtractions.

Recently Idilbi and Mehen [45, 46] reemphasized the necessity for zero-bin subtractions. They studied deep inelastic scattering and showed that the correct total amplitude has the form $I_n + I_{\bar{n}} - I_s$, the sum of the n-collinear, $\bar{n}$-collinear, *minus* the soft contributions, rather than the naive expectation $I_n + I_{\bar{n}} + I_s$. The sign change of I_s arises because the collinear contributions have to be properly thought of as zero-bin subtracted, $I_n \to I_n - I_s$. This converts the second (incorrect) form of the result into the first. In the case of deep inelastic scattering the effective

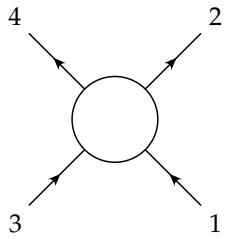

Figure 2.1: A scattering amplitude with four external particles defining four collinear directions n_1, n_2, n_3, and n_4.

theory graphs are scaleless, and so vanish in dimensional regularization. The net effect of the zero-bin subtractions is therefore to simply convert $1/\epsilon$ infrared divergent poles into $1/\epsilon$ ultraviolet divergent poles. This might lead one to think of the zero-bin subtraction as an academic issue. However, the conversion is necessary to obtain the correct form of the anomalous dimensions. In the case of a broken $SU(2)$ gauge theory we also find that the zero-bin subtractions are mandatory. In contrast to deep inelastic scattering, the effective theory graphs depend on the gauge boson mass M, and are no longer scaleless. As a result, the zero-bin subtractions are necessary not just to convert infrared divergences into ultraviolet ones, but also to correctly obtain the finite parts of the diagram.

2.1 Factorization and Collinear Wilson Lines

Consider a high energy scattering process with two or more particles, in the n_i direction, $i = 1, \ldots, r$ (see Fig. 2.1). n_i-collinear gauge bosons, which have momentum parallel to particle i can interact with particle i, or with the other particles $j \neq i$. The coupling of n_i-collinear gauge bosons to particle i is included explicitly in the SCET Lagrangian. The particle-gauge interactions are identical to those in the full theory, and there is no simplification on making the transition to SCET. However, if an n_i-collinear gauge boson interacts with a particle j not in the n_i-direction, then particle j becomes off-shell by an amount of order Q, and the intermediate particle j propagators can be integrated out, giving a Wilson line interaction in SCET. The form of these operators was derived in Ref. [18, 19], and gives the Wilson line interaction $W_{n_i}^\dagger \xi_{n_i}$, where W_{n_i} is a Wilson line in the $\bar{n}_i$ direction in the same representation as ξ_{n_i}. This is easy to see in processes with only two collinear particles. But even in complicated scattering processes with more than two collinear particles the Wilson line interaction still has the form $W_{n_i}^\dagger \xi_{n_i}$. Gluon emission from all particles other than the n_i-collinear particle combine (using the fact that the operator is a gauge singlet) to give a Wilson line in the representation of the n_i-collinear particle.

The Feynman rules for multiple gauge emission of n_i-collinear gluons from particle j

gives factors of the form

$$\frac{\epsilon \cdot n_j}{k \cdot n_j}. \tag{2.1}$$

The n_i-collinear gauge field has momentum k and polarization ϵ in the n_i-direction at leading order in SCET power counting, so the above expression can be replaced by

$$\frac{\epsilon \cdot n_j}{k \cdot n_j} \quad \to \quad \frac{n_i \cdot n_j}{n_i \cdot n_j} \frac{\epsilon \cdot \bar{n}_i}{k \cdot \bar{n}_i} = \frac{\epsilon \cdot \bar{n}_i}{k \cdot \bar{n}_i} \tag{2.2}$$

using the leading (first) term in Eq. (1.3) for the decomposition of both k and ϵ. This expression is independent of n_j. As a result, when one combines emission from all particles which are not in the n_i-direction, the term in Eq. (2.2) can be factored out, and the color matrices combined to form a single Wilson line in the $\bar{n}_i$ direction. This is the basis for factorization in SCET, since n_i-collinear interactions are independent of the dynamics of all particles not in the n_i-direction.

Unfortunately, Eq. (2.2), while valid at tree-level, can not be used for loop diagrams. The reason is that loop diagrams require a regulator for the Wilson lines. For example, with analytic regularization, Eq. (2.2) becomes

$$\begin{aligned} \frac{\epsilon \cdot n_j}{(k \cdot n_j)^{1+\delta}} \quad &\to \quad \frac{n_i \cdot n_j}{(n_i \cdot n_j)^{1+\delta}} \frac{\epsilon \cdot \bar{n}_i}{(k \cdot \bar{n}_i)^{1+\delta}} \\ &= \quad \frac{1}{(n_i \cdot n_j)^{\delta}} \frac{\epsilon \cdot \bar{n}_i}{(k \cdot \bar{n}_i)^{1+\delta}} \end{aligned} \tag{2.3}$$

and the j dependence no longer cancels. Thus the identities which allowed one to combine all the n_i-collinear emissions into a single Wilson line in the $\bar{n}_i$ direction no longer hold.

In this chapter, we regulate the Wilson lines using the Δ-regulator, which also introduces i-dependence into Eq. (2.2), and naively breaks factorization. We will see that after zero-bin subtraction, the j-dependence cancels, and factorization is restored.

2.2 Δ Regulator

The Δ-regulator for particle i is given by replacing the propagator denominators by

$$\frac{1}{(p_i + k)^2 - m_i^2} \to \frac{1}{(p_i + k)^2 - m_i^2 - \Delta_i}. \tag{2.4}$$

This regulator can be implemented at the level of the Lagrangian, since it corresponds to a shift in the particle mass. The on-shell condition remains $p_i^2 = m_i^2$.

In SCET, the collinear propagator denominators have the replacement of Eq. (2.4). If particle j interacts with an n_i-collinear gluon and becomes off-shell, then

$$\begin{aligned} &\frac{1}{(p_j + k)^2 - m_j^2 - \Delta_j} \\ &\qquad \to \frac{1}{\frac{1}{2}(\bar{n}_i \cdot k)(\bar{n}_j \cdot p_j)(n_i \cdot n_j) - \Delta_j}, \end{aligned} \tag{2.5}$$

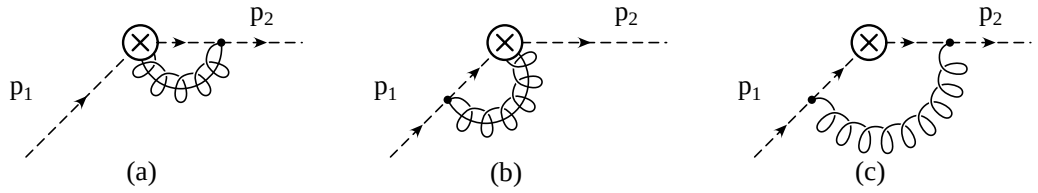

Figure 2.2: Diagrams of order $O(\alpha)$ in the effective theory. Wavefunction diagrams are not shown. The dashed line denotes a fermion, the spring denotes a mass-mode gauge boson and the spring with a line denotes a collinear gauge boson.

where k is n-collinear, and Eq. (2.2) becomes

$$\begin{aligned} \frac{\epsilon\cdot n_j}{k\cdot n_j} &\to \frac{\epsilon\cdot \bar{n}_i}{k\cdot \bar{n}_i - \delta_{j,n_i}}\,, \\ \delta_{j,n_i} &\equiv \frac{2\Delta_j}{(n_i\cdot n_j)(\bar{n}_j\cdot p_j)}\,. \end{aligned} \tag{2.6}$$

The denominator in Eq. (2.1) gets shifted by δ_{j,n_i}, as can be seen from the denominator of Eq. (2.5). The Wilson lines in the Δ-regulator method will be regulated using Eq. (2.6). As a result, in the multiparticle case, it is not possible to combine n_i-collinear gluon emission off the various particles into a single Wilson line in the $\bar{n}_i$ direction, since δ_{j,n_i} depends on the particle j. However, we will see that after zero-bin subtraction, the j-dependence drops out, and n_i-collinear gluon emission can be combined into a single Wilson line.

While $\delta_{i,n}$ and Δ_i are related by Eq. (2.6), it is useful to retain both variables during the computation.

2.3 Calculation in the effective theory

The one-loop effective theory vertex graphs are the n-collinear, $\bar{n}$-collinear and mass-mode graphs, shown in Fig. 1.4. The n-collinear diagram reads

$$I_n = -2ig^2 C_F f_\epsilon \int \frac{\mathrm{d}^d k}{(2\pi)^d} \frac{1}{[-\bar{n}\cdot k]} \frac{\bar{n}\cdot(p_2-k)}{[(p_2-k)^2]} \frac{1}{k^2-M^2}\,, \tag{2.7}$$

with $f_\epsilon = (4\pi)^{-\epsilon}\,\mu^{2\epsilon} e^{\epsilon\gamma_E}$. Since the gauge boson is massive, this integral is divergent even if p_2 is off-shell in $d = 4-2\epsilon$ dimensions. This can be seen as follows: Integrate over k^+ by contours and perform the substitution $k^- = z p_2^-$. Because the poles of k^+ lie in the same half-plane for $k^- > p_2^-$ and $k^- < 0$, one obtains (keeping $p_2^+ \neq 0$ to regulate the integral)

$$I_n = -2a\mu^{2\epsilon} e^{\epsilon\gamma_E}\Gamma(\epsilon) \int_0^1 dz \frac{1-z}{z} \left[M^2(1-z) - p_2^2 z(1-z)\right]^{-\epsilon} \tag{2.8}$$

where $a = C_F\alpha/(4\pi)$. For $z \to 0$ this integral diverges as long as the gauge boson is massive $M \neq 0$, even if $p_2^2 \neq 0$. For massless gauge bosons, $M = 0$, and the factor $z^{-\epsilon}$ from the $p_2^2 \neq 0$ term regulates the integral when the fermion is off-shell.

Introducing the Δ-regulator, the n-collinear diagram becomes

$$I_n = -2ig^2 C_F f_\epsilon \times \int \frac{\mathrm{d}^d k}{(2\pi)^d} \frac{1}{[-\bar{n}\cdot k - \delta_1]} \frac{\bar{n}\cdot(p_2-k)}{[(p_2-k)^2-\Delta_2]} \frac{1}{k^2-M^2}\,. \tag{2.9}$$

Doing the integrations in exactly the same way as described above, one obtains for the n-collinear integral with an on-shell external fermion $p_2^2 = 0$

$$\begin{aligned} I_n &= -2a\Gamma(\epsilon)(M^2)^{-\epsilon}\mu^{2\epsilon}e^{\epsilon\gamma_E}\int_0^1 dz\, \frac{(1-z)^{1-\epsilon}}{z+\delta_1/p_2^-} \\ &= a\left[\left(\frac{2}{\epsilon} - 2\mathsf{L}_M\right)\left(1+\log(\delta_1/p_2^-)\right) - \frac{\pi^2}{3} + 2\right]. \end{aligned} \tag{2.10}$$

Note that $\Delta_{1,2}$ and $\delta_1 \equiv \delta_{1,n}$, $\delta_2 \equiv \delta_{2,\bar{n}}$ are regulator parameters, and are set to zero unless they are needed to regulate any divergence. The regulator parameters are defined using Eq. (2.6),

$$\begin{aligned} \delta_1 &\equiv \delta_{1,n} = 2\frac{\Delta_1}{(n\cdot\bar{n})(n\cdot p_1)} = \frac{\Delta_1}{p_1^+}\,, \\ \delta_2 &\equiv \delta_{2,\bar{n}} = 2\frac{\Delta_2}{(n\cdot\bar{n})(\bar{n}\cdot p_2)} = \frac{\Delta_2}{p_2^-}\,., \end{aligned} \tag{2.11}$$

We recall that $n_1 = \bar{n}$ because p_1 is in the $\bar{n}$ direction, and similarly for δ_2. The terms δ_1 and δ_2 transform under boosts as the $-$ and $+$ component of a vector, and $\mathsf{L}_M, \mathsf{L}_Q$ are defined as

$$\mathsf{L}_M = \log\frac{M^2}{\mu^2}, \qquad \mathsf{L}_Q = \log\frac{Q^2}{\mu^2}. \tag{2.12}$$

Equation (2.9) depends on Δ_2 and δ_1 which regulate the collinear and Wilson line propagators, respectively. Δ_2 is not needed to regulate a divergence in the integral, so the result in Eq. (2.10) only depends on the Wilson line regulator δ_1. The n-collinear graph depends on the scale Q via the regulator dependence,

$$\log\frac{\delta_1}{p_2^-} = \log\frac{\Delta_1}{p_1^+ p_2^-} = \log\frac{\Delta_1}{Q^2}\,. \tag{2.13}$$

The n-collinear particle momentum is p_2, but the n-collinear graph Eq. (2.10) depends on particle 1 via its dependence on the regulator Δ_1 for particle 1. This leads to a violation of factorization in the collinear sector, since the n-collinear graph depends on the properties of the other particles. In the multiparticle case, this means that the Wilson lines for all the other particles cannot be combined into a single Wilson line in the $\bar{n}$ direction — the loop contributions from the other particles each depend on their own regulator δ_i, and the different contributions cannot be combined into a single amplitude.

The n-collinear wavefunction renormalization graph is identical to that in the full theory. It does not need any Δ-regularization, and reads

$$W_n = a\left[\frac{1}{\epsilon} - \frac{1}{2} - \mathsf{L}_M\right]. \tag{2.14}$$

The normalization convention is such that one gets a contribution of $-W_n/2$ for each external n-collinear fermion.

The $\bar{n}$-collinear integral $I_{\bar{n}}$ can be obtained from I_n by replacing p_2^- by p_1^+ and δ_1 by δ_2,

$$I_{\bar{n}} = a\left[\left(\frac{2}{\epsilon} - 2\mathsf{L}_M\right)\left(1+\log(\delta_2/p_1^+)\right) - \frac{\pi^2}{3} + 2\right], \tag{2.15}$$

and the $\bar{n}$-collinear wavefunction renormalization is $W_{\bar{n}} = W_n$.

For the mass-mode diagram, one finds

$$\begin{aligned} I_s &= -2ig^2 C_F f_\epsilon \int \frac{\mathrm{d}^d k}{(2\pi)^d} \frac{1}{k^2 - M^2} \frac{1}{-n\cdot k - \delta_2} \frac{1}{-\bar{n}\cdot k - \delta_1} \\ &= a\left[-\frac{2}{\epsilon^2} + \frac{2}{\epsilon}\log\frac{\delta_1\delta_2}{\mu^2} + \mathsf{L}_M^2 - 2\mathsf{L}_M \log\frac{\delta_1\delta_2}{\mu^2} + \frac{\pi^2}{6}\right]. \end{aligned} \tag{2.16}$$

Again, we only keep the leading terms in δ_i, and the integral depends on both δ_1 and δ_2. The mass-mode wavefunction contribution vanishes, $W_s = 0$, since $n^2 = \bar{n}^2 = 0$.

2.3.1 Zero-Bin Subtractions

In the effective theory, the gauge boson fields of the full theory are split up into several different fields which fluctuate over different scales. In order to avoid double counting of the mass-modes, one has to subtract the contribution from the collinear fields with vanishing label momenta [31]. The zero-bin subtraction for Eq. (2.7), which amounts to taking the soft limit in the integrand of the collinear integral, is

$$I_{n\varnothing} = -2ig^2 C_F f_\epsilon \int \frac{\mathrm{d}^d k}{(2\pi)^d} \frac{1}{[-\bar{n}\cdot k - \delta_1]} \frac{1}{\left[-n\cdot k - \Delta_2/p_2^-\right]} \frac{1}{k^2 - M^2}, \tag{2.17}$$

which is the same as the integral Eq. (2.16), with $\delta_2 \to \Delta_2/p_2^-$. One needs to retain Δ_2 to regulate the singularity, since the k^2 term in the collinear propagator has been expanded out. Subtracting this from the collinear integral yields

$$I_n - I_{n\varnothing} = a\left[\frac{2}{\epsilon^2} - \frac{2}{\epsilon}\log\frac{\Delta_2}{\mu^2} + \frac{2}{\epsilon} - 2\left(1 - \log\frac{\Delta_2}{\mu^2}\right)\mathsf{L}_M - \mathsf{L}_M^2 - \frac{\pi^2}{2} + 2\right]. \tag{2.18}$$

This combination only depends on the gauge boson mass and the regulator of the collinear fermion, Δ_2. The zero-bin subtraction $W_{n\varnothing}$ for the wavefunction renormalization W_n vanishes.

There are two very important differences between the zero-bin subtracted result $I_n - I_{n\varnothing}$ and the unsubtracted result I_n: The zero-bin subtracted integral no longer depends on the hard scale Q, and it depends only on the regulator Δ_2 for the n-collinear particle, rather than on the regulator Δ_1 for the other particle. This means it depends on the regulator of the collinear

particle rather than the regulator of the Wilson line, and it implies that zero-bin subtraction restores factorization in the effective theory. The hard scale has been factored out of the collinear contribution. In addition, in the multiparticle case, since the collinear graphs only depend on the n-collinear particle regulator (Δ_2 in our problem), the Wilson line contributions from all the other particles can be combined into a single Wilson line in the $\bar{n}$ direction, as was naively true at tree-level. This is because the zero-bin subtracted collinear graph does not need a regulator for the Wilson line.

The final result of the effective theory vertex computation is

$$\begin{aligned}&(I_n - I_{n\varnothing}) + (I_{\bar{n}} - I_{\bar{n}\varnothing}) + I_s - \frac{1}{2}(W_n - W_{n\varnothing}) - \frac{1}{2}(W_{\bar{n}} - W_{\bar{n}\varnothing}) - W_s \\ &\quad = a\left[\frac{2}{\epsilon^2} + \frac{2}{\epsilon}\log\frac{\delta_1\delta_2\mu^2}{\Delta_1\Delta_2} + \frac{3}{\epsilon} - \mathsf{L}_M^2 - 2\mathsf{L}_M\log\frac{\delta_1\delta_2\mu^2}{\Delta_1\Delta_2} - 3\mathsf{L}_M - \frac{5\pi^2}{6} + \frac{9}{2}\right], \quad (2.19)\end{aligned}$$

where we have added the zero-bin subtracted collinear graphs and the mass-mode graph. This result has to be independent of the regulators. Indeed, using Eq. (2.11), Eq. (2.19) can be simplified to

$$a\left[\frac{2}{\epsilon^2} - \frac{2}{\epsilon}\mathsf{L}_Q + \frac{3}{\epsilon} - \mathsf{L}_M^2 + 2\mathsf{L}_Q\mathsf{L}_M - 3\mathsf{L}_M - \frac{5\pi^2}{6} + \frac{9}{2}\right]. \quad (2.20)$$

This is the correct effective theory result, and when combined with the matching computation at Q [28] correctly reproduces the known full-theory computation of the form-factor.

Note that without zero-bin subtractions, the effective theory result would be

$$\begin{aligned}&I_n + I_{\bar{n}} + I_s - \frac{1}{2}W_n - \frac{1}{2}W_{\bar{n}} - W_s \\ &\quad = a\left[-\frac{2}{\epsilon^2} + \frac{2}{\epsilon}\log\frac{\Delta_1^2\Delta_2^2}{Q^6\mu^2} + \frac{3}{\epsilon} + \mathsf{L}_M^2 - 2\mathsf{L}_M\log\frac{\Delta_1^2\Delta_2^2}{Q^6\mu^2} - 3\mathsf{L}_M - \frac{\pi^2}{2} + \frac{9}{2}\right]. \quad (2.21)\end{aligned}$$

This is incorrect, and does not reproduce the full theory result when the matching condition at Q is included. The $1/\epsilon$ singularities, which are ultraviolet, do not give the correct anomalous dimension $\gamma = a(4\mathsf{L}_Q - 6)$ for the current in SCET. The result is also not independent of the regulator. Idilbi and Mehen [45, 46] have previously arrived at the same conclusions for QCD, where the gauge boson is massless. However, the necessity of zero-bin subtractions becomes more obvious with a massive gauge boson, since the effective theory graphs are no longer scaleless due to the gauge boson mass. One can see that Eq. (2.21) also does not give the correct finite parts of the diagram.

Using the Δ-regulator, we have seen that the vertex corrections are

$$(I_n - I_{n\varnothing}) + (I_{\bar{n}} - I_{\bar{n}\varnothing}) + I_s \quad (2.22)$$

after including zero-bin subtractions. Also, $I_{n\varnothing} = I_{\bar{n}\varnothing} = I_s$, so the vertex correction can be written as $I_n + I_{\bar{n}} - I_s$. Recently, Idilbi and Mehen [45, 46] showed in their study of deep inelastic scattering in QCD, that the combination $I_n + I_{\bar{n}} - I_s$ does not need any additional regulator

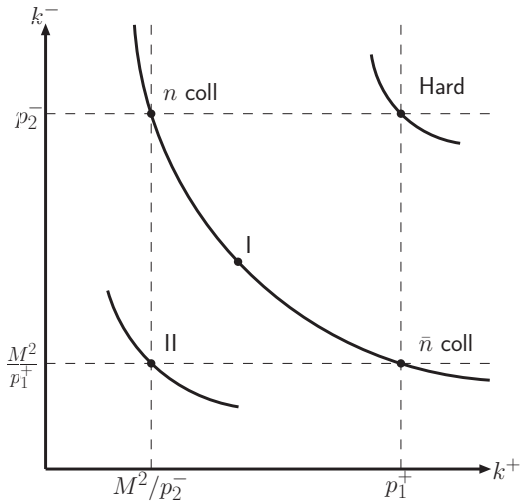

Figure 2.3: Modes which contribute to the effective theory. Mass-modes are shown as I. Additional massless gluons contribute modes shown as II.

beyond dimensional regularization. The same result continues to hold for broken $SU(2)$ with massive gauge bosons, where the role of the ultrasoft contribution is adopted by the mass-mode contribution I_s. Thus the integrand obtained by combining $I_n + I_{\bar{n}} - I_s$ does not need any Δ-regulator either, and can be evaluated explicitly to give

$$I_n + I_{\bar{n}} - I_s \quad = \quad a\left[\frac{2}{\epsilon^2} - \frac{2}{\epsilon}\mathsf{L}_Q + \frac{4}{\epsilon} - \mathsf{L}_M^2 + 2\mathsf{L}_Q\mathsf{L}_M - 4\mathsf{L}_M - \frac{5\pi^2}{6} + 4\right]. \tag{2.23}$$

When combined with the wavefunction graphs this gives the correct amplitude Eq. (2.20). The details of the computation are given in Appendix 2.4. The form of the expression, $I_n + I_{\bar{n}} - I_s$ in broken $SU(2)$ – and similarly in QCD – is counter-intuitive if one is used to thinking about effective field theories using the method of regions. This is because one has to subtract the mass-mode/ultrasoft region from the sum of the collinear regions to get the correct amplitude.

The above discussion shows that in practice one can identify the respective zero-bin contribution of the collinear integrals $I_{n\varnothing}$ and $I_{\bar{n}\varnothing}$ with the mass-mode integral I_s. Doing this identification also in the case where the integrals are done separately with the regulator, one does not need any relations between Δ_i and δ_i. Instead one regulates the collinear Wilson lines and propagators in the soft graphs with δ_i, and Eq. (2.18) is instead given by the same expression with $\delta_2 p_2^-$ in place of Δ_2.

2.3.2 Momentum Regions

In this section we discuss the various momentum regions that contribute to the computation of the Sudakov form factor paying particular attention in the role of the zero-bin sub-

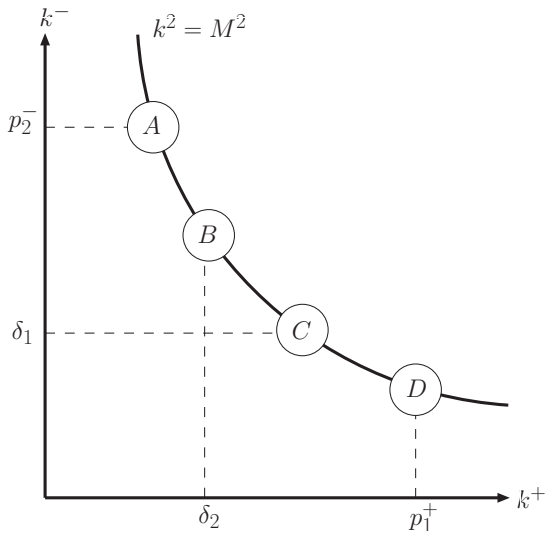

Figure 2.4: Momentum regions which contribute to the effective theory integrals. A and D are collinear, and B and C are regulator-dependent mass-mode regions.

tractions to the contributions from the n- and $\bar{n}$ collinear regions. The momentum regions which contribute to the Sudakov form factor are illustrated in Fig. 2.3. The hard contribution is the high-scale matching at Q, and the remaining contributions are given by the effective theory. The effective theory contributions are located along the curve $k^2 = M^2$. The n-collinear contribution arises from $k^- \sim p_2^- \sim Q$, so that $k^+ \sim M^2/Q$ and the $\bar{n}$-collinear contribution arises from $k^+ \sim p_1^+ \sim Q$, $k^- \sim M^2/Q$. The ultrasoft region with $k^+ \sim M^2/p_2^- \sim M^2/Q$ and $k^- \sim M^2/p_1^+ \sim M^2/Q$ is not on the $k^2 = M^2$ hyperbola, and does not contribute to the amplitude. Interestingly, it now turns out that the mass-mode region, with all components of k of order M, does not contribute to the amplitude either.[1] As shown in Ref. [21], the contributions to the amplitude from the mass-mode region vanish if the analytic regulator of Eq. (2.3) is employed, and only the n- and $\bar{n}$-collinear regions give nonzero results. As we show below, the same is true also when the Δ-regulator is used. However, in this case, the argument is more subtle and requires that zero-bin contributions to the n- and $\bar{n}$-collinear pieces are properly accounted for.

While the analytic regulator does not introduce any new dimensionful parameters, the Δ-regulator introduces the new dimensionful scales $\Delta_{1,2}$, and the picture changes because of contributions from unphysical regulator dependent regions, which are absent in the total amplitude. This has been noted previously [47, 48]. The n-collinear graph I_n, Eq. (2.10) gets contributions from $k^- \sim p_2^- \sim Q$, $k^+k^- \sim M^2$ and $k^- \sim \delta_1$, $k^+k^- \sim M^2$. This is shown as regions A and C in Fig. 2.4. The $\bar{n}$-collinear graph gets contributions from regions D and B.

The zero-bin integral $I_{n\varnothing}$ gets contributions from the region with $k^+ \sim \Delta_2/p_2^-$ and from

[1] It is important to include the mass-mode contribution. The mass-mode region does not contribute, because of a cancellation between the collinear modes and mass-modes in the mass-mode region. See below.

$k^- \sim \delta_1$, i.e. from regions B and C. Thus, for the zero-bin subtracted collinear integral $I_n - I_{n\varnothing}$, region C cancels, and the resulting contributions are from regions A and B. Similarly, $I_{\bar{n}} - I_{\bar{n}\varnothing}$ gets contributions from D and C. On the other hand, the mass-mode graphs get a contribution from the region $k^- \sim \delta_1$, $k^+k^- \sim M^2$ and from $k^+ \sim \delta_2$, $k^+k^- \sim M^2$, i.e. regions B and C. We now see that the total amplitude only gets contributions from A and D. The additional regions B and C introduced by the regulator drop out, as they should. To achieve the cancellation of the unphysical regions B and C it is essential to account for the zero-bin subtractions for the collinear regions.

2.3.3 Gauge dependence

So far, we have been working in Feynman gauge, $\xi = 1$. Let us now analyze the gauge dependence of the different parts of the effective theory calculation by using a general R_ξ gauge with the gauge boson propagator

$$i\Delta_{\alpha\beta}(k) = \frac{1}{k^2 - M^2}\left[g_{\alpha\beta} + (\xi - 1)\,\frac{k_\alpha k_\beta}{k^2 - \xi M^2}\right]. \tag{2.24}$$

In the full theory, the new ξ dependent contribution to the vertex graph, $I^{(\xi)}$, stemming from the second part of the gauge boson propagator is

$$\begin{aligned} I^{(\xi)} &= \frac{\alpha_s}{4\pi} C_F \Gamma J \\ J &= -16\pi^2 i(\xi - 1) f_\epsilon \int \frac{\mathrm{d}^d k}{(2\pi)^d} \frac{1}{k^2 - M^2} \frac{1}{k^2 - \xi M^2} \\ &= \frac{\xi - 1}{\epsilon_{\mathrm{UV}}} - (\xi - 1)\log\frac{M^2}{\mu^2} + (\xi - 1) - \xi \log \xi\,. \end{aligned} \tag{2.25}$$

The full theory vertex graph gets shifted, $I_V \to I_V + aJ$. There is a similar shift in the full theory wavefunction contribution, $W \to W + aJ$ so that the on-shell S-matrix element $I_V - W$ is ξ-independent. The high scale matching coefficient is the full theory result with all infrared scales set to zero, and so is gauge invariant.

In terms of the method of regions, J only has contributions from the mass mode region where $k^+ \sim k^- \sim k^\perp \sim M$, given ξ is counted as order $O(1)$. Therefore, one might not expect this additional piece to show up in the collinear vertex diagrams in the effective theory. However, doing the calculation of the additional parts $I_n^{(\xi)}$ and $I_{\bar{n}}^{(\xi)}$ of the collinear integrals yields (see Ref. [18] for the Feynman rules)

$$\begin{aligned} I_n^{(\xi)} &= -ig^2 C_F f_\epsilon \int \frac{d^d k}{(2\pi)^d}\left[n^\alpha - \frac{\gamma_\perp^\alpha \not{k}_\perp}{\bar{n}\cdot(p_2 - k)}\right] \\ &\quad \times \frac{\bar{n}\cdot(p_2 - k)}{(p_2 - k)^2 - \Delta_2}\Gamma \frac{1}{-\bar{n}\cdot k - \delta_1}\bar{n}^\beta \frac{1}{k^2 - M^2} \\ &\quad \times \left[(\xi - 1)\,\frac{k_\alpha k_\beta}{k^2 - \xi M^2}\right] \\ &= \frac{\alpha}{4\pi} C_F \Gamma J\,, \end{aligned} \tag{2.26}$$

and similarly for $I_{\bar{n}}^{(\xi)}$. Note that for Eq. (2.26) we have adopted $p_2^+ = p_2^\perp = 0$.

For the mass-mode diagram, the additional piece reads

$$\begin{aligned} I_s^{(\xi)} &= -ig^2 C_F f_\epsilon \int \frac{d^d k}{(2\pi)^d} \frac{1}{-n\cdot k - \delta_2} \Gamma \frac{1}{-\bar{n}\cdot k - \delta_1} \\ &\quad \times \frac{1}{k^2 - M^2} \left[(\xi - 1) \frac{(n\cdot k)(\bar{n}\cdot k)}{k^2 - \xi M^2} \right] \\ &= \frac{\alpha}{4\pi} C_F \Gamma J \,. \end{aligned} \tag{2.27}$$

The collinear and soft wavefunction renormalization graphs also get shifted by

$$J, W_n \to W_n + aJ \qquad , W_{\bar{n}} \to W_{\bar{n}} + aJ \qquad , W_s \to W_s + aJ.$$

Without accounting for zero-bin subtractions, the effective theory result

$$I_n + I_{\bar{n}} + I_s - (W_n/2 + W_{\bar{n}}/2 + W_s)$$

would get shifted by

$$aJ + aJ + aJ - (aJ/2 + aJ/2 + aJ) = aJ,$$

and is not gauge invariant. With zero-bin subtractions, however, the effective theory collinear vertex graph is $I_n - I_{n\varnothing}$, which is gauge invariant, since both terms shift by aJ. Similarly, the collinear wavefunction graph is $W_n - W_{n\varnothing} = W_n - W_s$ which is also gauge invariant, since again both terms are shifted by aJ. Thus, the collinear vertex and wavefunction contributions are each separately gauge invariant. The mass-mode contributions I_s and W_s are each shifted by aJ, so the net soft contribution $I_s - W_s$ is gauge invariant as well.

Thus zero-bin subtractions are also necessary to maintain gauge invariance of the two collinear and the mass-mode sectors of the effective theory, as required by factorization.

2.4 Calculation without a regulator

In this appendix, we calculate the effective field amplitude including zero-bin subtractions by first adding and then performing the integration. No regulators are needed in this case, as in the massless case [45, 46].

$$
\begin{aligned}
R &= I_n + I_{\bar{n}} - I_s \\
&= -2ig^2 C_F f_\epsilon \int \frac{\mathrm{d}^d k}{(2\pi)^d} \left[\frac{p_1^+ - k^+}{(-p_1^+ k^- + k^2)(-k^+)(k^2 - M^2)} \right. \\
&\quad \left. + \frac{p_2^- - k^-}{(-p_2^- k^+ + k^2)(-k^-)(k^2 - M^2)} - \frac{1}{(-k^+)(-k^-)(k^2 - M^2)} \right] \\
&= -2ig^2 C_F f_\epsilon \int \frac{\mathrm{d}^d k}{(2\pi)^d} \left[\frac{2k^2 + p_1^+ p_2^- - p_1^+ k^- - p_2^- k^+}{(-p_1^+ k^- + k^2)(-p_2^- k^+ + k^2)(k^2 - M^2)} \right. \\
&\quad \left. - \frac{k^4}{(-p_1^+ k^- + k^2)(-p_2^- k^+ + k^2)(-k^+)(-k^-)(k^2 - M^2)} \right] .
\end{aligned}
\tag{2.28}
$$

The total integral is IR finite. It can be decomposed as

$$
R = -2ig^2 C_F \left[Q^2 I_0 - 2(p_1 + p_2)_\mu I_1^\mu + 2I_2 - I_3 \right] \tag{2.29}
$$

with

$$
\begin{aligned}
I_0 &= f_\epsilon \int \frac{\mathrm{d}^d k}{(2\pi)^d} \frac{1}{(k - p_1)^2 (k - p_2)^2 (k^2 - M^2)} \\
I_1^\mu &= f_\epsilon \int \frac{\mathrm{d}^d k}{(2\pi)^d} \frac{k^\mu}{(k - p_1)^2 (k - p_2)^2 (k^2 - M^2)} \\
I_2 &= f_\epsilon \int \frac{\mathrm{d}^d k}{(2\pi)^d} \frac{k^2}{(k - p_1)^2 (k - p_2)^2 (k^2 - M^2)} \\
I_3 &= f_\epsilon \int \frac{\mathrm{d}^d k}{(2\pi)^d} \frac{k^2}{(-p_1^+ k^- + k^2)(-p_2^- k^+ + k^2)(-k^+)(-k^-)} .
\end{aligned}
\tag{2.30}
$$

Since we are not interested in subleading terms in M^2/Q^2 for all these integrals, we simplify the last part of the integrand in Eq. (2.28) and set $M = 0$ to obtain I_3. One finds

$$
\begin{aligned}
I_0 &= -\frac{i}{16\pi^2} \int_0^1 \mathrm{d}z \int_0^1 \mathrm{d}x \frac{z}{Q^2 x(1-x) z^2 + M^2 (1 - z)} \\
&= -\frac{i}{16\pi^2 Q^2} J_1 , \\
I_1^\mu &= -\frac{i}{16\pi^2} \frac{1}{2} \int_0^1 \mathrm{d}z \int_0^1 \mathrm{d}x \frac{z^2 (p_1 + p_2)^\mu}{Q^2 x(1-x) z^2 + M^2 (1 - z)} \\
&= -\frac{i}{16\pi^2 Q^2} J_2 \frac{1}{2} (p_1 + p_2)^\mu ,
\end{aligned}
$$

$$
\begin{aligned}
I_2 &= M^2 I_0 + f_\epsilon \int \frac{\mathrm{d}^d k}{(2\pi)^d} \frac{1}{(k-p_1)^2 (k-p_2)^2} \\
&= M^2 I_0 + \frac{i}{16\pi^2} \left[\frac{1}{\epsilon} + \log \frac{\mu^2}{Q^2} + 2 \right] , \\
I_3 &= -\frac{i}{2} \int_0^{p_2^-} \frac{\mathrm{d}k^-}{2\pi} \frac{\mathrm{d}^{d-2} k_\perp}{(2\pi)^{d-2}} \\
&\quad \frac{p_1^+ k^-}{[\mathbf{k}_\perp^2 + p_1^+ k^-][(k^-)^2 p_1^+ - p_2^- \mathbf{k}_\perp^2 - p_1^+ p_2^- k^-]} \\
&\quad + \frac{i}{2} f_\epsilon \int_{p_2^-}^{\infty} \frac{\mathrm{d}k^-}{2\pi} \frac{\mathrm{d}^{d-2} k_\perp}{(2\pi)^{d-2}} \frac{1}{(-p_1^+ k^- - \mathbf{k}_\perp^2)(k^-)} \\
&= -\frac{i}{16\pi^2} \left[\frac{1}{\epsilon^2} - \frac{1}{\epsilon} \log \frac{Q^2}{\mu^2} + \frac{1}{2} \log^2 \frac{Q^2}{\mu^2} - \frac{\pi^2}{12} \right] , \qquad (2.31)
\end{aligned}
$$

with

$$
J_n = \int_0^1 \mathrm{d}z \int_0^1 \mathrm{d}y \frac{4 z^n}{z^2 (1-y^2) + \lambda^2 (1-z)} \qquad (2.32)
$$

and $\lambda^2 = 4M^2/Q^2$. To calculate the integral J_1, integrate first over y and substitute $w = z + \sqrt{z^2 + \lambda^2 (1-z)}$, leading to

$$
J_1 = \frac{\pi^2}{3} + \frac{1}{2} \log^2 \frac{Q^2}{M^2} . \qquad (2.33)
$$

For J_2, one can simply expand in λ after the integration over y to obtain

$$
J_2 = 2 \log \frac{Q^2}{M^2} - 2 . \qquad (2.34)
$$

Adding everything up, one finally finds

$$
R = a \Big[\frac{2}{\epsilon^2} - \frac{2}{\epsilon} \mathsf{L}_Q + \frac{4}{\epsilon} - \mathsf{L}_M^2 + 2 \mathsf{L}_Q \mathsf{L}_M - 4 \mathsf{L}_M - \frac{5\pi^2}{6} + 4 \Big] . \qquad (2.35)
$$

2.5 Final Remarks

SCET with massive gauge bosons requires an additional regulator on top of the common dimensional regularization to obtain well defined expressions for individual Feynman diagrams. We have proposed the Δ-regulator to regularize the singularity from the Wilson line propagators. Using the Δ-regulator, the effective theory only gives the correct result for the scattering amplitude if zero-bin subtractions for the n- and $\bar{n}$-collinear contributions are included. For the Sudakov form factor in a broken $SU(2)$ gauge theory with a common gauge boson mass M, the total amplitude then is $I_n + I_{\bar{n}} - I_s$ as a result of the subtractions. Here I_n and $I_{\bar{n}}$ refer to the n- and $\bar{n}$-collinear diagrams and I_s refers to the contributions of the mass-mode graphs related to gluons with momenta $k^+ \sim k^- \sim k^\perp \sim M$. This result is in analogy to previous results obtained for unbroken gauge theories with massless gauge bosons [45, 46]. The result appears to

contradict the method-of-regions approach, where one has to add up the contributions from all different regions.

We have demonstrated that one needs to subtract the mass-mode region from the sum of the collinear regions to avoid double-counting, and that gauge invariance of the effective theory is only maintained if the zero-bin subtractions are accounted for.

Zero-bin subtractions also restore factorization between the different collinear sectors. Naively, one implements factorization by redefining the collinear fields as [18, 19]

$$W_n^\dagger \xi_n \quad \to \quad S_n W_n^{(0)\dagger} \xi_n^{(0)} \tag{2.36}$$

where the mass-mode fields are in the Wilson line S_n, and no longer couple to the collinear fields in $W_n^{(0)}$ and $\xi_n^{(0)}$. This redefinition is not valid at the loop-level, because the regulator dependence of the collinear graphs breaks factorization. Factorization is restored after zero-bin subtraction, and thus the proper replacement is

$$W_n^\dagger \xi_n \quad \to \quad S_n \left[W_n^{(0)\dagger} \xi_n^{(0)} \right]_\varnothing \tag{2.37}$$

where the subscript $\varnothing$ is a reminder that the collinear sector requires zero-bin subtraction.[2]

Partial text of chapter 2 is extracted from J. y. Chiu, A. Fuhrer, A. H. Hoang, R. Kelley and A. V. Manohar,"Soft-Collinear Factorization and Zero-Bin Subtractions," Phys. Rev. D 79, 053007 (2009).

[2] We note that in the presence of massless ultrasoft gauge fields the RHS of Eq. (2.37) reads $Y_n S_n \left[W_n^{(0)\dagger} \xi_n^{(0)} \right]_\varnothing$, with an ultrasoft Y-Wilson line.

Chapter 3

The Goldstone Boson Equivalence Theorem

In the first two chapters, we calculated the radiative corrections for processes involving fermionic or scalar external states. Naturally, we would like to generalize these results for external gauge bosons and this will be the subject of the next chapter. In the SCET framework, the calculation for transversely polarized gauge bosons is a straightforward generalization of the methods of the first two chapters. The calculation of the radiative corrections for *longitudinally* polarized gauge bosons will require the use of the Goldstone boson equivalence theorem (ET) which states that

$$\langle \cdots | \, S \, | A_L^{a_1} \cdots A_L^{a_n} \cdots \rangle = (i\mathcal{E})^n \, \langle \cdots | \, \text{“}S\text{”} \, | \varphi^{a_1} \cdots \varphi^{a_n} \cdots \rangle + \mathcal{O}\Big(\frac{M}{E_1}, \cdots, \frac{M}{E_n}\Big) \tag{3.1}$$

where E_i is the energy of the ith gauge boson and terms of order M/E_i have been neglected. Eq. (3.1) says that the S matrix element for longitudinal production of a gauge boson A^a is related to the S matrix element for production of the corresponding Goldstone boson φ^a. The quotation marks on the S matrix on the right hand side will be explained in detail later, but in short, it stems from the fact that the Goldstone bosons are not physical modes and so these states cannot contribute to the S-matrix. Such a quantity is gauge dependent and this dependence is canceled by the gauge dependence of $\mathcal{E}$, thus rendering the right hand side gauge invariant. This simple relation was first noticed by Cornwall, Levin, and Tiktopoulous and by Vayonakis at tree level [49, 50]. A sketch of the proof was later provided in 't Hooft-Feynman gauge by Lee, Quigg, and Thacker [51] and then the extension to general R_ξ gauge and an arbitrary Higgs mass was given by Chanowitz and Gaillard [52] and followed by Gounaris, Kögerler, and Neufeld [53]. The initial discussions of the equivalence theorem were limited to tree level and a more careful analysis at one loop, carried out by Bagger and Schmidt [54] and by Yao and Yan [55] showed there should in general be a correction factor – this is the factor $\mathcal{E}$ that appears in Eq. 3.1. This

chapter will focus on the derivation of the equivalence theorem and give an explicit calculation for the spontaneously broken $SU(2)$ theory of the appendix. For the first of these two objectives we will follow the approach of Bohm et al. [56].

3.1 BRS invariance

The lagrangian given in Eq (A.1) for the $SU(2)$ gauge theory is *not* gauge invariant due to the appearance of the gauge fixing and ghost terms. These extra terms arise when using the Faddeev-Popov method to make the functional integral well defined [57]. It was noticed by Becchi, Rouet, and Stora (BRS) that the lagrangian, while not invariant under a normal gauge transformation, is invariant under an extended gauge transformation involving a Grassmann-valued constant ζ [58]. Explicitly, the transformation on a general field F is given by

$$\delta F = \zeta(sF) \tag{3.2}$$

where sF is defined below for each of the fields in the theory

$$\begin{aligned} sA^a_\mu &= D^{ab}_\mu \theta^b = (\delta^{ab}\partial_\mu + g\epsilon^{abc}A^c_\mu)\theta^b \\ s\psi &= -ig\theta^a T^a \psi \\ s\phi &= -ig\theta^a T^a \phi \\ sH &= -ig\theta^a T^a H \\ s\theta^a &= \frac{1}{2} g\epsilon^{abc}\theta^b\theta^c \\ s\bar{\theta}^a &= -\frac{1}{\xi}G^a. \end{aligned} \tag{3.3}$$

Here ψ and ϕ are generic massless fermion and scalar fields, respectively and H is the Higgs field defined in Eq. (A.4) and is responsible for the spontaneous symmetry breakdown. Such a transformation, called a BRS transformation, has been given in terms of the BRS operator s, which is defined as the left derivative with respect to ζ on the BRS transformed fields. Due to the anticommutating nature of ζ, the BRS operator s has a slightly modified product rule.

$$s(FG) = (sF)G \pm F(sG) \tag{3.4}$$

where the minus sign occurs if F contains an odd number of Grassmann variables. The last equation in Eq. (3.3), giving the BRS transformation of $\bar{\theta}$, involves the gauge fixing term and will play an important role in the derivation of the ET. Individually, the ghost and gauge fixing lagrangians, $\mathcal{L}_{\rm gf}$ and $\mathcal{L}_{\rm ghost}$, are not gauge invariant; however, the rest of the lagrangian is invariant since the BRS transformation is just a gauge transformation with an anticommuting parameter. It remains to show that $\mathcal{L}_{\rm gf} + \mathcal{L}_{\rm ghost}$ is invariant, i.e.

$$s\Big(\mathcal{L}_{\rm gf} + \mathcal{L}_{\rm ghost}\Big) = 0. \tag{3.5}$$

We will postpose the proof of Eq. (3.5) until we derive a few identities that will make the proof easier.

The theory is spontaneously broken and so the gauge fixing term G^a will in general have dependence on A^a_μ and φ^a, where φ^a is the would-be Goldstone boson associated with A^a. An explicit example of a gauge fixing term which has such a dependence is

$$G^a = \partial_\mu A^{a\mu} - \xi' M \varphi^a, \tag{3.6}$$

which corresponds to choosing t'-Hooft R_ξ gauge. The details of this choice are worked out in Appendix B. The derivation that follows does not depend on this choice and in the meantime we will not restrict ourselves to this gauge. Since the gauge fixing term contains φ^a, we need the BRS transformation for this field. The transformation rule for h and φ is obtained from the BRS transformation of H.

$$\begin{aligned} sh &= \frac{g}{2}\theta^a\varphi^a \\ s\varphi^a &= \frac{g}{2}\Big(-\theta^a(h+v) + \epsilon^{abc}\theta^b\varphi^c\Big) \end{aligned} \tag{3.7}$$

The BRS operator is nilpotent – specifically that is for a general field F, two successive operators with s yields zero for all fields except $\bar\theta^a$.

$$s^2 F = 0 \tag{3.8}$$

For the anti-ghost field the we have

$$s^2\bar\theta^a = -\frac{1}{\xi} sG^a(x) \tag{3.9}$$

yet,

$$s^3\bar\theta^a = 0 \tag{3.10}$$

For ψ, ϕ, the result follows from a straightforward application of s^2. For the A field, it is slightly more complicated.

$$\begin{aligned} s^2 A^a_\mu &= s(\partial_\mu\theta^a + g f^{abc} A^c_\mu \theta^b) \\ &= \frac{g}{2}\epsilon^{abc}\partial_\mu(\theta^b\theta^c) + g\epsilon^{abd}\partial_\mu(\theta^d)\theta^b \\ &\quad + g^2\epsilon^{abc}\epsilon^{cde}A^e_\mu\theta^d\theta^b + \frac{g^2}{2}\epsilon^{abc}\epsilon^{bde}A^c_\mu\theta^d\theta^e \end{aligned} \tag{3.11}$$

Notice the first two terms cancel. Using the anticommuting properties of the ghost fields and relabeling indices, we can write the last two terms in the form

$$\frac{g^2}{2}(\epsilon^{ade}\epsilon^{bcd} + \epsilon^{bde}\epsilon^{cad} + \epsilon^{abd}\epsilon^{cde})A^e_\mu\theta^c\theta^b \tag{3.12}$$

which vanishes by the Jacobi identity. So $s^2 A^a_\mu = 0$. For the φ^a field, we have

$$\begin{aligned} s^2\varphi^a &= s\Big(-\theta^c(h+v) + \epsilon^{abc}\theta^b\varphi^c\Big)\frac{g}{2} \\ &= \frac{g}{2}\Big(-(s\theta^a)(h+v) + \theta^a(sh) + \epsilon^{abc}(s\theta^b)\varphi^c - \epsilon^{abc}\theta^b(s\varphi^c)\Big) \\ &= \frac{g^2}{4}\Big(-\epsilon^{abc}\theta^b\theta^c(h+v) + \theta^a\theta^b\varphi^b \\ &\quad +\epsilon^{abc}\epsilon^{bde}\theta^d\theta^e\varphi^c + \epsilon^{abc}\theta^b\theta^c(h+v) - \epsilon^{abc}\epsilon^{cde}\theta^b\theta^d\varphi^e\Big). \end{aligned} \tag{3.13}$$

and we have used the anticommuting minus sign for s and the fact that $s(v) = 0$ in the second line, i.e. the VEV does not transform. The first and the third clearly cancel and so after some tedious algebra, the remaining terms become

$$\theta^a\theta^b\varphi^b + \epsilon^{abc}\epsilon^{bde}\theta^d\theta^e\varphi^c - \epsilon^{abc}\epsilon^{cde}\theta^b\theta^d\varphi^e = \varphi^a(\theta^b\theta^b) \tag{3.14}$$

which vanishs due to the anticommutating nature of the ghost fields. For the θ^a field, we have

$$\begin{aligned} s^2\theta^a &= s\Big(\epsilon^{abc}(s\theta^b)\theta c + \epsilon^{abc}\theta^b(s\varphi^c)\Big)\frac{g}{2} \\ &= \frac{g}{2}\Big(\epsilon^{abc}\epsilon^{bde}\theta^d\theta^e\theta^c - \epsilon^{abc}\epsilon^{bde}\theta^c\theta^d\theta^e\Big) \\ &= 0 \end{aligned} \tag{3.15}$$

where the last line follows from expanding out the sums involving permutation symbols and setting to zero terms with two identical ghost fields such as $\theta^1\theta^1\theta^2$. It remains to show $s^3\bar{\theta}^a = 0$. We begin by first considering s^2 applied to $\bar{\theta}^a$, that is

$$\begin{aligned} s^2\bar{\theta} &= -\frac{1}{\xi}sG^a \\ &= -\frac{1}{\xi}\int dy\left[\frac{\delta G^a\{A,\varphi\}}{\delta A^b_\mu(y)}sA^b_\mu(y) + \frac{\delta G^a\{A,\varphi\}}{\delta\varphi^b(y)}s\varphi^b(y)\right]. \end{aligned} \tag{3.16}$$

We now apply the BRS operator again and use $s^2 W^a_\mu = 0$ and $s^2\varphi^b = 0$ to get

$$\begin{aligned} s^3\bar{\theta} &= -\frac{1}{\xi}s^2G^a \\ &= -\frac{1}{\xi}\int dy\int dz\left[\frac{\delta^2 G^a\{A,\varphi\}}{\delta A^c_\mu(z)\delta A^b_\mu(y)}(sA^c_\mu(z))(sA^b_\mu(y)) + \frac{\delta^2 G^a\{A,\varphi\}}{\delta\varphi^c(z)\delta A^b_\mu(y)}(s\varphi^c(z))(sA^b_\mu(y))\right. \\ &\quad \left. +\frac{\delta^2 G^a\{A,\varphi\}}{\delta A^c_\mu(z)\delta\varphi^b(y)}(sA^c_\mu(z))(s\varphi^b(y)) + \frac{\delta^2 G^a\{A,\varphi\}}{\delta\varphi^c(z)\delta\varphi^b(y)}(s\varphi^c(z))(s\varphi^b(y))\right]. \end{aligned} \tag{3.17}$$

$G^a\{W,\varphi\}$ is a function of A^a and φ^a only, and since it does not have any ghost fields, there are no minus signs from the s operator. Since the terms sA^a_μ and $s\varphi^a$ each contain an odd number of ghost fields, the quantities

$$(sA^c_\mu(z))(sA^b_\mu(y)) \qquad \text{and} \qquad (s\varphi^c(z))(s\varphi^b(y)) \tag{3.18}$$

are anti-symmetric in the exchange of its indices and spatial dependence. This means the first and last terms in Eq. (3.17) vanish since they each multiply expressions which are symmetric in the exchange $b \leftrightarrow c$ and $z \leftrightarrow y$. After exchanging $b \leftrightarrow c$ and $z \leftrightarrow y$, the third term can be re-written so that Eq. (3.17) becomes

$$s^3\bar{\theta} = -\frac{1}{\xi}\int dy \int dz\ \frac{\delta^2 G^a\{A,\varphi\}}{\delta\varphi^c(z)\delta A^b_\mu(y)}\Big[(s\varphi^c(z))(sA^b_\mu(y)) + (sA^b_\mu(y))(s\varphi^c(z))\Big] = 0. \quad (3.19)$$

Again, sA^a_μ and $s\varphi^a$ each contain an odd number of ghost fields, so the expression in the brackets vanishes. We have now shown that the BRS operator s is nilpotent.

There is one final simplification we will make before proving Eq. (3.5). The ghost lagrangian in Eq. (A.14) is

$$\begin{aligned}\mathcal{L}_{\rm ghost} &= -\int dy\ \bar{\theta}^a(x)\frac{\delta G^a(x)}{\delta\alpha^c(y)}\theta^c(y) \\ &= -\int dy \int dz\ \bar{\theta}^a(x)\Big[\frac{\delta G^a(x)}{\delta A^b_\mu(z)}\frac{\delta A^b_\mu(z)}{\delta\alpha^c(y)} + \frac{\delta G^a(x)}{\delta\varphi^b(z)}\frac{\delta\varphi^b(z)}{\delta\alpha^c(y)}\Big]\theta^c(y). \end{aligned} \quad (3.20)$$

where $A^b_\mu(z)$ and $\varphi^b(z)$ are gauge transformed fields and $\alpha^c(y)$ is the parameter governing the transformation. The transformation properties of these fields are given in Eq. (A.16) and by using these transformations we notice that

$$\frac{\delta A^b_\mu(z)}{\delta\alpha^c(y)}\theta^c(y) = sA^b_\mu(z)\delta(y-z) \qquad \text{and} \qquad \frac{\delta\varphi^b(z)}{\delta\alpha^c(y)}\theta^c(y) = s\varphi^b(z)\delta(y-z). \quad (3.21)$$

Eq. (3.20) then becomes

$$\begin{aligned}\mathcal{L}_{\rm ghost} &= -\int dy\ \bar{\theta}^a(x)\frac{\delta G^a(x)}{\delta\alpha^c(y)}\theta^c(y) \\ &= -\int dy\ \bar{\theta}^a(x)\Big[\frac{\delta G^a(x)}{\delta A^b_\mu(y)}sA^b_\mu(y) + \frac{\delta G^a(x)}{\delta\varphi^b(y)}s\varphi^b(y)\Big]. \end{aligned} \quad (3.22)$$

Inspection of Eq. (3.16) shows that the ghost lagrangian can be written in the simple form

$$\mathcal{L}_{\rm ghost} = -\bar{\theta}^a(x)sG^a(x). \quad (3.23)$$

This form will be useful for proving Eq. (3.5) and the ET.

With all of these preliminary results, proving Eq. (3.5) is now easy. First consider the BRS transformed ghost lagrangian,

$$\begin{aligned}s\mathcal{L}_{\rm ghost} &= -s\bar{\theta}^a(x)sG^a(x) + \bar{\theta}^a(x)s^2G^a(x) \\ &= -s\bar{\theta}^a(x)sG^a(x) \end{aligned} \quad (3.24)$$

where have used $s^2G^a = 0$ as shown in Eqs. (3.18) through (3.19). Now consider the BRS transformed gauge fixing lagrangian,

$$\begin{aligned}s\mathcal{L}_{\rm gf} &= -\frac{G^a(x)}{\xi}sG^a(x) \\ &= s\bar{\theta}^a(x)sG^a(x) \end{aligned} \quad (3.25)$$

We now see that the sum of BRS transformed ghost and gauge fixing lagrangians vanishes which demonstrates the validity of Eq. (3.5). The full lagrangian in Eq. (A.1) is invariant under a BRS transformation given in Eq. (3.3). Though we haven't shown it, the measure of the functional integration is also invariant under a BRS transformation and thus the BRS is a symmetry of the theory.

Before leaving this section, we can formulate the BRS symmetry in a more symmetric form by introducing a commuting auxiliary scalar field B^a into the lagrangian and then integrating it out of the theory by performing a functional integral. We alter the gauge fixing term to now read

$$\mathcal{L}_{\rm gf} = -\frac{\xi}{2} B^a B^a + B^a G^a. \tag{3.26}$$

There are no derivatives in the quadratic term in B^a and so this field does not propagate. By performing the functional integral and using the resulting equations of motion, we recover the original lagrangian.

With this altered lagrangian, we must change the BRS transformation of the anti-ghost field and introduce one for B^a. The BRS transformations for B^a and $\bar{\theta}^a$ which leave the theory invariant are

$$\begin{aligned} s\bar{\theta}^a &= B^a \\ sB^a &= 0. \end{aligned} \tag{3.27}$$

The BRS transformations are now independent of the gauge fixing term and the BRS operator satisfies

$$s^2\bar{\theta}^a = sB^a = 0. \tag{3.28}$$

Making this change will be useful when considering how physical states are related to BRS invariance.

3.2 Physical States

We have seen that (covariant) quantization of the gauge theory has led to the introduction of additional unphysical degrees of freedom and care must be taken in order to separate the physical from the unphysical states. Following the arguments of Kugo and Ojima [59], we will *define* physical degrees of freedom as all states which are invariant under a BRS transformation. To make this more precise, we introduce the BRS current and BRS charge. Since BRS symmetry is a good symmetry of the lagrangian, Neother's theorem implies there is a conserved current

$$j_\mu^{\rm BRS} = \sum \frac{\delta \mathcal{L}}{\delta(\partial_\mu \Psi)} s\Psi \tag{3.29}$$

Here Ψ is any field in the theory and the sum extends over all fields $A^a_\mu, \varphi^a, \psi, \cdots$. The conserved charge is then the spatial integral over the time-like component.

$$Q_{\text{BRS}} = \int d^3x \; j_0^{\text{BRS}} \tag{3.30}$$

The charge generates an infinitesimal BRS transformation on the Hilbert space of states, and a physical state is one in which

$$Q_{\text{BRS}} \left|\alpha\right\rangle = 0. \tag{3.31}$$

When acting on fields, the charge behaves as follows

$$[Q_{\text{BRS}}, \Psi]_\mp = s\Psi \tag{3.32}$$

where the $\mp$ denotes either commutator or anticommutator depending on whether the field Ψ is commuting or Grassmann, and s is the BRS operator defined in Eq. (3.3). We showed at the end of the previous section, that after introducing the auxiliary field B^a, the s operator is strictly nilpotent and so this implies that

$$Q^2_{\text{BRS}} = 0. \tag{3.33}$$

Furthermore, since the charge is conserved it commutes with the hamiltonian and thus the S-matrix.

$$[Q_{\text{BRS}}, H] = 0 \qquad\qquad [Q_{\text{BRS}}, S] = 0 \tag{3.34}$$

The charge is hermitian provided we choose ghost fields to have the following hermiticity properties

$$(\theta^a)^\dagger = \theta^a \qquad\qquad (\bar\theta^a)^\dagger = -\bar\theta^a. \tag{3.35}$$

The minus sign for the second equation is present due to the anticommutating nature of the ghost fields and is required to make the lagrangian hermitian [59]:

The commuting of Q_{BRS} with the hamiltonian implies that the eigenspace of H can be divided into three subsets:

- The subset of states not annihilated by Q_{BRS}:

$$\mathcal{V}_2 = \{\left|\alpha\right\rangle, \; Q_{\text{BRS}} \left|\alpha\right\rangle \neq 0\} \tag{3.36}$$

- The subset of states obtained by applying Q_{BRS} to states in $\mathcal{V}_2$:

$$\mathcal{V}_0 = \{\left|\alpha\right\rangle, \; \left|\alpha\right\rangle = Q_{\text{BRS}} \left|\alpha'\right\rangle, \; \left|\alpha'\right\rangle \in \mathcal{V}_2\} \tag{3.37}$$

- The subset of states annihilated by Q_{BRS} but not in $\mathcal{V}_0$:

$$\mathcal{V}_1 = \{\left|\alpha\right\rangle, \; Q_{\text{BRS}} \left|\alpha\right\rangle = 0, \; \left|\alpha\right\rangle \notin \mathcal{V}_0\}. \tag{3.38}$$

An additional superscript on the states will be used when it is necessary to denote which subset a state belongs to, that is $|\alpha^{(i)}\rangle \in \mathcal{V}_i$. We can see immediately that states in $\mathcal{V}_2$ are not physical states since they are not annihilated by Q_{BRS}. States in the other two subsets are annihilated by the BRS charge and thus their union $\mathcal{V}_1 \cup \mathcal{V}_0$ forms a subspace which is invariant under the S matrix.

The subspace $\mathcal{V}_1 \cup \mathcal{V}_0$ can be further reduced. Notice that all states in $\mathcal{V}_0$ have zero norm since for any two states $|\alpha^{(0)}\rangle$ and $|\beta^{(0)}\rangle$, the inner product vanishes. That is

$$\langle \alpha^{(0)} | \beta^{(0)} \rangle = \langle \alpha^{(2)} | \, Q_{\text{BRS}} \, | \beta^{(0)} \rangle = 0, \tag{3.39}$$

where we have used the hermiticity of Q_{BRS}. Also the states in $\mathcal{V}_0$ are orthogonal to the states in $\mathcal{V}_1$,

$$\langle \alpha^{(0)} | \beta^{(1)} \rangle = \langle \alpha^{(2)} | \, Q_{\text{BRS}} \, | \beta^{(1)} \rangle = 0. \tag{3.40}$$

The states in $\mathcal{V}_0$ have zero norm and provide zero contribution to any physical matrix element. Furthermore, Eq. (3.40) implies that these decouple from the $\mathcal{V}_1$ and so we see that any two states in $\mathcal{V}_1 \cup \mathcal{V}_0$ which differ by zero norm states only are physically equivalent. We thus define the physical subspace to be the quotient space of $\mathcal{V}_1 \cup \mathcal{V}_0$ with respect to $\mathcal{V}_0$

$$\mathcal{H}_{\text{phys}} = \frac{\mathcal{V}_1 \cup \mathcal{V}_0}{\mathcal{V}_0}, \tag{3.41}$$

where we have defined two states to be equivalent if they differ by a zero norm state,

$$|\alpha\rangle \sim |\alpha'\rangle \;\text{ if }\; |\alpha\rangle - |\alpha'\rangle = Q_{\text{BRS}} \, |\beta\rangle \,, \;\text{ for }\; |\beta\rangle \in \mathcal{V}_2. \tag{3.42}$$

The physical subspace, $\mathcal{H}_{\text{phys}}$, is the set of all equivalence classes of elements in $\mathcal{V}_1 \cup \mathcal{V}_0$. We will see shortly that ghost fields and certain polarizations of the gauge fields have zero norm states and so we will usually take the representative member of the equivalence class to be a state in V_1.

In a quantum field theory the physical space is the Fock space of asymptotic fields, which are generated by the creation operators of the Fourier representation of the asymptotic field operators. Typically in a QFT with a sufficiently small coupling, calculations are not performed using asymptotic fields, but rather by using free fields in the presence of interactions. Physical matrix elements are computed by considering truncated Green's functions and using the LSZ reduction formula to account for the fact that the overlap of states created by the free field with those created by the physical field is not unity. In order to separate which fields correspond to physical states and which ones are unphysical or zero normed, we now work out the action of the Q_{BRS} charge on physical, asymptotic fields.

Consider a generic asymptotic field corresponding to a physical degree of freedom in

momentum space

$$\Psi^{\text{as,phys}} = \frac{1}{(2\pi)^3}\sum_\sigma \int \frac{d^3\mathbf{p}}{2E_p}\Big[u_\alpha(p,\sigma)a(p,\sigma)e^{-ip\cdot x} + v_\alpha(p,\sigma)b^\dagger(p,\sigma)e^{+ip\cdot x}\Big]$$
$$p = (E_p, \mathbf{p}) \quad \text{and} \quad E_p^2 - |\mathbf{p}|^2 = m^2 \tag{3.43}$$

where $u_\alpha(p,\sigma)$ and $v_\alpha(p,\sigma)$ are generic polarization tensors (or spinors). If we now apply the BRS charge to this field, we get

$$[Q_{\text{BRS}}, \Psi^{\text{as,phys}}]_\mp = \frac{1}{(2\pi)^3}\sum_\sigma \int \frac{d^3\mathbf{p}}{2E_p}\Big[u_\alpha(p,\sigma)[Q_{\text{BRS}}, a(p,\sigma)]_\mp e^{-ip\cdot x}$$
$$+v_\alpha(p,\sigma)[Q_{\text{BRS}}, b^\dagger(p,\sigma)]_\mp e^{+ip\cdot x}\Big] \tag{3.44}$$

When acting on a physical state the annihilation operator $a(p,\sigma)$ will remove one quantum from the system. As a concrete example, consider a state with a single mode of $\Psi^{\text{as,phys}}$ with momentum p' and polarization σ' and an arbitrary number of other physical states and denote this state by $|p',\sigma';\cdots\rangle$. The action of $[Q_{\text{BRS}}, a(p,\sigma)]_\mp$ on this state gives

$$\begin{aligned}[Q_{\text{BRS}}, a(p,\sigma)]_\mp |p',\sigma';\cdots\rangle &= \Big(Q_{\text{BRS}}\ a(p,\sigma) \mp a(p,\sigma)Q_{\text{BRS}}\Big)|p',\sigma';\cdots\rangle \\ &= 2E_p(2\pi)^3\delta(\mathbf{p}-\mathbf{p}')\delta_{\sigma\sigma'}Q_{\text{BRS}}\,|0,\cdots\rangle \\ &= 0 \end{aligned} \tag{3.45}$$

since Q_{BRS} annihilates any physical state. A similar procedure can be carried out for the the creation operator $b^\dagger(p,\sigma)$. We conclude that physical components of asymptotic fields must have vanishing BRS variation

$$[Q_{\text{BRS}}, \Psi^{\text{as,phys}}]_\mp = s\Psi^{\text{as,phys}} = 0. \tag{3.46}$$

Not all fields in the theory describe physical modes and in order to distinguish the physical fields from the unphysical fields, we must derive the BRS transformations for asymptotic fields. The transformation properties of asymptotic fields can be studied by considering the Green's functions with one external field Ψ_I replaced with its BRS transformed field $s\Psi_I$. Here the label I indicates the spacetime dependence x_I, and contains all other quantum numbers as well as distinguishing between different fields.

$$\langle T\Psi_I\Psi_{I_1}\cdots\Psi_{I_n}\rangle \to \langle T(s\Psi_I)\Psi_{I_1}\cdots\Psi_{I_n}\rangle \tag{3.47}$$

We can now analyze the Green's function using the LSZ reduction formula [60] and place all external particles on shell and extract the pole terms. Since the pole terms require one-particle intermediate states, we find

$$\langle T(s\Psi_I)\Psi_{I_1}\cdots\Psi_{I_n}\rangle = \sum_K \langle T(s\Psi_I)\underline{\Psi}_K\rangle\langle T\Psi_K\Psi_{I_1}\cdots\Psi_{I_n}\rangle + \text{ non-pole terms} \tag{3.48}$$

The underline means that the Green's function has been truncated for the field Ψ_K and the summation over K mean that all space-time and group theoretic indices have been contracted and the proper integration over x_K has been performed. Diagrammatically, Eq. (3.48) reads

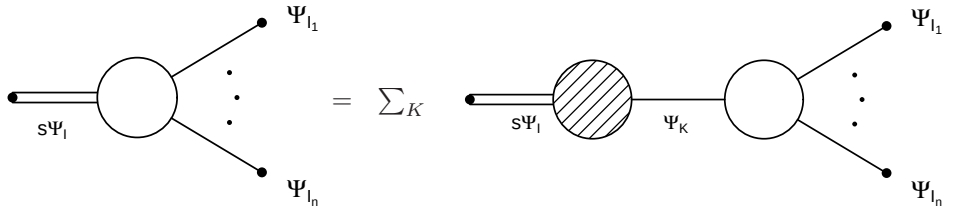

+ non-pole

where the double line represents insertion of the composite operator $s\Psi_I$. In order to couple with a single external leg, asymptotic BRS transformation must be linear and so it can be expressed as

$$s\Psi_I^{as} \underset{\text{on-shell}}{\longrightarrow} C_{IK}\Psi_K^{as} \tag{3.49}$$

and C_{IK} is given by

$$C_{IK} = \langle T(s\Psi_I)\underline{\Psi}_K\rangle|_{\text{on-shell}}. \tag{3.50}$$

A field Ψ_K will only give a non-zero contribution to Eq. (3.49) if the field has the same mass as Ψ_I. Usually, Ψ_K will be an anti-ghost field since the linear terms for $s\Psi$ involve ghost fields. For the anti-ghost field, this will not be true since its BRS transformation involves the gauge fixing term and does not contain the gauge field.

The manipulations of the previous paragraph have been very formal and we would like to apply them to the specific fields in the toy theory. The first field we will consider is the gauge field. The argument begins with Eq. (3.48) and we proceed through the same line of reasoning that lead us to Eq. (3.49) where we use $A_\mu(x)^a$ instead of Ψ_I. Inserting the BRS variation of the free gauge field into Eq. (3.3) gives

$$\langle T(sA_\mu(x)^a)\Psi_{I_1}\cdots\Psi_{I_n}\rangle = \tag{3.51}$$

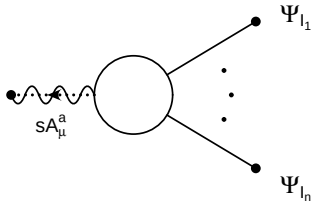

where the wiggle line on top of the ghost line represents insertion of the composite operator $sA_\mu^a(x)$. After inserting the expression for $sA_\mu^a(x)$ from Eq. (3.3), the diagram becomes

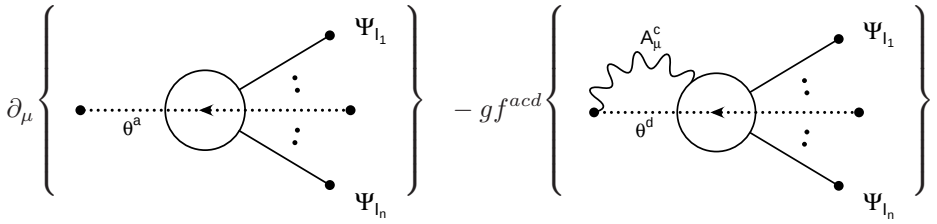

(3.52)

Since each term in $sA^a_\mu(x)$ contains a ghost field and since ghost number is conserved, we have extended the ghost line through the blob and have included it as an external leg. Since we want the asymptotic fields, we look for the pole terms

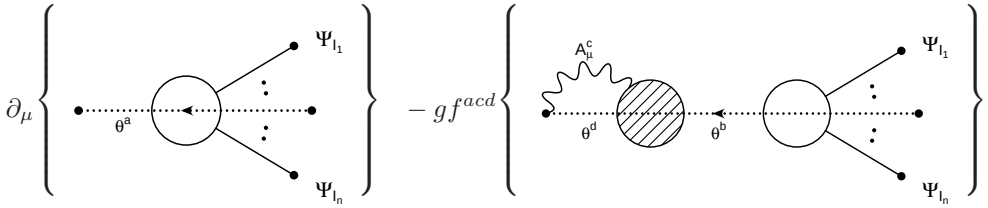

+non-pole terms (3.53)

The shading in the second diagram denotes that the blob is one particle irredicible. The second diagram gives a contribution proportional to the first, and so Eq. (3.49) for a gauge field takes the form

$$sA^{\mathrm{as},a}_\mu = \Big[1 + \mathcal{O}\Big(\frac{g}{4\pi}\Big)\Big]\partial_\mu\theta^{\mathrm{as},a}. \tag{3.54}$$

In the literature, there exist renormalization schemes in which the coefficient in the brackets is unity; however, in this work the $\overline{MS}$ scheme is used exclusively and so no such renormalization will be made. The conclusion we draw from Eq. (3.54) is that $sA^{\mathrm{as},a}_\mu$ depends linearly on $\theta^{\mathrm{as},a}$. From this result we conclude that states created by A^{as}_μ which have polarization for which $\epsilon \propto k_\mu$ are elements of $\mathcal{V}_2$ – they are not physical. In short, we see that dropping the non-linear terms in the Eq. 3.49 gives the asymptotic BRS transformation. If we proceeded similarly for the rest of the fields, we would find that this rule indeed holds. We will not go through the detailed diagrammatic derivation for each field, but instead summarize the results. The BRS transformations for the asymptotic fields in $SU(2)$ theory are

$$\begin{aligned}
&sA^{\mathrm{as},a}_\mu \sim \partial_\mu\theta^a && s\psi^{\mathrm{as}} = 0\\
&s\Phi^{\mathrm{as}} = 0 && sh^{\mathrm{as}} = 0\\
&s\theta^{\mathrm{as},a} = 0 && s\varphi^{\mathrm{as},a} \sim -M\theta^{\mathrm{as},a}\\
&s\bar{\theta}^{\mathrm{as},a} = B^{\mathrm{as},a} \sim -\frac{1}{\xi}G^{\mathrm{as},a} && sB^{\mathrm{as},a} = 0
\end{aligned} \tag{3.55}$$

where we have use $M = \frac{gv}{2}$ for $s\varphi^{\mathrm{as},a}$ and $\sim$ denotes equality up to a (calculable) factor of order one.

The states which are produced by these asymptotic fields can now be classified as belonging to $\mathcal{V}_0, \mathcal{V}_1$ or $\mathcal{V}_2$ by inspecting Eq. (3.55). We have already mentioned that gauge boson states with polarization of $\epsilon_\mu \sim k_\mu$, are not physical and thus are in $\mathcal{V}_2$. Similarly we see that the would-be Goldstone boson fields, φ^a, and the anti-ghost fields, $\bar{\theta}^a$, are not annihilated by the BRS charge and thus also belong to $\mathcal{V}_2$. The remaining states are all part of $\mathcal{V}_1 \cup \mathcal{V}_0$. The ghost fields, θ^a and the auxiliary fields B^a are the result of a BRS transformation and so states created from these fields belong to $\mathcal{V}_0$ and have zero norm. The remainder of the fields, massless scalars, massless fermions, and the three remaining polarizations of the gauge field, have physical, positively-normed states which belong to $\mathcal{V}_1$.

Since the gauge fixing term for a broken theory usually contains both gauge fields and would-be Goldstone boson fields, it is worth examining B^a in more detail.

$$B^{\mathrm{as},a} \sim -\frac{1}{\xi} G^{\mathrm{as},a} \tag{3.56}$$

The calculations in this work were all done in R_ξ gauge by using the gauge fixing term of Eq. (3.6) and so we now specialize to this case.

$$B^{\mathrm{as},a} \sim -\frac{1}{\xi}(\partial_\mu A^{\mathrm{as},a}_\mu - \xi' M \varphi^{\mathrm{as},a}) \tag{3.57}$$

Even though the gauge boson states with (scalar) polarization $\epsilon_\mu \sim k_\mu$ and the Goldstone boson states are unphysical, a linear combination of these states given by the previous equation has zero norm and is an element of $\mathcal{V}_0$. The orthogonal linear combination remains in $\mathcal{V}_2$. For a massive gauge boson, the two transverse polarizations $\epsilon_{\perp\mu}$ and the longitudinal polarization $\epsilon_{L\mu} = \frac{1}{M}(|\mathbf{k}|, E\hat{k})$ are physical states and the fourth polarization – the so called scalar polarization, for which $\epsilon_{s\mu} \propto k_\mu$, and the would-be Goldstone boson states are either unphysical or zero normed, depending on which linear combination we consider. The equivalence theorem stems from the observation that at high energy, the longitudinal polarization tensor has a large component proportional to k_μ and thus $\epsilon_{s\mu}$,

$$\epsilon_{L\mu} = \frac{k_\mu}{M} + \mathcal{O}\Big(\frac{E}{M}\Big). \tag{3.58}$$

In order to compute the largest part of the amplitude, instead of considering longitudinal polarizations, we can consider scalar polarizations, and due to Eq. (3.57), this amplitude is related to the one involving the Goldstone boson. This statement will be made more precise in the next section when we formulate the Goldstone boson equivalence theorem.

3.3 Proof of the equivalence theorem

In this section we formulate the equivalence theorem by recognizing that the BRS transformations generate a continuous symmetry and so there must be a set of Ward identities. The

equivalence theorem follows as a consequence of one such Ward identity. First we will discuss Ward identities in general and then proceed with the proof of the equivalence theorem. The discussion of the Ward identities will only be a brief summery and a more complete treatment can be found in Bohm et al. [56]

The Ward identities associated with BRS invariance are called the Slavnov-Taylor identities; we will briefly summarize the main ideas. The identities follow from the BRS invariance of the functional integral with sources. We begin by introducing sources for the BRS transformed fields into the generating functional

$$Z\{J_{I_1},\cdots,K_{I_1},\cdots\} = \int \prod_L \mathcal{D}\Psi_L \exp\Big(i\int dx\ \mathcal{L}_{\rm tot}\Big) \tag{3.59}$$

where Ψ_L denotes any one of the fields in the theory and L, as usual, denotes the space-time dependence and other quantum numbers for this field. The lagrangian $\mathcal{L}_{\rm tot}$ is the lagrangian given in Eq. (A.1) plus the source terms

$$\begin{aligned}\mathcal{L}_{\rm tot} &= \mathcal{L} + J^{a,\mu}A^a_\mu + J^i_\Phi\Phi^i + J^i_{\Phi^\dagger}\Phi^{i\dagger} + J^a_\theta\theta^a - \bar\theta^a J^a_{\bar\theta} + J^i_\psi\psi^i - \bar\psi^i J^i_{\bar\psi} + J^a_\varphi\varphi^a + J_h h \\ &\quad + K^{a,\mu}(sA^a_\mu) + K^i_\Phi(s\Phi^i) + K^i_{\Phi^\dagger}(s\Phi^{i\dagger}) + K^a_\theta(s\theta^a) \\ &\quad + K^i_\psi(s\psi^i) - (s\bar\psi^i)K^i_{\bar\psi} + K^a_\varphi\varphi^a + K_h h.\end{aligned} \tag{3.60}$$

All of the sources are assumed to be BRS invariant. The BRS transformed anti-ghost field, $s\bar\theta^a$, does not have a source coupled to it since in the original formulation of the BRS transformation, without the auxiliary fields defined, we have that $s^2\bar\theta^a \neq 0$. The generating function is BRS invariant, and so if we apply a BRS transformation to Eq. (3.59) and expand in the anticommuting parameter ζ, the linear coefficient must vanish. That is

$$\begin{aligned}0 &= \int \prod_L \mathcal{D}\Psi_L \exp\Big(i\int dx\ \mathcal{L}_{\rm tot}\Big) \\ &\quad \times\Big[\int dx\ J^{a,\mu}(sA^a_\mu) + J^i_\Phi(s\Phi^i) + J^i_{\Phi^\dagger}(s\Phi^{i\dagger}) - J^a_\theta(s\theta^a) - (s\bar\theta^a)J^a_{\bar\theta} \\ &\quad - J^i_\psi(s\psi^i) - (s\bar\psi^i)J^i_{\bar\psi} + J^a_\varphi(s\varphi^a) + J_h(sh)\Big]\end{aligned} \tag{3.61}$$

We can replace the BRS transformed fields with a functional derivative with respect to the corresponding source acting on the generating function

$$\begin{aligned}0 &= \int dx\ \Big[J^{a,\mu}\frac{\delta}{i\delta K^{a,\mu}} - J^a_\theta\frac{\delta}{i\delta K^a_\theta} + \frac{1}{\xi}G^a\Big\{\frac{\delta}{i\delta J^{a,\mu}},\frac{\delta}{i\delta J^a_\varphi}\Big\}J^a_{\bar\theta} - J^i_\psi\frac{\delta}{i\delta K^i_\psi} - \frac{\delta}{i\delta K^i_{\bar\psi}}J^i_{\bar\psi} \\ &\quad + J^a_\varphi\frac{\delta}{i\delta K^a_\varphi} + J_h\frac{\delta}{i\delta K_h}\Big] \times \int \prod_L \mathcal{D}\Psi_L \exp\Big(i\int dx\ \mathcal{L}_{\rm tot}\Big)\end{aligned} \tag{3.62}$$

This complicated expression is a manifestation of the BRS symmetry and it is used to generate relationships between seemingly unrelated Green's function. The Green's functions are generated by differentiating this expression with respect to the external sources and then putting the sources

on-shell. The following example serves to illustrate this procedure. Consider the expression,

$$\begin{aligned} 0 &= \frac{\delta}{i\delta J^{b,\nu}(y)}\frac{\delta}{i\delta J^{a,\mu}(x)}\int dx' \left[J^{a,\mu}\frac{\delta}{i\delta K^{a,\mu}} - J^a_\theta\frac{\delta}{i\delta K^a_\theta} + \frac{1}{\xi}G^a\Big\{\frac{\delta}{i\delta J^{a,\mu}},\frac{\delta}{i\delta J^a_\varphi}\Big\}J^a_{\bar\theta}\right. \\ &\quad \left. -J^i_\psi\frac{\delta}{i\delta K^i_\psi} - \frac{\delta}{i\delta K^i_{\bar\psi}}J^i_{\bar\psi} + J^a_\varphi\frac{\delta}{i\delta K^a_\varphi} + J_h\frac{\delta}{i\delta K_h}\right] Z\{J_{I_1},\cdots,K_{I_1},\cdots\}\Big|_{\text{all } J=0}. \end{aligned} \tag{3.63}$$

After performing the differentiation and setting the sources to zero we get

$$0 = \langle T(sA^a_\mu(x))A^b_\nu(y)\rangle + \langle T(sA^b_\nu(y))A^a_\mu(x)\rangle \tag{3.64}$$

More generally, for any Green's function, we have

$$\begin{aligned} 0 &= s\langle T\prod_i \Psi_{L_i}\rangle \\ &= \sum_k \sigma_k \langle T\prod_{i<k}\Psi_{L_i}(s\Psi)_{L_k}\prod_{j>k}\Psi_{L_j}\rangle \end{aligned} \tag{3.65}$$

where is σ_k is the sign that results from anticommuting s past Grassmann valued fields. Eq. (3.65) defines the action of s on a green's function and does not imply that the Green's function itself is BRS invariant. Instead, it provides a very useful way to derive the Ward identities of the BRS symmetry and will be the starting point for the proof of the equivalence theorem.

Before we proceed, we pause to derive an expression for the equation of motion in terms of Green's function. This is achieved by considering an small shift in a given (arbitrary) field, $\Psi_K \to \Psi_K + \epsilon\delta\Psi_K$, on the generating functional of Eq. (3.59). After inserting this shift into the generating function and then expanding to first order in ϵ, we get

$$Z \to \int\prod_L \mathcal{D}\Psi_L\left[1 + i\epsilon\delta\Psi_K\Big(\frac{\delta S}{\delta\Psi_K} + J_K\Big)\right]\exp\Big(iS + i\langle\sum_L J_L\Psi_L\rangle\Big) \tag{3.66}$$

where S is the action, obtained by integrating $\mathcal{L}$ in Eq. (A.1)

$$S = \int dx\ \mathcal{L} \qquad \text{and} \qquad \langle\cdots\rangle = \int dx\ (\cdots). \tag{3.67}$$

For the equation of motion, the sources for the BRS fields do not play a role and so these have been set to zero. The functional will be stationary when the linear term in ϵ vanishes so we have

$$0 = \int\prod_L \mathcal{D}\Psi_L\Big(\frac{\delta S}{\delta\Psi_K} + \frac{\delta}{i\delta\Psi_K}\Big)\exp\Big(iS + i\langle\sum_L J_L\Psi_L\rangle\Big) \tag{3.68}$$

where we have replaced the current with a functional derivative with respect to the field. This identity can be used to generate relationships among various Green's functions by differentiating Eq. (3.68) with respect to the sources and then setting all the sources to zero. The resulting expression takes the form

$$0 = \langle T\frac{\delta S}{\delta\Psi_K}\prod_i\Psi_{L_i}\rangle + \langle T\frac{\delta}{i\delta\Psi_K}\prod_i\Psi_{L_i}\rangle \tag{3.69}$$

where $\prod_i \Psi_{L_i}$ is any product of fields. This expression will be useful in what follows.

Now that we have finished our brief discussion of the Ward identities of the BRS symmetry, we focus on one such Ward identity. Consider a Green's function with one anti-ghost field and one gauge fixing term, and apply the BRS operator. The result is

$$\begin{aligned} 0 &= s\langle T\bar{\theta}^a(x)G^b(y)\rangle \\ &= \langle T(s\bar{\theta}^a(x))G^b(y)\rangle - \langle T\bar{\theta}^a(x)(sG^b(y))\rangle. \end{aligned} \tag{3.70}$$

The second line follows from Eq. (3.65) and the minus sign between the terms is due to the anticommuting nature of s. Now we insert the equation of motion in the form of Eq. (3.69) for the anti-ghost field

$$\begin{aligned} \frac{\delta S}{\delta\bar{\theta}^b(y)} &= \frac{\delta}{\delta\bar{\theta}^b(y)}\int dx\ \mathcal{L}_{\rm ghost} \\ &= -\frac{\delta}{\delta\bar{\theta}^b(y)}\int dx\ \bar{\theta}^a(x)sG^a(x) = -sG^b(y) \end{aligned} \tag{3.71}$$

to remove $sG^b(y)$, and then use Eq. (3.69). Furthermore, we replace $s\bar{\theta}^a$ with its expression from Eq. (3.3), and with these changes Eq. (3.70) becomes

$$\begin{aligned} 0 &= \langle T(s\bar{\theta}^a(x))G^b(y)\rangle - \langle T\bar{\theta}^a(x)\frac{\delta S}{\delta\bar{\theta}^b(y)}\rangle \\ &= -\frac{1}{\xi}\langle TG^a(x)G^b(y)\rangle + \langle T\frac{\delta}{i\delta\bar{\theta}^b(y)}\bar{\theta}^a(x)\rangle \\ &= -\frac{1}{\xi}\langle TG^a(x)G^b(y)\rangle - i\delta^{ab}\delta(x-y) \end{aligned} \tag{3.72}$$

or in the final form

$$\langle TG^a(x)G^b(y)\rangle = -i\xi\delta^{ab}\delta(x-y) \tag{3.73}$$

This Ward identity is valid for any covariant gauge; however, we will now specialize to R_ξ gauge where the Ward identity will then take the very explicit form

$$\begin{aligned} -i\xi\delta^{ab}\delta(x-y) &= \langle T\{(\partial\cdot A^a)_x(\partial\cdot A^b)_y - \xi' M(\varphi^a)_x(\partial\cdot A^b)_y \\ &\quad -\xi' M(\partial\cdot A^a)_x(\varphi^b)_y + (\xi' M)^2(\varphi^a)_x(\varphi^b)_y\}\rangle. \end{aligned} \tag{3.74}$$

In Fourier space this expression becomes

$$-i\xi\delta^{ab} = k^\mu k^\nu G_{\mu\nu}^{A^aA^b}(k) + i\xi' Mk^\mu G_\mu^{\varphi^aA^b}(k) - i\xi' Mk^\mu G_\mu^{A^a\varphi^b}(k) + \xi'^2M^2G^{\varphi^a\varphi^b}(k), \tag{3.75}$$

where we have used the convention that the momentum is flowing from x to y as in Fig. (3.1). Furthermore, we have defined $G_{\mu\nu}^{A^aA^b}$ as the Green's function involving A^a and A^b, $G_\mu^{\phi^aA^b}$ as the Green's function involving φ^b and A^b, etc. We can make Eq. (3.75) look simpler if we write the

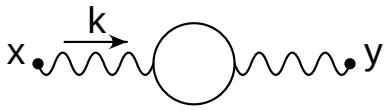

Figure 3.1: The momentum is positive flowing into y.

tensor valued Green's functions in terms of simpler (scalar) functions, defined as follows

$$\begin{aligned} G_{\mu\nu}^{A^a A^b}(k) &= \delta^{ab}(P_{\mu\nu}^T G_T^{AA}(k) + P_{\mu\nu}^L G_L^{AA}(k)) \\ G_{\mu}^{A^a \varphi^b}(k) &= ik_\mu \delta^{ab} G^{A\varphi}(k) \\ G_{\mu}^{\varphi^a A^b}(k) &= -ik_\mu \delta^{ab} G^{A\varphi}(k) \\ G^{\varphi^a \varphi^b}(k) &= \delta^{ab} G^{\varphi\varphi}(k) \end{aligned} \tag{3.76}$$

where

$$\begin{aligned} P_{\mu\nu}^T &= g_{\mu\nu} - \frac{k_\mu k_\nu}{k^2} \\ P_{\mu\nu}^L &= \frac{k_\mu k_\nu}{k^2}. \end{aligned} \tag{3.77}$$

are the transverse and the longitudinal projectors, respectively. The Ward identity then takes a more simple form,

$$-i\xi = k^2 G^{AA}(k) + 2\xi' M k^2 G^{A\varphi}(k) + \xi'^2 M^2 G^{\varphi\varphi}(k). \tag{3.78}$$

It will be useful to introduce the (full) propagator matrix

$$\begin{aligned} G_{(\mu\nu)}^{ab} &= \begin{pmatrix} G_{\mu\nu}^{A^a A^b} & G_{\mu}^{A^a \varphi^b} \\ G_{\nu}^{\varphi^a A^b} & G^{\varphi^a \varphi^b} \end{pmatrix} \\ &= \delta^{ab} \begin{pmatrix} P_{\mu\nu}^T G_T^{AA} + P_{\mu\nu}^L G_L^{AA} & ik_\mu G^{A\varphi} \\ -ik_\nu G^{A\varphi} & G^{\varphi\varphi} \end{pmatrix}. \end{aligned} \tag{3.79}$$

Similarly, we can define the (full) matrix (1PI) proper functions,

$$\begin{aligned} \Gamma_{(\mu\nu)}^{ab} &= \begin{pmatrix} P_{\mu\nu}^T \Gamma_T^{A^a A^b} + P_{\mu\nu}^L \Gamma_L^{A^a A^b} & \Gamma_{\mu}^{A^a \varphi^b} \\ \Gamma_{\nu}^{\varphi^a A^b} & \Gamma^{\varphi^a \varphi^b} \end{pmatrix} \\ &= \delta^{ab} \begin{pmatrix} P_{\mu\nu}^T \Gamma_T^{AA} + P_{\mu\nu}^L \Gamma_L^{AA} & -ik_\mu \Gamma^{A\varphi} \\ ik_\nu \Gamma^{A\varphi} & \Gamma^{\varphi\varphi} \end{pmatrix} \end{aligned} \tag{3.80}$$

where we have defined the scalar functions

$$\begin{aligned} \Gamma_{\mu\nu}^{W^a W^b}(k) &= \delta^{ab}(P_{\mu\nu}^T \Gamma_T^{AA}(k) + P_{\mu\nu}^L \Gamma_L^{AA}(k)) \\ \Gamma_{\mu}^{W^a \varphi^b}(k) &= -ik_\mu \delta^{ab} \Gamma^{W\varphi}(k) \\ \Gamma_{\nu}^{\varphi^a W^b}(k) &= ik_\mu \delta^{ab} \Gamma^{W\varphi}(k) \\ \Gamma^{\varphi^a \varphi^b}(k) &= \delta^{ab} \Gamma^{\varphi\varphi}(k). \end{aligned} \tag{3.81}$$

$G^{ab}_{(\mu\nu)}$ and $\Gamma^{ab}_{(\mu\nu)}$ are inverses of each other.

$$\begin{aligned} G^{ac}_{(\mu\lambda)}\Gamma^{cb(\lambda\nu)} &= \delta^{ab}\begin{pmatrix} P^{T\nu}_{\mu}G^{AA}_{T}\Gamma^{AA}_{T} + P^{L\nu}_{\mu}(G^{AA}_{L}\Gamma^{AA}_{L} - k^2 G^{A\varphi}\Gamma^{A\varphi}) & -ik_{\mu}(G^{AA}_{L}\Gamma^{A\varphi} - G^{A\varphi}\Gamma^{\varphi\varphi}) \\ -ik^{\nu}(G^{A\varphi}\Gamma^{AA}_{L} - G^{\varphi\varphi}\Gamma^{A\varphi}) & -k^2 G^{A\varphi}\Gamma^{A\varphi} + G^{\varphi\varphi}\Gamma^{\varphi\varphi} \end{pmatrix} \\ &= i\delta^{ab}\begin{pmatrix} \delta^{\nu}_{\mu} & 0 \\ 0 & 1 \end{pmatrix} \end{aligned} \tag{3.82}$$

The relationships between the scalar functions can now be read off

$$\begin{aligned} & G^{WW}_{T}\Gamma^{AA}_{T} = i \\ & -G^{WW}_{T}\Gamma^{AA}_{T} + G^{AA}_{L}\Gamma^{AA}_{L} - k^2 G^{A\varphi}\Gamma^{A\varphi} = 0 \\ & G^{WW}_{L}\Gamma^{A\varphi} - G^{A\varphi}\Gamma^{\varphi\varphi} = 0 \\ & G^{W\varphi}\Gamma^{AA}_{L} - G^{\varphi\varphi}\Gamma^{A\varphi} = 0 \\ & -k^2 G^{W\varphi}\Gamma^{A\varphi} + G^{\varphi\varphi}\Gamma^{\varphi\varphi} = i. \end{aligned} \tag{3.83}$$

After solving for the G's in terms of the Γ's, we have

$$\begin{aligned} G^{AA}_{T} &= \frac{i}{\Gamma^{AA}_{T}} \\ G^{A\varphi} &= \frac{i\Gamma^{A\varphi}}{\Gamma^{AA}_{L}\Gamma^{\varphi\varphi} - k^2\Gamma^{A\varphi}\Gamma^{A\varphi}} \\ G^{AA}_{L} &= \frac{i\Gamma^{\varphi\varphi}}{\Gamma^{AA}_{L}\Gamma^{\varphi\varphi} - k^2\Gamma^{A\varphi}\Gamma^{A\varphi}} \\ G^{\varphi\varphi} &= \frac{i\Gamma^{AA}}{\Gamma^{AA}_{L}\Gamma^{\varphi\varphi} - k^2\Gamma^{A\varphi}\Gamma^{A\varphi}}. \end{aligned} \tag{3.84}$$

After substituting for the G's into the Ward identity of Eq. (3.75), we get

$$-\xi(\Gamma^{AA}_{L}\Gamma^{\varphi\varphi} - k^2\Gamma^{A\varphi}\Gamma^{A\varphi}) = k^2\Gamma^{\varphi\varphi} + 2\xi' M k^2\Gamma^{A\varphi} + \xi'^2 M^2\Gamma^{AA}_{L}. \tag{3.85}$$

This expression and the one of Eq. (3.75) are consequences of the BRS symmetry – they relate the two point functions involving gauge fields and Goldstone bosons to one another.

We are finally in a position to derive the equivalence theorem and, for simplicity, we will only consider the case of a single longitudinally polarized gauge boson. We start with the generalized Ward identity of Eq. (3.65) for the case of a Green's function involving one anti-ghost field and an arbitrary number of physical fields,

$$0 = s\langle T\bar{\theta}^{a}(x)\prod_{l}\Psi^{\rm phys}_{I_l}\rangle \tag{3.86}$$

where again I_i denotes all of the appropriate quantum numbers and space-time dependencies. Since we are ultimately interested in calculating S matrix elements, we place all of the states on-shell which amounts to replacing the free fields with their asymptotic values. The BRS operator

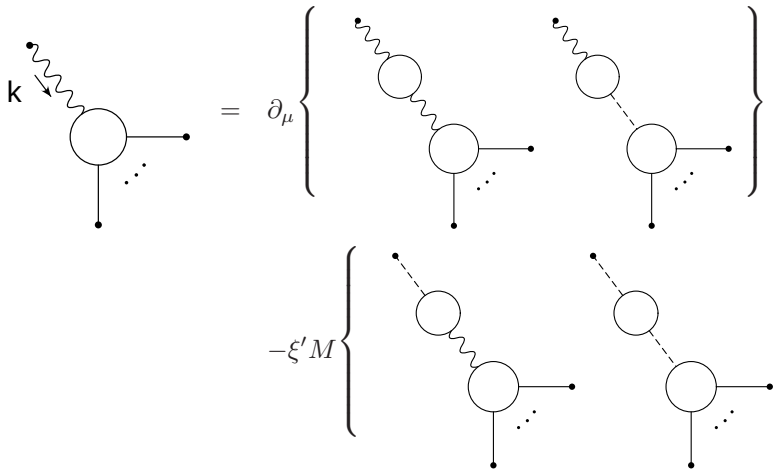

$$= \partial_\mu \left\{ \right\} \tag{3.89}$$

$$-\xi' M \left\{ \right\} \tag{3.90}$$

Figure 3.2: Diagrammatic description of Eq. (3.91)

annihilates all of these fields except the first one, and so we have

$$\begin{aligned} 0 &= \langle T(s\bar{\theta}^a(x)) \prod_l \Psi_{I_l}^{\text{phys}} \rangle \\ &= -\frac{1}{\xi} \langle T G^a(x) \prod_l \Psi_{I_l}^{\text{phys}} \rangle \\ &= \langle T\Big(\partial^\mu A_\mu^a(x) - \xi' M \varphi^a(x)\Big) \prod_l \Psi_{I_l}^{\text{as,phys}} \rangle, \end{aligned} \tag{3.87}$$

and after passing to Fourier space

$$0 = \langle T(ik^\mu A_\mu^a - \xi' M \varphi^a) \prod_l \Psi_{I_l}^{\text{as,phys}} \rangle. \tag{3.88}$$

The momentum of the A is chosen to flow into the diagram as shown in Fig. (3.2). For the calculation of the S matrix element, we need to truncate the external legs and since the A_μ^a field is contracted with a derivative, it can mix into the φ^a field as shown diagrammatically in Fig. (3.2). The amplitude corresponding to the diagrams in Fig. (3.2) can be written, after using the full propagator, as

$$\begin{aligned} 0 &= (ik_\mu, -\xi' M) G^{ab(\mu\nu)}(k) \begin{pmatrix} \langle T \underline{A}_\nu^b \prod_l \Psi_{I_l}^{\text{as,phys}} \rangle \\ \langle T \underline{\varphi}^b \prod_l \Psi_{I_l}^{\text{as,phys}} \rangle \end{pmatrix} \\ &= \Big(ik^\nu (G_L^{AA} + \xi' M G^{A\varphi}), -(k^2 G^{A\varphi} + \xi' M G^{\varphi\varphi})\Big) \begin{pmatrix} \langle T \underline{A}_\nu^b \prod_l \Psi_{I_l}^{\text{as,phys}} \rangle \\ \langle T \underline{\varphi}^b \prod_l \Psi_{I_l}^{\text{as,phys}} \rangle \end{pmatrix} \end{aligned} \tag{3.91}$$

Or after some rearrangement,

$$k^\nu \langle T \underline{A}_\nu^b \prod_l \Psi_{I_l}^{\text{as,phys}} \rangle = iMC(k^2) \langle T \underline{\varphi}^b \prod_l \Psi_{I_l}^{\text{as,phys}} \rangle \tag{3.92}$$

where $C(k^2)$ is defined by

$$C(k^2) \equiv -\frac{1}{M}\frac{k^2 G^{A\varphi} + \xi' M G^{\varphi\varphi}}{G_L^{AA} + \xi' M G^{A\varphi}} \tag{3.93}$$

Later we will calculate the expression for $C(k^2)$ for R_ξ gauge with the $\overline{MS}$ renormalization scheme, and for such a calculation, it is far easier to write the expression in terms of the proper functions instead of Green's functions. After replacing the G's with the Γ's, we get

$$C(k^2) \quad = \quad -\frac{1}{M}\frac{k^2\Gamma^{A\varphi} + \xi' M\Gamma_L^{AA}}{(\Gamma_L^{\varphi\varphi} + \xi' M\Gamma^{A\varphi})}. \tag{3.94}$$

This expression involves three two point functions, and we can eliminate one in favor of the other two using the Ward identity involving the Γ's. Using Eq. (3.85), the denominator becomes,

$$\Gamma^{\varphi\varphi} + \xi' M\Gamma^{A\varphi} \quad = \quad \frac{(k^2\Gamma^{A\varphi} + \xi' M\Gamma_L^{AA})(\xi\Gamma^{A\varphi} - \xi' M)}{\xi\Gamma_L^{AA} + k^2} \tag{3.95}$$

and after inserting this into the expression for $C(k^2)$ we get

$$C(k^2) \quad = \quad \frac{1}{M}\frac{\xi\Gamma_L^{AA} + k^2}{\xi' M - \xi\Gamma^{A\varphi}}. \tag{3.96}$$

We note that there could have been a different factor of $C(k^2)$ for each $a = 1, 2, 3$; however, the custodial symmetry, $SO(3)_C$, guarantees that each field has the same correction factor. In the standard model the custodial symmetry is broken and the charged weak gauge bosons ($W^\pm$), the neutral gauge boson (Z), and the photon (γ) each receive a different factor.

Ultimately we are after the S matrix element for A production and so the LSZ reduction formula tells us that we must truncate each external leg, place them on-shell, and then multiply by the R-factor and the appropriate polarization tensor. The S matrix involving a single gauge boson in the initial state then reads

$$\langle \cdots | \, S \, | A_L^a(k) \cdots \rangle = \epsilon_\mu^a(k, L)\langle T\underline{A}_\mu^a(k) \cdots \rangle \sqrt{R_A} \tag{3.97}$$

where $k^2 = M_{\text{phys}}^2$ and a subscript has been placed on M_{phys} in order to distinguish the physical mass from M, which is a parameter in the lagrangian. The longitudinal polarization for a massive gauge boson is

$$\begin{aligned} \epsilon_\mu^a(k, L) &= \frac{E}{M_{\text{phys}}}(\beta, \hat{k}) \\ &= \frac{k_\mu}{M_{\text{phys}}} - \frac{M_{\text{phys}}}{E(1+\beta)}(1, \hat{k}) \end{aligned} \tag{3.98}$$

with $\beta = \sqrt{1 - M_{\text{phys}}^2/E^2}$ the velocity in the CM frame. At energies large compared to the physical mass, the polarization becomes parallel to k_μ

$$\epsilon_\mu^a(k, L) \sim \frac{k^\mu}{M_{\text{phys}}} + \mathcal{O}\left(\frac{M_{\text{phys}}}{E}\right). \tag{3.99}$$

The longitudinal polarization becomes nearly parallel to the non-physical (scalar) polarization and the dominant contribution to the amplitude comes from replacing the truncated Green's function involving the A^a with the one involving φ^a. More precisely, we use Eq. (3.99) to express the S matrix for the A^a as

$$\langle \cdots | \, S \, | A_L^a(k) \cdots \rangle \;=\; \frac{k^\mu}{M_{\rm phys}} \langle T \underline{A}_\mu^a(k) \cdots \rangle \sqrt{R_A} + \mathcal{O}\left(\frac{M_{\rm phys}}{E}\right). \tag{3.100}$$

We can then replace the expression on the right hand side with one involving a truncated φ^a field using Eq. (3.92)

$$\langle \cdots | \, S \, | A_L^a(k) \cdots \rangle \;=\; i \frac{MC(M_{\rm phys}^2)}{M_{\rm phys}} \sqrt{R_A} \langle T \underline{\varphi}^a \cdots \rangle + \mathcal{O}\left(\frac{M_{\rm phys}}{E}\right) \tag{3.101}$$

Higher order loop corrections introduce an unphysical scale μ. The left hand side of Eq. (3.101) is a physical S-matrix element and is μ independent and so must be the right hand side; however, each term on the right hand side is dependent on μ and only after combining all of the terms does this dependence cancel. In t'Hooft-Feynman gauge ($\xi = 1$), the (unphysical) pole of the Goldstone boson propagator occurs at the same location as that for the physical polarizations of the gauge boson and so we can make the multiplicative factor independent of μ by absorbing a factor of $\sqrt{R_\varphi}$.

$$\langle \cdots | \, S \, | A_L^a(k) \cdots \rangle \;=\; i \frac{MC(M_{\rm phys}^2)}{M_{\rm phys}} \sqrt{\frac{R_A}{R_\varphi}} \langle T \underline{\varphi}^a \cdots \rangle \sqrt{R_\varphi} + \mathcal{O}\left(\frac{M_{\rm phys}}{E}\right) \tag{3.102}$$

To write this expression in the final form given at the beginning of the chapter we introduce $\mathcal{E}$,

$$\begin{aligned} \mathcal{E} &= \frac{MC(M_{\rm phys}^2)}{M_{\rm phys}} \sqrt{\frac{R_A}{R_\varphi}} \\ &= \frac{1}{M_{\rm phys}} \frac{\xi \Gamma_L^{AA} + k^2}{\xi' M - \xi \Gamma^{A\varphi}} \sqrt{\frac{R_A}{R_\varphi}} \end{aligned} \tag{3.103}$$

and the S matrix element becomes

$$\langle \cdots | \, S \, | A_L^a(k) \cdots \rangle \;=\; i\mathcal{E} \langle T \underline{\varphi}^a(k) \cdots \rangle \sqrt{R_\varphi} + \mathcal{O}\left(\frac{M_{\rm phys}}{E}\right). \tag{3.104}$$

The expression

$$\langle T \underline{\varphi}^a(k) \cdots \rangle \sqrt{R_\varphi} \tag{3.105}$$

is μ independent and looks very similar to an S matrix element for Goldstone boson production; however, no such matrix element exists since the Goldstone bosons are unphysical modes. This is not to say that the expression in Eq. (3.105) is zero, but rather that we cannot interpret it as an S-matrix element. It is a quantity that must be computed. Furthermore, this expression is gauge dependent and since k^2 is taken to be $M_{\rm phys}^2$ and not $\frac{\xi'^2}{\xi} M^2$, the pole of the tree-level propagator of φ, it is not even on-shell. The factor $\mathcal{E}$ also gauge dependent, but the combination

$$\mathcal{E} \langle T \underline{\varphi}^a(k) \cdots \rangle \sqrt{R_\varphi} \tag{3.106}$$

is gauge independent, as it must be since the S matrix for A production is a gauge invariant quantity. These comments justify the use of the quotations in Eq. (3.1) at the beginning of the chapter. We have shown that for a single gauge boson, the leading terms of the S matrix involving A can be calculated by considering the so called "S" matrix of the corresponding would-be Goldstone boson.

$$\langle \cdots | \, S \, | A_L^a(k) \cdots \rangle \quad = \quad i\mathcal{E} \, \langle \cdots | \, \text{“}S\text{”} \, | \varphi^a(k) \cdots \rangle + \mathcal{O}\left(\frac{M_{\rm phys}}{E} \right) \tag{3.107}$$

For production of multiple A's, the generalization is straight-foward.

$$\langle \cdots | \, S \, | A_L^{a_1} \cdots A_L^{a_n} \cdots \rangle = (i\mathcal{E})^n \, \langle \cdots | \, \text{“}S\text{”} \, | \varphi^{a_1} \cdots \varphi^{a_n} \cdots \rangle + \mathcal{O}\Big(\frac{E_1}{M}, \cdots, \frac{E_n}{M} \Big) \tag{3.108}$$

For matrix elements involving A_L in the final state, we can use crossing symmetry and since the momentum changes sign, there is an additional factor of (-1) for each final states A_L. We close this section by making one final comment. Grouping $\sqrt{R_\varphi}$ together with the multiplicative factors $\frac{MC}{M_{\rm phys}}\sqrt{R_A}$ was convenient only in Feynman gauge where the poles of the unphysical modes agree with those of the physical ones. While Eq. (3.108) is formally correct, when performing explicit calculations in R_ξ gauge, is it more convenient to use Eq. (3.104).

3.4 Calculation of the equivalence theorem coefficient, $\mathcal{E}$.

We now turn to the calculation of the multiplicative factor $\mathcal{E}$ introduced at the beginning of the chapter and whose expression was derived in the previous section. The explicit form of $\mathcal{E}$ was given in Eq. (3.103) and we see that in order to calculate this factor we need to calculate the 1PI two point (scalar) functions Γ^{AA} and $\Gamma^{A\varphi}$. Calculation of $\Gamma^{\varphi\varphi}$ is not required, but it can provide a check on the calculation by requiring that the Ward identity is satisfied. The calculation of the renormalized two point functions is summarized in Appendix B.

Placing the longitudinal modes on-shell requires that the factor $C(k^2)$ is evaluated at $k^2 = M^2_{\rm phys}$. The physical mass of the gauge boson is given by the real part of the pole of the propagator, or equivalently the zero of the proper functions. For the gauge boson proper two point function, $\Gamma^{A^aA^b}_{\mu\nu}$, there are two zeros. The first zero is for the transverse component, Γ^{AA}_T, and gives the physical pole. The second zero is for Γ^{AA}_L and corresponds to the unphysical scalar polarizations whose contributions cancel with those from the Goldstone boson, the ghost, and anti-ghost states in the calculation of any gauge invariant quantity. In what follows, we will assume that $M_h < 2M$ to ensure the expressions are all real. The physical mass of the gauge boson must satisfy

$$\begin{aligned} 0 = \Gamma^{AA}_T(M^2_{\rm phys}) \quad &= \quad -M^2_{\rm phys} + M^2 + \Pi^{AA}_T(M^2_{\rm phys}) + 2M^2\frac{\delta v}{v} \\ &\quad -M^2_{\rm phys}\delta Z_A + M^2\delta Z_{M^2} + M^2\delta Z_A. \end{aligned} \tag{3.109}$$

If we only keep terms to one loop, this expression becomes

$$M^2_{\rm phys} = M^2\Big(1+\frac{1}{M^2}\Pi^{AA}_T(M^2)+\frac{2\delta v}{v}+\delta Z_{M^2}\Big) \tag{3.110}$$

or, after taking the square root,

$$M_{\rm phys} = M\Big(1+\frac{1}{2M^2}\Pi^{AA}_T(M^2)+\frac{\delta v}{v}+\frac{\delta Z_{M^2}}{2}\Big). \tag{3.111}$$

The explicit expression for the physical mass is gauge invariant as can be seen by inserting the values of $\Pi^{AA}_L(M^2)$ and $\delta v/v$ calculated in R_ξ gauge.

$$\begin{aligned} M_{\rm phys} &= M+\frac{g^2}{16\pi^2}M\Big[-\left(\frac{3z^2}{8}+\frac{59}{24}+\frac{9}{4z^2}\right)\log\frac{M^2}{\mu^2}-\frac{z^4}{24}+\frac{5z^2}{8}+\frac{3}{4z^2} \\ &\quad -\frac{11\sqrt{3}\pi}{8}+\frac{139}{18}+\left(\frac{z^6}{48}-\frac{z^4}{8}\right)\log\left(z^2\right) \\ &\quad +\left(\frac{z^5}{12}-\frac{z^3}{3}+z\right)\sqrt{4-z^2}\arctan\sqrt{\frac{2-z}{2+z}}\Big] \end{aligned} \tag{3.112}$$

where we have defined $z = M_h/M$. If we want expressions with $z > 2$, we can analytically continue the previous expression.

Using the one loop expressions for Γ^{AA} and $\Gamma^{A\varphi}$ from Eq. (B.10), we can compute $C(k^2)$ using the expression we derived in the previous section. The numerator and denominator for $C(k^2)$ are

$$\begin{aligned} \xi\Gamma^{AA}_L+k^2 &= \xi M^2\Big(1+\frac{1}{M^2}\Pi^{AA}_L+2\frac{\delta v}{v}+\delta Z_{M^2}+\delta Z_A\Big) \\ \xi M-\xi\Gamma^{A\varphi} &= \xi M\Big(1-\frac{1}{M}\Pi^{A\varphi}+\frac{\delta v}{v}+\frac{\delta Z_{M^2}}{2}+\frac{\delta Z_\varphi}{2}+\frac{\delta Z_A}{2}\Big), \end{aligned} \tag{3.113}$$

and after these expression are inserted into Eq. (3.93), we get the one loop expression for $C(k^2)$. It reads

$$\begin{aligned} C(k^2) &= \frac{1}{M}\frac{\xi\Gamma^{AA}_L+k^2}{\xi M-\xi\Gamma^{A\varphi}} \\ &= 1+\frac{1}{M^2}\Pi^{AA}_L(k^2)+\frac{1}{M}\Pi^{A\varphi}(k^2)+\frac{\delta v}{v}+\frac{\delta Z_A}{2}-\frac{\delta Z_\varphi}{2}+\frac{\delta Z_{M^2}}{2}. \end{aligned} \tag{3.114}$$

The Z-factors are needed to render the expression finite. The expressions for Π^{AA}_L, $\Pi^{A\varphi}$ and $\delta v/v$, calculated in t'Hooft-Feynman gauge ($\xi = 1$) and evaluated at $k^2 = M^2_{\rm phys} \approx M^2$ are inserted into Eq. (3.114) to get

$$\begin{aligned} C(M^2_{\rm phys}) &= C(M^2)+\mathcal{O}(g^4) \\ &= 1+\frac{g^2}{16\pi^2}\left[-\Big(\frac{9}{4z^2}+\frac{3z^2}{8}+\frac{13}{8}\Big)\log\frac{M^2}{\mu^2}-\frac{\sqrt{3}\pi}{2}+\frac{23}{8}+\frac{3}{4z^2}+\frac{3z^2}{8}\right. \\ &\quad \left.-\frac{z^2}{2}\log z+\frac{z\sqrt{4-z^2}}{2}\arctan\sqrt{\frac{2-z}{2+z}}\right] \end{aligned} \tag{3.115}$$

where $z = M_h/M$ and we have assumed $M_h < M$. In a general R_ξ gauge, the same expression becomes

$$\begin{aligned} C(M^2) &= 1+\frac{g^2}{16\pi^2}\left[-\Big(\frac{23}{24}-\frac{\xi}{8}\Big)\log\frac{M^2}{\mu^2}+\frac{103}{18}+\frac{11\sqrt{3}\pi}{8}-\frac{z^2}{4}+\frac{z^4}{24}+\frac{11\xi}{8}-\frac{\xi^2}{2}\right. \\ &\quad +\left(-\frac{1}{2}+\frac{5\xi}{4}-\frac{z^2\xi}{8}-\frac{11\xi^2}{8}+\frac{\xi^6}{4}\right)\log\xi+(\xi^2-1)\sqrt{4\xi-1}\arctan\sqrt{\frac{1}{4\xi-1}} \\ &\quad -\frac{z^2}{2}\log z-\left(z-\frac{z^3}{3}+\frac{z^5}{12}\right)\sqrt{4-z^2}\arctan\sqrt{\frac{2-z}{2+z}} \\ &\quad -(4\xi-\xi^2)^{\frac{3}{2}}\arctan\sqrt{\frac{2-\xi}{2+\xi}} \\ &\quad \left.+\frac{\xi}{2}\sqrt{-(z^2-\xi-1)^2}\arctan\sqrt{-\frac{(z-\sqrt{\xi})^2-1}{(z+\sqrt{\xi})^2-1}}\right] \end{aligned} \tag{3.116}$$

To calculate $\mathcal{E}$ in Eq. (3.103) , we divide by $M_{\rm phys}$ and then multiply by the appropriate one loop expression for the R-factors. We find that

$$\begin{aligned} \mathcal{E} &= \frac{MC(M^2_{\rm phys})}{M_{\rm phys}}\sqrt{\frac{R_A}{R_\varphi}} \\ &= 1+\frac{1}{M^2}\Pi_L^{AA}(M^2)-\frac{1}{2M^2}\Pi_T^{AA}(M^2)+\frac{1}{M}\Pi^{A\varphi}(M^2) \\ &\quad +\frac{\delta Z_A}{2}-\frac{\delta Z_\varphi}{2}+\frac{R_A}{2}-\frac{R_\varphi}{2} \end{aligned} \tag{3.117}$$

The expression for $\mathcal{E}$ in t'Hooft-Feynman gauge is

$$\begin{aligned} \mathcal{E} &= 1+\frac{g^2}{16\pi^2}\left[-\frac{z^2}{4}+\frac{47\pi}{12\sqrt{3}}-\frac{73}{12}+\left(\frac{z^4}{8}-\frac{7z^2}{16}+\frac{5}{16}\right)\log(z^2)\right. \\ &\quad \left.+\left(-\frac{z^4}{2}+\frac{7z^2}{4}+\frac{1}{4}\right)\frac{z}{\sqrt{4-z^2}}\arctan\sqrt{\frac{2-z}{2+z}}\right]. \end{aligned} \tag{3.118}$$

Notice the expression is μ independent as discussed earlier. In R_ξ gauge, the pole of the Goldstone boson propagator is not at M^2 and so expression

$$\langle T\underline{\varphi}^a\cdots\rangle\sqrt{R_\varphi} \tag{3.119}$$

no longer acts like an S matrix. In this case it is more convenient to use the expression in Eq. (3.104).

$$\begin{aligned} \frac{MC(M^2)}{M_{\rm phys}}\sqrt{R_A} &= 1+\frac{g^2}{16\pi^2}\left[-\left(\frac{9}{4}-\frac{3\xi}{4}\right)\log\frac{M^2}{\mu^2}-\frac{25}{4}+\frac{11\pi}{2\sqrt{3}}-\frac{z^2}{2}+\frac{z^4}{8}+\frac{37\xi}{24}-\frac{\xi^2}{2}\right. \\ &\quad +\left(-\frac{5}{24}+\frac{7\xi}{8}-\frac{z^2\xi}{16}-\frac{11\xi^2}{16}+\frac{\xi^3}{8}\right)\log\xi \\ &\quad +\left(\frac{5}{6}-\frac{11\xi}{3}+\frac{4\xi^2}{3}\right)\frac{1}{\sqrt{4\xi-1}}\arctan\sqrt{\frac{1}{4\xi-1}} \\ &\quad +\frac{\xi}{2}\sqrt{-[(z+\xi)^2-1][(z-\xi)^2-1]}\arctan\sqrt{-\frac{(z-\xi)^2-1}{(z-\xi)-1}} \\ &\quad \left.+\left(7-5z^2+\frac{7z^4}{4}-\frac{z^6}{4}\right)\frac{-z}{\sqrt{4-z^2}}\arctan\sqrt{\frac{2-z}{2+z}}\right] \end{aligned} \tag{3.120}$$

Chapter 4

Electroweak Corrections: Massive Gauge Fields

In the first chapter, we performed an effective theory calculation involving external fermionic and scalar particles, first within a toy theory to understand the structure of the calculation and then within the framework of the standard model. In this chapter we extend the formalism to include external (massive) gauge bosons. There are three physical polarizations for a massive gauge field, two in the transverse direction and one in the longitudinal direction. The fourth (scalar) polarization is unphysical. The EFT theory calculation for the transverse polarization is a straightforward generalization of the calculation with external matter fields; however, the longitudinal polarization is quite different. The equivalence theorem of the previous chapter will be needed for the EFT theory calculation involving external gauge bosons with longitudinal polarization. This chapter will demonstrate the effective theory calculation involving external gauge bosons, first for transversely polarized and then longitudinally polarized states.

4.1 Transverse Polarization

In the first chapter, the Sudakov form factor was studied for fermion and scalar scattering by the set of operators $\bar{\psi}\Gamma\psi$, $\phi^\dagger\phi$, etc. The complete set of operators is listed in Table (1.1) as well as the effective theory operators that they were matched onto. We follow the same procedure to study the scattering of two gauge bosons via the following operator.

$$\mathcal{O} = F^{a\mu\nu}F^a_{\mu\nu} \tag{4.1}$$

where $F^a_{\mu\nu}$ is given by Eq. (A.2). The form factor, $F(Q)$, is the coefficient that multiplies the tree level matrix element of this operator after all higher orders are accounted for. The corrected

matrix element then becomes

$$\begin{aligned}\langle p_2,\sigma_2|\,\mathcal{O}\,|p_2,\sigma_1\rangle &= F(Q)\Big[4(p_2\cdot p_1)(\epsilon^{a*}(p_2,\sigma_2)\cdot\epsilon^a(p_1,\sigma_1)) \\ &\quad -4(\epsilon^{a*}(p_2,\sigma_2)\cdot p_1)(\epsilon^a(p_1,\sigma_1)\cdot p_2)\Big] \end{aligned} \tag{4.2}$$

where $\epsilon^a(p_i,\sigma_i)$ are the polarization vectors for particle i with momentum p_i. The polarization index σ_i will take on values $1,-1,L$ and S for the two transverse, one longitudinal and scalar polarizations. There is an extra factor of two from the two ways that the identical fields can be Wick contracted with the external states. The physical polarization vectors obey

$$\epsilon^a(p_i,\sigma_i)\cdot p_i = 0 \;\text{ and }\; \epsilon^{a*}(p_i,\sigma_i)\cdot\epsilon^a(p_i,\sigma_i) = -1, \quad \sigma_i = \pm 1, L. \tag{4.3}$$

The calculation will be done in the Breit frame using the same kinematics from the first chapter ($q = p_2 - p_1$). In this frame, the transverse polarizations have an additional condition,

$$\epsilon^a(p_1,\sigma_1)\cdot p_2 = \epsilon^a(p_2,\sigma_2)\cdot p_1 = 0. \tag{4.4}$$

The expression in the brackets in Eq. (4.2) vanishes for the unphysical scalar polarizations, $\epsilon^\mu(p,S) = p^\mu/M$. For the longitudinal polarization, $\epsilon^\mu(p,L) = \frac{1}{M}(|\mathbf{p}|, E\hat{p})$, the term in the brackets becomes

$$4(p_2\cdot p_1)(\epsilon^{a*}(p_2,L)\cdot\epsilon^a(p_1,L)) - 4(\epsilon^{a*}(p_2,L)\cdot p_1)(\epsilon^a(p_1,L)\cdot p_2) = 4M^2. \tag{4.5}$$

The corresponding expression for transverse polarization reads

$$4(p_2\cdot p_1)(\epsilon^{a*}(p_2,\sigma_2)\cdot\epsilon^a(p_1,\sigma_1)) - 4(\epsilon^{a*}(p_2,\sigma_2)\cdot p_1)(\epsilon^a(p_1,\sigma_1)\cdot p_2) = 4(E^2+|\mathbf{p}_2|^2)\delta_{\sigma_1,-\sigma_2} \tag{4.6}$$

where $\mathbf{p}_2$ is the spatial part of p_2 and $\sigma_{1,2}$ have been restricted to values ± 1. The tree level amplitude for longitudinal production is suppressed relative to the transverse by a factor $\sim M^2/Q^2$. In our calculation, we have dropped all such terms and so this operator cannot describe the production of longitudinally polarized gauge boson. For these polarizations we will have to invoke the equivalence theorem of the previous chapter. This will be the subject of the second half of this chapter.

4.1.1 High Scale Matching

The full theory operator is matched onto the effective theory at a scale $\mu \sim Q$ and so we begin by constructing the appropriate effective theory operator. In SCET, the appropriate field that we match the external gauge fields onto is

$$B^\mu_{n,p} = \frac{1}{g}[W_n^\dagger i D_n^\mu W_n], \qquad\qquad iD_n^\mu = i\partial_n + gA_{n,p}, \tag{4.7}$$

where the derivative only acts within the square brackets. This combination of operators is collinear gauge invariant and were first discussed by Ref. [62] and, in the form of Eq. (4.7), by

Ref. [63]. If we expand the Wilson lines to first order in the coupling constant we get, after breaking the field into light cone components,

$$\begin{aligned}
\bar{n}\cdot B_{n,p} &= 0 \\
B_{n,p}^{\perp\mu} &= A_{n,p}^{\perp\mu} - \frac{\mathcal{P}_\perp^\mu}{\bar{\mathcal{P}}}\bar{n}\cdot A_{n,p} \\
&\quad -g\bar{n}\cdot A_{n,p}^*\frac{1}{\bar{\mathcal{P}}^\dagger}\left(A_{n,p}^{\perp\mu} - \frac{\mathcal{P}_\perp^\mu}{\bar{\mathcal{P}}}\bar{n}\cdot A_{n,p}\right) \\
&\quad -g\left(A_{n,p}^{\perp\mu} - \frac{\mathcal{P}_\perp^\mu}{\bar{\mathcal{P}}}\bar{n}\cdot A_{n,p}\right)\frac{1}{\bar{\mathcal{P}}}\bar{n}\cdot A_{n,p} \\
n\cdot B_{n,p} &= n\cdot A_{n,p} - \frac{n\cdot i\partial}{\bar{\mathcal{P}}}(\bar{n}\cdot A_{n,p}) \\
&\quad -g\bar{n}\cdot A_{n,p}^*\frac{1}{\bar{\mathcal{P}}^\dagger}\left(A_{n,p}^{\perp\mu} - \frac{(n\cdot i\partial)}{\bar{\mathcal{P}}}\bar{n}\cdot A_{n,p}\right) \\
&\quad -g\left(A_{n,p}^{\perp\mu} - \frac{(n\cdot i\partial)}{\bar{\mathcal{P}}}\bar{n}\cdot A_{n,p}\right)\frac{1}{\bar{\mathcal{P}}}\bar{n}\cdot A_{n,p}.
\end{aligned} \tag{4.8}$$

Here $A_{n,p} = T^a A_{n,p}^a$ are the n-collinear fields describing the energetic gauge boson modes, which are not collinear gauge invariant and can only appear when expanding the Wilson lines. We can extract the component field $B_{n,p}^a$ by using $\mathrm{Tr}[T^a T^b] = \delta^{ab}/2$ for T^a in the fundamental representation. The components are given by

$$B_{n,p}^a = 2\mathrm{Tr}[T^a B_{n,p}]. \tag{4.9}$$

Notice the n^μ component of $B_{n,p}$ vanishes in Eq. (4.8). This is true at all orders in g and follows from a well know fact about Wilson lines,

$$i\bar{n}\cdot D_n W_n = W_n i\partial_n \tag{4.10}$$

where ∂_n only acts on the residual spatial dependence. The operator $\bar{n}\cdot D_n$ in Eq. (4.7) becomes ∂_n acting on unity since the derivative only acts inside the brackets. Moreover, if such a component were to existed, the field would create gauge boson states with polarization $\epsilon \propto p^\mu = (\bar{n}\cdot p)\frac{n^\mu}{2}$ and there would be a non-zero amplitude for production of bosons with scalar polarization. These polarizations are unphysical and their vanishing is a consequence of that. In the full theory, the operator $F_{\mu\nu}F^{\mu\nu}$ also annihilated states with scalar polarization.

The full theory operator $\mathcal{O}$ is matched onto the SCET operator

$$\widetilde{\mathcal{O}} = B_{n,p_2}^{a\perp\dagger}\cdot B_{\bar{n},p_1}^{a\perp}. \tag{4.11}$$

The n-collinear field B_{n,p_2}^a describes the outgoing gauge boson and the $\bar{n}$-collinear field $B_{\bar{n},p_1}^b$ describes the incoming one. The tree level matrix element is simply $\epsilon(p_2,\pm 1)\cdot\epsilon(p_1,\mp 1)$ and comparison with the full theory (tree) level amplitude gives the lowest order contribution to the matching coefficient,

$$C^{(0)} = 4(p_1\cdot p_2) = 2Q^2 \tag{4.12}$$

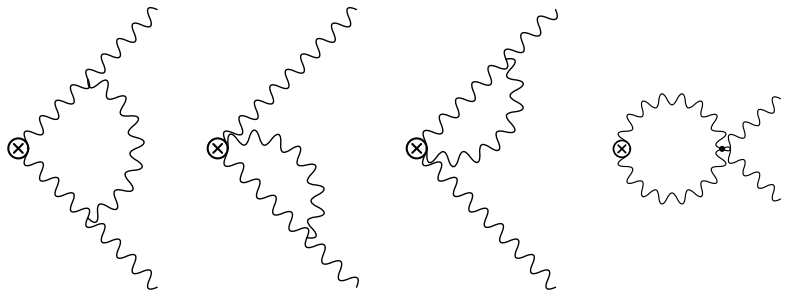

Figure 4.1: One loop corrections for $\mathcal{O} = F^a_{\mu\nu} F^{a\mu\nu}$.

where we have used the kinematics of the Breit frame where $p_1 = (n \cdot p_1)\frac{\bar{n}^\mu}{2}$, $p_2 = (\bar{n} \cdot p_2)\frac{n^\mu}{2}$ and $q^2 = -Q^2 = (p_2 - p_1)^2 \approx 2(p_1 \cdot p_2)$. At one loop, the full theory graphs are shown in Fig. (4.1). The evaluation of these diagrams is much simpler when restricting ourselves to the Breit frame and by assuming transverse polarization. The effective theory graphs, at one loop, are shown in Fig. (4.2), and by comparing the matrix elements in the two theories, we extract the one loop contribution to the matching coefficient. Since the calculation is done at $\mu \sim Q$, all infrared scales such as the mass of the gauge boson have been set to zero. With all masses set to zero, the effective theory diagrams give rise to scaleless integrals which are set to zero in dimensional regularization. The one loop matching is given from the finite part of the full theory diagrams and it is

$$C^{(1)}(\mu) = 2Q^2 \left[\frac{\alpha}{4\pi} C_A \left(-\log^2 \frac{Q^2}{\mu^2} + \frac{\pi^2}{6} \right) \right]. \tag{4.13}$$

However, the poles in $1/\epsilon_{IR}$ in the full theory calculation must be same as those in the effective theory, and so we can extract the $1/\epsilon_{UV}$ poles of the effective theory calculation from the full theory calculation. Once these poles are identified, and after accounting for the poles from wavefunction renormalization, the anomalous dimension of the effective theory operator can be computed. For this calculation, the one loop contribution to the anomalous dimension for the effective theory operator is

$$\gamma^{(1)} = \frac{\alpha}{4\pi} C_A \left(4 \log \frac{Q^2}{\mu^2} - 4 \right) + 2\gamma_A \tag{4.14}$$

where γ_A is the contribution to the anomalous dimension from the wavefunction renormalization, or equivalently the anomalous dimension of the field. The expression for γ_A is given by taking minus two times the $1/\epsilon$ pole from the wavefunction renormalization given in Eq. (B.15) in the appendix.

$$\gamma_A = \frac{\alpha}{4\pi} \left(-\frac{10}{3} C_A + \frac{4}{3} T_F n_F + \frac{2}{3} T_F n_S + \frac{1}{3} \right) \tag{4.15}$$

Using the anomalous dimension, the high scale matching coefficient $C(\mu)$ can be evolved from

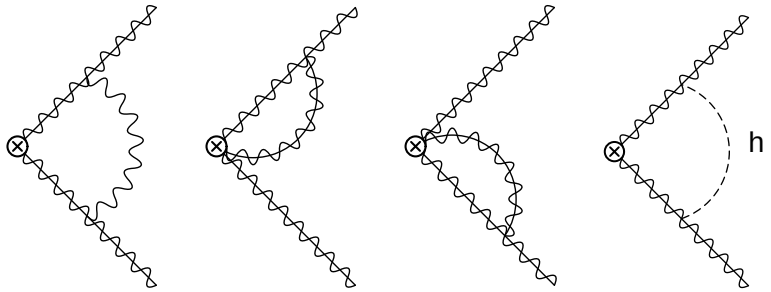

Figure 4.2: One loop corrections for $\widetilde{\mathcal{O}} = B^{\perp *}_{n,p_2} \cdot B^{\perp}_{\bar{n},p_1}$. The last diagram is suppressed by one power of M and does not contribute.

$\mu_1 \sim Q$ to $\mu_2 \sim M$, using

$$C(\mu_2) = C(\mu_1) \exp\left[\int_{\mu_1}^{\mu_2} \frac{d\mu}{\mu} \gamma^{(1)}(\mu)\right]. \tag{4.16}$$

4.1.2 Low Scale Matching

After the effective theory has been evolved to the scale M, the propagating gauge boson modes are integrated out of the theory and we transition from a theory in which the external gauge bosons are treated as collinear SCET fields to one in which they are treated as heavy fields, h^{μ}_{v}. The residual momentum of the SCET fields, k, becomes the momentum for these fields and it is further decomposed into

$$k = Mv + r \tag{4.17}$$

where v, the four velocity, labels the field and r is now the momentum associated with the residual spatial dependence. We compute the low scale matching coefficient, D, by comparing the matrix elements calculated in SCET with the matrix elements computed in a theory with heavy background fields. The matching coefficient is unity at tree level and, since there are no one loop diagrams in the theory below M, the one loop coefficient is given by computing the diagrams of Fig. (4.2). The matching scale is of order M and we cannot neglect the gauge boson masses when calculating these diagrams. We begin by analyzing the first diagram of Fig. (4.2). The EFT operator $\widetilde{\mathcal{O}}$ involves the adjoint field $B^{a\perp}_{n,p}$ and not the full gauge invariant field $B^{\perp}_{n,p}$. The easiest way to keep track of the group theory indices is to use $B^{a\perp}_{n,p} = 2\mathrm{Tr}[T^a B^{\perp}_{n,p}]$ and only perform the trace after the loop integration has been done.

We see from Eq. (4.8) that the four operators that contribute to $B^{\perp}_{n,p}$ at order g are

$$-g\bar{n}\cdot A^{*}_{n,p}\frac{1}{\bar{\mathcal{P}}^{\dagger}}\left(A^{\perp\mu}_{n,p} - \frac{\mathcal{P}^{\mu}_{\perp}}{\bar{\mathcal{P}}}\bar{n}\cdot A_{n,p}\right) - g\left(A^{\perp\mu}_{n,p} - \frac{\mathcal{P}^{\mu}_{\perp}}{\bar{\mathcal{P}}}\bar{n}\cdot A_{n,p}\right)\frac{1}{\bar{\mathcal{P}}}\bar{n}\cdot A_{n,p}. \tag{4.18}$$

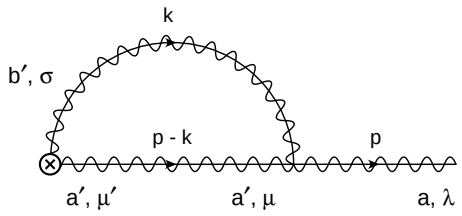

Figure 4.3: The momentum routing for the n-collinear diagram.

When contracting these operators with the transverse external state, the parts involving $\mathcal{P}_\perp$ vanish since the polarization tensors are perpendicular to the momentum. Therefore, we only need to consider the operators

$$-g\bar{n}\cdot A^*_{n,p}\frac{1}{\bar{\mathcal{P}}^\dagger}A^{\perp\mu}_{n,p} - gA^{\perp\mu}_{n,p}\frac{1}{\bar{\mathcal{P}}}\bar{n}\cdot A_{n,p}. \tag{4.19}$$

The first operator gives a contribution of

$$\begin{aligned} & f_\epsilon\int\frac{d^dk}{(2\pi)^d}\frac{-gT^{b'}\bar{n}_\sigma}{-k^-+i0^+}T^{a'}\frac{-i(g^{\mu\mu'}-\frac{n^\mu\bar{n}^{\mu'}+\bar{n}^\mu n^{\mu'}}{2})}{(p-k)^2-M^2+i0^+} \\ & \times gf^{a'b'a}[g_{\mu'\sigma}(p-2k)^\lambda+g_{\sigma\lambda}(k+p)^{\mu'}+g_{\lambda\mu'}(k-2p)^\sigma]\frac{-i}{k^2-M^2+i0^+}\epsilon^{a\mu}(p_2,\sigma_2) \\ = \; & -g^2f^{a'b'a}T^{b'}T^{a'}\epsilon^{a\mu}(p_2,\sigma_2)f_\epsilon\int\frac{d^dk}{(2\pi)^d}\frac{\bar{n}\cdot(2p-k)}{[-k^-+i0^+][(p-k)^2-M^2+i0^+][k^2-M^2+i0^+]}. \end{aligned} \tag{4.20}$$

The momentum routing and indices for this integral are shown in Fig. (4.3). The projection in the first gauge propagator is due to the fact that only transversely polarized modes are propagating along the that line. The second operator gives a contribution of

$$g^2f^{a'b'a}T^{a'}T^{b'}\epsilon^{a\mu}(p_2,\sigma_2)f_\epsilon\int\frac{d^dk}{(2\pi)^d}\frac{\bar{n}\cdot(2p-k)}{[-k^--i0^+][(p-k)^2-M^2+i0^+][k^2-M^2+i0^+]}. \tag{4.21}$$

After reshuffling group theory indices, the two contributions add together to give

$$-2ig^2T^a\epsilon^{a\mu}(p_2,\sigma_2)\frac{C_A}{2}f_\epsilon\int\frac{d^dk}{(2\pi)^d}\frac{(2p-k)^-}{[-k^-+i0^+][(p-k)^2-M^2+i0^+][k^2-M^2+i0^+]} \tag{4.22}$$

To complete the diagram, we take the trace to extract the contribution from $B^{a\perp}_{n,p}$ using Eq. (4.9) and then contract the $\bar{n}$-collinear field, $B^{a\perp}_{\bar{n},p}$, with the incoming state $|p_1,\pm1\rangle$ to pick up a polarization tensor $\epsilon^a_\mu(p_1,\pm1)$. Putting all of the pieces together gives the following for I_n.

$$\begin{aligned} I_n = & -ig^2C_A[\epsilon^{a*}(p_2,\sigma_2)\cdot\epsilon^a(p_1,\sigma_1)] \\ & \times f_\epsilon\int\frac{\mathrm{d}^dk}{(2\pi)^d}\frac{\bar{n}\cdot(2p_2-k)}{[(p_2-k)^2-M^2+i0^+][-\bar{n}\cdot k+i0^+][k^2-M^2+i0^+]} \end{aligned} \tag{4.23}$$

As we have seen many times at this point, this diagram is divergent due to the $\bar{n}\cdot k$ term from the Wilson line. We can perform this integral by regulating it either with the analytic regulator

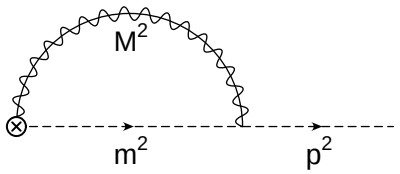

Figure 4.4: The mass assignments for the collinear integral of Eq. (4.24). The dashed line can represent a collinear scalar or gauge field.

of chapter 1 or the Δ-regulator of chapter 2. We will use the latter. Moreover, when evaluating the integral, it will be convenient to consider a generalized version of Eq. (4.23) in which there will be three different mass scales which are all of the same order. The generalized integral is

$$J_n(p^2, m^2, M^2) = f_\epsilon \int \frac{\mathrm{d}^d k}{(2\pi)^d} \frac{\bar{n}\cdot(2p-k)}{[(p-k)^2 - m^2 - \Delta_2 + i0^+][-\bar{n}\cdot k - \delta_1 + i0^+][k^2 - M^2 + i0^+]} \tag{4.24}$$

where we have introduced the Δ-regulator from chapter 2 for which we defined $\delta_i \equiv \frac{\Delta_i}{\bar{n}_i \cdot p_i}$. The three scales are shown in Fig. (4.4) where M^2 is the mass of the gauge boson, p^2 is the square of the external momentum, and m^2 is the mass of the internal propagator. The external dashed line in Fig. (4.4) can represent a scalar or a gauge field. The evaluation of this integral can be simpilified by the method of Sec. 1.7.4, where we isolated the singular part of the integral. We break the integral into pieces through the following equation.

$$J_n(p^2, m^2, M^2) = I_n(0, 0, M^2) + f_S\left(\frac{p^2}{M^2}, \frac{m^2}{M^2}\right) \tag{4.25}$$

where we recall that

$$f_S\left(\frac{p^2}{M^2}, \frac{m^2}{M^2}\right) = J_n(p^2, m^2, M^2) - J_n(0, 0, M^2). \tag{4.26}$$

The integral $J_n(0, 0, M^2)$ is computed just as the one for fermions from chapter 2 in Sec. 2.3 and the integral f_S is tabulated in Appendix C. If the diagram represented a fermion, the numerator in Eq. (4.24) becomes $\bar{n}\cdot(p-k)$ and the function f_S is replaced by f_F.

The diagram must be zero-bin subtracted. The zero-bin contribution does not have dependence on m^2 and M^2, nor does it depend on the particle's spin, and so it is the same as Eq. (2.17) from chapter 2. After zero-bin subtractions, the contribution from the first diagram becomes

$$I_n - I_{n\varnothing} = \frac{\alpha}{4\pi} C_A \left[\frac{2}{\epsilon^2} + \frac{1}{\epsilon} - \frac{2}{\epsilon}\log\frac{\Delta_2}{\mu^2} + 2\log\frac{\Delta_2}{\mu^2}\mathsf{L}_M - \mathsf{L}_M^2 - \mathsf{L}_M + 1 - \frac{\pi^2}{2} + f_S(1,1)\right] \langle \widetilde{O}\rangle_{tree} \tag{4.27}$$

Note that we have used the notation of chapters 1 and 2 in which $\mathsf{L}_Q = \log Q^2/\mu^2$, $\mathsf{L}_M = \log M^2/\mu^2$. The second diagram of Fig. (4.1) represents virtual exchange of a $\bar{n}$-collinear gauge

field and is evaluated in the same way as the first diagram. The external particles are evaluated on-shell and so the soft diagram is same as the zero-bin contribution. The last diagram in Fig. (4.1), representing the exchange of a soft Higgs mode, is suppressed by a factor M^2/Q^2 and has been dropped. The sum of diagrams, together with one factor of $\delta R_A/2$ and $\delta Z_A/2 = -\gamma_A/2\epsilon$ for each external gauge field is

$$\begin{aligned}(I_n - I_{n\varnothing}) + (I_{\bar{n}} - I_{\bar{n}\varnothing}) + I_s + \delta R_A = \\ \frac{\alpha}{4\pi} C_A \left[\frac{2}{\epsilon^2} + \frac{2}{\epsilon} - \frac{2\mathsf{L}_Q}{\epsilon} + 2\mathsf{L}_M \mathsf{L}_Q - \mathsf{L}_M^2 - 2\mathsf{L}_M + 2 - \frac{5\pi^2}{6} + 2 f_S(1,1) \right] - \frac{\gamma_A}{\epsilon} + \delta R_A .\end{aligned} \tag{4.28}$$

Once all of the diagrams are added together, with the proper zero-bin subtractions, all dependence on the Δ-regulator has vanished. Indeed, the entire calculation could have been performed using the analytic regulator of Chapter 1. The low scale matching is extracted from the finite part,

$$D(\mu) = 1 + \frac{\alpha}{4\pi} C_A \left[2\mathsf{L}_M \mathsf{L}_Q - \mathsf{L}_M^2 - 2\mathsf{L}_M + 2 - \frac{5\pi^2}{6} + 2 f_S(1,1) \right] + \delta R_A . \tag{4.29}$$

and the anomalous dimension is extracted from the $1/\epsilon$ terms,

$$\gamma^{(1)} = \frac{\alpha}{4\pi} C_A (4\mathsf{L}_Q - 4) + 2\gamma_A . \tag{4.30}$$

The anomalous dimension calculated directly in the effective theory agrees with the results from the high scale matching calculation in Eq. (4.14). After integrating out the gauge bosons, there are no longer modes which can give a one loop correction, and so the operator does not run below this scale. In the standard model, the heavy gauge bosons can still couple to the massless photon and so the running below the matching scale would come from QED radiative corrections only.

4.2 Longitudinal Polarization

The $B_{n,p}$ operator is unsuitable for the calculation of the leading order contribution for processes involving longitudinal gauge bosons. At energies greater than Q the infrared scales such as the mass of the gauge boson (M) or the Higgs mass (M_h) are irrelevant and so the states can be described by the unbroken gauge theory, in which there are no physical longitudinal polarizations. However, at the scale of symmetry breaking the Goldstone boson modes (φ) of the unbroken Higgs doublet (H) become intertwined with the longitudinally polarized modes, the details of which were the subject of the previous chapter in the statement of the Goldstone boson equivalence theorem. In short, the S matrix element for longitudinal gauge boson production is the "S" matrix element for production of the Goldstone boson modes, weighted by the correction factor $\mathcal{E}$. We are interested in the scattering of a single longitudinally polarized gauge boson, and so Eq. (3.1) applied to this case gives

$$\langle p_2, 0 | \, S \, | p_1, 0 \rangle = -i^2 \mathcal{E}^2 \, \langle p_2 | \, \text{“}S\text{”} \, | p_1 \rangle + \mathcal{O}\Big(\frac{E}{M}\Big) \tag{4.31}$$

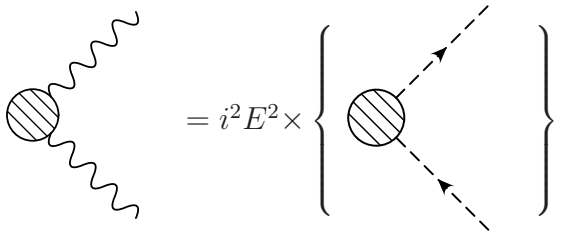

Figure 4.5: The S-matrix for gauge boson production is given by considering the "S" matrix from Goldstone boson production.

The extra minus sign is due to crossing and the quotation marks are a reminder that the expression

$$\langle p_2 | \text{“}S\text{”} | p_1 \rangle = \langle 0 | T \underline{\varphi^a \varphi^b} | 0 \rangle R_\varphi \tag{4.32}$$

is not an S matrix element. The form of the equivalence theorem in Eq. (4.31) was more convenient in 't-Hooft Feynman gauge, whereas, in a general R_ξ gauge, the form of Eq. (3.104) was more convenient. This subtlety was discussed at the end of Sec. 3.3. We proceed by using the effective theory methods outlined in chapters 1 and 2 to calculate Goldstone boson production, and then use the equivalence theorem to relate this to the production of the longitudinal gauge bosons . This calculation is shown schematically in Fig. (4.5). The calculation of the factor $\mathcal{E}$ was done at the end of the previous chapter and so all that remains is the calculation of the amplitude in Eq. (4.32).

4.2.1 High Scale Matching

The high scale matching proceeds as in all of the previous calculations. All infrared scales are neglected at the high scale Q and so we consider scattering of the Higgs doublet modes rather than the individual Goldstone boson modes. The scattering process is mediated by the full theory operator

$$\mathcal{O} = H^\dagger H \tag{4.33}$$

where H is the Higgs doublet

$$H \;=\; \frac{1}{\sqrt{2}} \begin{pmatrix} \varphi^2 + i\varphi^1 \\ h - i\varphi^3 \end{pmatrix}. \tag{4.34}$$

The vacuum expectation value of the Higgs field, discussed at length in Appendix A, has been set to zero since we are in the unbroken phase. The fields were chosen this way so that φ^a describes the would-be Goldstone boson modes for A^a when the Higgs doublet develops a non-zero expectation value with the alignment of Eq. (A.4). The field h describes the remaining physical Higgs mode.

In the effective theory, the Higgs doublet is discribed by a scalar n-collinear field $\Phi^{(H)}_{n,p}$ in the same representation as H. At scale Q the full theory operator, $\mathcal{O}$, is matched onto the effective theory operator $\widetilde{\mathcal{O}}$ given by

$$\widetilde{\mathcal{O}} = [\Phi^{(H)\dagger}_{n,p_2} W_n][W^\dagger_{\bar{n}} \Phi^{(H)}_{\bar{n},p_1}]. \tag{4.35}$$

Since the masses are neglected and the $SU(2)$ symmetry is unbroken, the high scale matching coefficient and anomalous dimension are the same as that for the light scalar operator $\phi^\dagger\phi$ from Sec. (1.4). They are given by the $\phi^\dagger\phi$ entry in Table 1.1 and are repeated here for convenience.

$$\begin{aligned} C(\mu) &= 1 + \frac{\alpha}{4\pi} C_F \left(-\log^2 \frac{Q^2}{\mu^2} + 4 \log \frac{Q^2}{\mu^2} - 2 + \frac{\pi^2}{6} \right), \\ \gamma^{(1)}(\mu) &= \frac{\alpha}{4\pi} C_F \left(4 \log \frac{Q^2}{\mu^2} - 8 \right). \end{aligned} \tag{4.36}$$

The matching coefficient is then evolved to the scale $\mu \sim M$.

4.3 Low Scale Matching

Once the high scale matching coefficient is evolved to $\mu \sim M$, the propagating gauge boson modes are integrated out of the theory. The global $SO(4)$ symmetry of the Higgs sector has been broken by the non-zero VEV; however, there remains a custodial $SO(3)$ symmetry. The φ^a fields transform as a triplet and h transforms as a singlet under $SO(3)_C$. Therefore, the Goldstone boson modes φ^a gain a common mass $\sqrt{\xi}M$ whereas the physical Higgs mode h gains a different mass M_h and ,when transitioning to the broken theory, the gauge invariant operators $W_n \Phi^{(H)}_{n,p_2}$ $W_n \Phi^{(H)}_{\bar{n},p_1}$ break into $SO(3)_C$ invariant pieces.

When matching, we will only need to consider two-particle processes with no external gauge fields, and so at one loop, the gauge fields from the Wilson lines are connected to the external legs. When the external particle is a Goldstone boson, we need to consider the n-collinear diagrams shown in Fig. (4.6). The first diagram gives a contribution

$$\begin{aligned} &-ig^2 \left(\frac{1}{2}\right) f_\epsilon \int \frac{\mathrm{d}^d k}{(2\pi)^d} \frac{\bar{n}\cdot(2p_2 - k)}{[(p_2-k)^2 - M^2 + i0^+][-\bar{n}\cdot k + i0^+][k^2 - M^2 + i0^+]} \\ &\quad = -ig^2 \left(\frac{1}{2}\right) \left[J_n(0,0,M^2) + f_S(1,1) \right] \end{aligned} \tag{4.37}$$

and the second gives

$$\begin{aligned} &-ig^2 \left(\frac{1}{4}\right) f_\epsilon \int \frac{\mathrm{d}^d k}{(2\pi)^d} \frac{\bar{n}\cdot(2p_2 - k)}{[(p_2-k)^2 - M_h^2 + i0^+][-\bar{n}\cdot k + i0^+][k^2 - M^2 + i0^+]} \\ &\quad = -ig^2 \left(\frac{1}{4}\right) \left[J_n(0,0,M^2) + f_S\left(1, \frac{M_h^2}{M^2}\right) \right]. \end{aligned} \tag{4.38}$$

Both diagrams have been evaluated on-shell, $p_2^2 = M^2$. The sum of these two contributions is

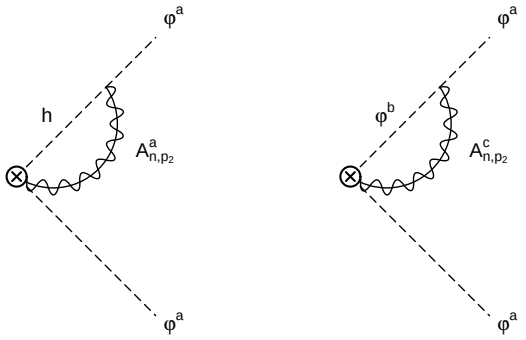

Figure 4.6: A massive collinear mode couples to the external φ^a mode. These diagrams give a contribution $I_n^{(\varphi)}$ to the low scale matching.

denoted by $I_n^{(\varphi)}$, and after zero-bin subtraction we get,

$$\begin{aligned} I_n^{(\varphi)} - I_{n\varnothing}^{(\varphi)} &= \frac{\alpha}{4\pi} C_F \left[\frac{2}{\epsilon^2} + \frac{1}{\epsilon} - \frac{2}{\epsilon} \log \frac{p_2^- \delta_2}{\mu^2} \right. \\ &\quad \left. + 2\mathsf{L}_M \log \frac{p_2^- \delta_2}{\mu^2} - \mathsf{L}_M^2 - \mathsf{L}_M + 1 - \frac{\pi^2}{2} + \frac{2}{3} f_S(1,1) + \frac{1}{3} f_S\left(1, \frac{M_h^2}{M^2}\right) \right]. \end{aligned} \tag{4.39}$$

We remark that had we considered a light scalar instead of the Higgs doublet, the last two terms would not have appeared. When the external particle is the physical Higgs scalar, h, we instead consider the diagram in Fig. (4.7). This diagram is denoted by $I_n^{(h)}$ and is computed just as for $I_n^{(\varphi)}$ and after zero-bin subtractions it is

$$\begin{aligned} I_n^{(h)} - I_{n\varnothing}^{(h)} &= \frac{\alpha}{4\pi} C_F \left[\frac{2}{\epsilon^2} + \frac{1}{\epsilon} - \frac{2}{\epsilon} \log \frac{p_2^- \delta_2}{\mu^2} \right. \\ &\quad \left. + 2\mathsf{L}_M \log \frac{p_2^- \delta_2}{\mu^2} - \mathsf{L}_M^2 - \mathsf{L}_M + 1 - \frac{\pi^2}{2} + f_S\left(\frac{M_h^2}{M^2}, 1\right) \right]. \end{aligned} \tag{4.40}$$

The soft diagrams, being independent of mass, are the same for external h and φ^a modes and are given by Eq. (2.17).

At the low scale, the $SU(2)$ invariant operator splits into $SO(3)_C$ invariant operators since the virtual diagrams involving the Wilson line give a different contribution for the external Goldstone boson modes than for external Higgs modes. The one loop contribution from the n-collinear Wilson line, when the gauge fields are contracted with the external legs, can be expressed as

$$W_n^\dagger \Phi_{n,p_2}^{(H)} \to \Phi_{n,p_2}^{(H)} + \frac{1}{\sqrt{2}} \begin{pmatrix} \tilde{I}_n^{(\varphi)} (\Phi_{n,p_2}^{(\varphi^2)} + i \Phi_{n,p_2}^{(\varphi^1)}) \\ \tilde{I}_n^{(\varphi)} \Phi_{n,p_2}^{(h)} - i \tilde{I}_n^{(\varphi)} \Phi_{n,p_2}^{(\varphi^3)} \end{pmatrix} \tag{4.41}$$

where the tilde indicates that zero-bin subtractions have been made ($\tilde{I}_n = I_n - I_{n\varnothing}$) and the doublet field $\Phi_{n,p_2}^{(h)}$ has been replaced by its component fields $\Phi_{n,p_2}^{(\varphi^a)}$ and $\Phi_{n,p_2}^{(h)}$. The $\bar{n}$-collinear

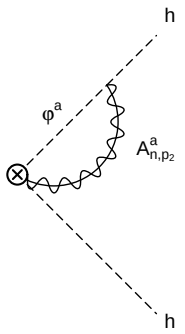

Figure 4.7: A massive collinear gauge mode couples to the external h mode. This diagram gives a contribution $I_n^{(h)}$ to the low scale matching.

direction gives the same results with $n \to \bar{n}$, $p_2^- \to p_1^+$ and $\delta_2 \to \delta_{-1}$. The one loop matrix element splits into two pieces, one involving Goldstone boson fields and one involving physical Higgs fields.

$$\begin{aligned}\langle\cdots|\,[\Phi_{n,p_2}^{(H)\dagger}W_n][W_{\bar{n}}^\dagger\Phi_{\bar{n},p_1}^{(H)}]\,|\cdots\rangle_{1\text{ loop}} &= (1+I_n^{(\varphi)}+I_{\bar{n}}^{(\varphi)}+I_s^{(\varphi)})\frac{1}{2}\langle\cdots|\,\Phi_{n,p_2}^{(\varphi^a)}\Phi_{\bar{n},p_1}^{(\varphi^a)}\,|\cdots\rangle_{\text{tree}} \\ &\quad +(1+I_n^{(h)}+I_{\bar{n}}^{(h)}+I_s^{(h)})\frac{1}{2}\langle\cdots|\,\Phi_{n,p_2}^{(h)}\Phi_{\bar{n},p_1}^{(h)}\,|\cdots\rangle_{\text{tree}}\end{aligned} \tag{4.42}$$

The expresssions for δR_φ and δR_h are given in the appendix in Eqs. (B.23) and Eqs. (B.22), respectively. The physical Higgs and the Goldstone boson modes have masses of order M and so these modes are integrated out of the theory at the same time as the gauge fields. In the theory below M, the SCET fields for the Goldstone boson and physical Higgs fields are replaced by a heavy scalar field,

$$\begin{aligned}\Phi_{n,p}^{(\varphi^a)} &\to h_v^{(\varphi^a)} \\ \Phi_{n,p}^{(h)} &\to h_v^{(h)}.\end{aligned} \tag{4.43}$$

In this theory, there are no one loop corrections since all of the propagating modes which could have contributed at one loop have been removed from the theory. The EFT operators above M are matched onto the following two operators,

$$\begin{aligned}\mathcal{O}^{\varphi\varphi} &= h_{v_2}^{(\varphi^a)}h_{v_1}^{(\varphi^a)} \\ \mathcal{O}^{hh} &= h_{v_2}^{(h)}h_{v_1}^{(h)}.\end{aligned} \tag{4.44}$$

The matching coefficients are extracted from the finite part of Eq. (4.42).

$$\begin{aligned}D^{(\varphi\varphi)}(\mu) &= 1+\frac{\alpha}{4\pi}C_F\left[2\mathsf{L}_M\mathsf{L}_Q-\mathsf{L}_M^2-2\mathsf{L}_M+2-\frac{5\pi^2}{6}+\frac{4}{3}f_S(1,1)+\frac{2}{3}f_S\left(1,\frac{M_h^2}{M^2}\right)\right]+\delta R_\varphi \\ D^{(hh)}(\mu) &= 1+\frac{\alpha}{4\pi}C_F\left[2\mathsf{L}_M\mathsf{L}_Q-\mathsf{L}_M^2-2\mathsf{L}_M+2-\frac{5\pi^2}{6}+2f_S\left(\frac{M_h^2}{M^2},1\right)\right]+\delta R_h\end{aligned} \tag{4.45}$$

The infinite part of Eq. (4.42) gives the anomalous dimension of $\widetilde{\mathcal{O}}$, which is identical to the result extracted from the full theory.

After assembling all of the pieces, the matrix element of the full theory operator becomes,

$$\begin{aligned}\langle\cdots|\, H^\dagger H\,|\cdots\rangle_{1\text{ loop}} &= \left[C(Q)\exp\left(\int_Q^M \frac{d\mu}{\mu}\gamma^{(1)}\right) D^{(\varphi\varphi)}(M)\right]\langle\cdots|\,\mathcal{O}^{\varphi\varphi}\,|\cdots\rangle_{\text{tree}} \\ &\quad + \left[C(Q)\exp\left(\int_Q^M \frac{d\mu}{\mu}\gamma^{(1)}\right) D^{(hh)}(M)\right]\langle\cdots|\,\mathcal{O}^{hh}\,|\cdots\rangle_{\text{tree}}\,.\end{aligned} \tag{4.46}$$

The high and low scales have been conveniently choosen to be Q and M, respectively. Since we are interested in the S-matrix element for the scattering of longitudinal bosons, we take the initial and final states to be Goldstone boson modes $|p_1\rangle$ and $|p_2\rangle$. Had we been interested in Higgs scattering we would instead interpret these states as Higgs modes. To complete the calculation the equivalence theorem requires that we multiply by one factor $i\mathcal{E}$ for each external leg. The factor $\mathcal{E}$ is given in Eq. (3.118). Thus, the matrix element for longitudinal gauge boson production is then

$$\langle p_2, L|\, S\,|p_1, L\rangle = \mathcal{E}^2\,\langle p_2|\, H^\dagger H\,|p_1\rangle \tag{4.47}$$

The methods of this chapter were demonstrated for the two particle scattering case only, but it is straightforward to generalize the results to many particles.

Appendix A

Spontaneously Broken SU(2)

Throughout the main text, a broken SU(2) theory was used as a toy to illustrate how the techniques work in the simplest non-abelian group. The theory consists of an $SU(2)$ gauge theory with n_F massless (Weyl) fermions and n_S massless scalars in the fundamental representation. The theory is broken by a single scalar doublet, suggestively called the Higgs scalar, which is also taken to be a massless fundamental scalar; however, the Higgs potential is chosen so the field will have a non-zero vacuum expectation value. The purpose of this appendix is to work through the lagrangian of this toy theory to standardize conventions and to provide the Feynman rules used throughout the main text. The toy lagrangian takes the form

$$\mathcal{L} = \mathcal{L}_{\text{gauge}} + \mathcal{L}_{\text{gf}} + \mathcal{L}_{\text{ghost}} + \mathcal{L}_{\text{fermions}} + \mathcal{L}_{\text{scalars}} + \mathcal{L}_{\text{Higgs}} \tag{A.1}$$

where

$$\begin{aligned} D_\mu &= \partial_\mu + igA^a_\mu T^a \\ F^a_{\mu\nu} &= \partial_\mu A^a_\nu - \partial_\nu A^a_\mu - g\epsilon^{abc} A^b_\mu A^c_\nu \end{aligned} \tag{A.2}$$

and

$$\begin{aligned} \mathcal{L}_{\text{gauge}} &= -\frac{1}{4} F^{a\mu\nu} F^a_{\mu\nu}, \\ \mathcal{L}_{\text{scalar}} &= \sum_i (D_\mu \phi^i)^\dagger D_\mu \phi^{i\dagger} - V(\phi^{i\dagger}\phi^i) \\ \mathcal{L}_{\text{Higgs}} &= (D_\mu H)^\dagger D_\mu H - V(H^\dagger H) \\ \mathcal{L}_{\text{fermion}} &= \sum_i \bar{\psi}^i_L i \not{D} \psi^i_L \end{aligned} \tag{A.3}$$

The gauge fixing lagrangian, $\mathcal{L}_{\text{gf}}$, and the ghost lagrangian, $\mathcal{L}_{\text{ghost}}$ will be discussed below.

The SU(2) gauge symmetry is broken down when the dynamics causes the Higgs doublet field H to have a non-zero vacuum expectation value (VEV). Below the symmetry breaking scale,

it is no longer useful to describe the field as a doublet, but instead we will examine how each of the component fields behave. The following convention will be used for the Higgs doublet.

$$H = \frac{1}{\sqrt{2}} \begin{pmatrix} \varphi^2 + i\varphi^1 \\ \langle\varphi\rangle + h - i\varphi^3 \end{pmatrix} \tag{A.4}$$

The parameter $\langle\varphi\rangle$ suggestively looks like the VEV of the Higgs doublet, but it is worth noting that at this stage it is only a parameter. The Higgs scalar potential is chosen to provide a phenomenological model for the symmetry breaking. It has the form,

$$V(H^\dagger H) = \mu^2 H^\dagger H + \lambda (H^\dagger H)^2. \tag{A.5}$$

If $\mu^2 < 0$, then the potential has a minimum at $\langle\varphi\rangle = \sqrt{\frac{|\mu^2|}{\lambda}}$ and the lagrangian becomes

$$V(H^\dagger H) = \lambda\langle\varphi\rangle^2 h^2 + \lambda\langle v\rangle\Big(h^3 + h(\varphi^a\varphi^a)\Big) + \frac{\lambda}{4}\Big((\varphi^a\varphi^a)^2 + 2h^2(\varphi^a\varphi^a) + h^4\Big). \tag{A.6}$$

The quantum corrections add a contribution to the potential and the $\langle\varphi\rangle = \sqrt{\frac{|\mu^2|}{\lambda}}$ no longer represents the true vacuum expectation value of the Higgs doublet field. In order to account for this, one can choose $\langle\varphi\rangle$ to minimize the effective potential including all of the quantum corrections. The VEV is written $\langle\varphi\rangle = v + \delta v$ where $v = \sqrt{\frac{|\mu^2|}{\lambda}}$ minimizes the tree level potential and δv account for the quantum corrections. δv is chosen so that $\langle\varphi\rangle$ minimizes the potential. Since the calculation of the main text only involves first order corrections, δv is treated as a one loop correction. To first order in δv, the lagrangian becomes

$$\begin{aligned} V(H^\dagger H) &= \frac{1}{2}(2\lambda v^2)h^2 + \lambda v\Big(h^3 + h(\varphi^a\varphi^a)\Big) + \frac{\lambda}{4}\Big((\varphi^a\varphi^a)^2 + 2h^2(\varphi^a\varphi^a) + h^4\Big) \\ &\quad + \lambda\delta v\Big(2v^2 h + 3vh^2 + v(\varphi^a\varphi^a) + h(\varphi^a\varphi^a) + h^3\Big). \end{aligned} \tag{A.7}$$

It is now clear that $M_h^2 \equiv 2\lambda v^2$. The condition $\langle h\rangle = 0$ can now be used to fix δv and the Higgs potential now has additional interactions from terms involving $h^2, \varphi^a\varphi^a, h^3, h(\varphi^a\varphi^a)$ whose strength is proportional to δv.

The kinetic term, $\mathcal{L}_{\text{Higgs}}$, written out in terms of the component fields of H, becomes

$$\begin{aligned} \mathcal{L}^{\text{KE}}_{\text{Higgs}} &= \frac{1}{2}\partial_\mu h\partial^\mu h + \frac{1}{2}\partial_\mu\varphi^a\partial^\mu\varphi^a - \frac{g\langle\varphi\rangle}{8}\partial_\mu A^{a\mu}\varphi^a \\ &\quad - i\frac{g}{2}A^a_\mu\Big(h\partial^\mu\varphi^a - \partial^\mu h\varphi^a\Big) + i\frac{g}{2}\epsilon^{abc}A^a_\mu\Big(\varphi^b\partial^\mu\varphi^c - \partial^\mu\varphi^b\varphi^c\Big) \\ &\quad + \frac{g^2}{4}A^a_\mu A^{a\mu}\left[\frac{h^2}{2} + h\langle\varphi\rangle + \frac{\varphi^a\varphi^a}{2}\right] + \frac{g^2\langle\varphi\rangle^2}{8}A^a_\mu A^{a\mu}. \end{aligned} \tag{A.8}$$

A few remarks are in order. First, the last term is interpreted as the mass term for the gauge fields and so one defines $M = \frac{gv}{2}$. With this choice the quadratic term in A has an additional contribution at one loop

$$\frac{M^2}{2}\Big(1 + \frac{2\delta v}{v} + \cdots\Big)A^a_\mu A^{a\mu}. \tag{A.9}$$

The second term involving δv in the previous equation gives a contribution to the AA (proper) two point function, and is necessary to render the one-loop corrections to the physical mass gauge invariant. Second, it is worth emphasizing that parameter M is the physical mass for the gauge boson as discussed in section 3.4. Finally, the third term involves mixing between the A and φ fields and a proper choice of the gauge fixing term will remove this term.

Due to the $SU(2)$ gauge symmetry, the functional integral for the gauge sector,

$$\int \mathcal{D}A^a \exp\Big[\int dx\ \mathcal{L}_{\rm gauge}\Big], \tag{A.10}$$

is not well defined since, for each physically equivalent configuration, there are infinitely many equivalent configurations that we are integrating over. The Faddeev-Popov method [57] ensures these equivalent configurations are not overcounted in the functional integral. In their method, one selects a gauge fixing term by inserting an identity into the functional derivative of the form

$$\mathbf{1} = \int \mathcal{D}\alpha^a(x)\delta(G^a(A^\alpha))\det\Big(\frac{\delta G^a(A^\alpha)}{\delta\alpha^a}\Big) \tag{A.11}$$

Here A^α is the gauge transformed field. The gauge fixing term, G^a, is usually chosen to cancel the A-φ mixing from Eq. (A.8). It is

$$G^a \;=\; \partial_\mu A^{a\mu} - \xi' M\varphi^a. \tag{A.12}$$

Furthermore, removing the delta function in Eq. (A.11) involves introducing an additional gaussian integration which involves the gauge fixing parameter ξ. The result is an additional contribution to the lagrangian and the details are given in any field theory text book (see for example Ref. [61]). This gauge fixing lagrangian is

$$\begin{aligned}\mathcal{L}_{\rm gf} &= -\frac{1}{2\xi}(G^a)^2 \\ &= -\frac{1}{2\xi}\partial_\mu A^{a\mu}\partial_\nu A^{a\nu} + \frac{\xi'}{\xi}M\partial_\mu A^{a\mu}\varphi^a - \frac{1}{2}\frac{\xi'^2M^2}{\xi}\varphi^a\varphi^a.\end{aligned} \tag{A.13}$$

Such a choice of the gauge fixing term gives a class of gauges which depends on the two parameters ξ and ξ'. Making the choice $\xi' = \xi$ gives the so called renormalizable (R_ξ) gauges. In this manuscript, this choice will normally be made unless otherwise specified. The first term gives a contribution to the longitudinal component of the gauge boson two point (1PI) function. The second term combines with the third term in Eq. A.8 and, with the choice of $\xi' = \xi$, these terms cancel to eliminate A-φ mixing in the tree level propagator. The third term gives the mass terms for the non-physical Goldstone bosons.

The Faddeev-Popov method introduces additional unphysical degrees of freedom in the theory in the form of ghosts in order to account for the functional determinant that arises when performing a gauge transformation on the integrand. In order to evaluate this determinant, one introduces anticommuting scalar fields $\theta^a(x)$ and $\bar\theta^a(x)$, called ghost fields, and expresses the

functional determinant as an additional contribution to the functional integral.

$$\begin{aligned} S_{\text{ghost}} &= -\int dx \int dy\ \bar{\theta}^a(x)\frac{\delta G^a(x)}{\delta\alpha^c(y)}\theta^c(y) \\ &= \int dx\ \mathcal{L}_{\text{ghost}} \end{aligned} \tag{A.14}$$

where the fields $\alpha^c(y)$ are the parameters governing an infinitesimal gauge transformation. The action now has a contributions from the gauge fixing lagrangian and ghost lagrangian, so that the functional integral becomes

$$\int \mathcal{D}W^a \exp\Big[\int dx\ \Big(\mathcal{L}_{\text{gauge}} + \mathcal{L}_{\text{gf}} + \mathcal{L}_{\text{ghost}}\Big)\Big]. \tag{A.15}$$

In order to evaluate $\frac{\delta G^a(x)}{\delta\alpha^c(y)}$ which appears in Eq. (A.14), consider the transformation of the fields involved in the gauge fixing term governed by α^a,

$$\delta\varphi^a = \frac{g}{2}\Big(-\alpha^a(h+v) + \epsilon^{abc}\alpha^b\varphi^c\Big) \qquad \delta h = \frac{g}{2}\alpha^a\varphi^a \qquad \delta A^a_\mu = -g\epsilon^{abc}A^b_\mu\alpha^c + \partial_\mu\alpha^a. \tag{A.16}$$

Using these transformations, the expression for $\frac{\delta G^a(x)}{\delta\alpha^c(y)}$ becomes

$$\frac{\delta G^a(x)}{\delta\alpha^c(y)} = \left[\delta^{ac}\partial^2 + g\epsilon^{abc}\overleftarrow{\partial^\mu}\ A^b_\mu - \xi'\frac{g}{2}M\epsilon^{acb}\varphi^b + \xi'\frac{g}{2}M(h+v)\delta^{ac}\right]\delta^{(4)}(x-y). \tag{A.17}$$

where $\overleftarrow{\partial^\mu}$ acts to the left and the minus sign used when integrating by parts on the second term has already been included. After inserting the result of Eq. (A.17) into Eq. (A.14), using the delta function to eliminate the y-integral, the integrand of the x-integral is the ghost lagrangian. The expression is

$$\mathcal{L}_{\text{ghost}} = \bar{\theta}^a(x)\left[-\delta^{ac}\partial^2 - \xi' M^2\delta^{ac} - g\epsilon^{abc}\overleftarrow{\partial^\mu}\ A^b_\mu - \xi'\frac{g}{2}M\epsilon^{abc}\varphi^b - \xi'\frac{g}{2}Mh\delta^{ac}\right]\theta^c(x) \tag{A.18}$$

where $M = g\langle\varphi\rangle/2$ was used on the last term of Eq. (A.17). The second term is a mass term for ghost fields; however, the pole of the propagator,

$$\Delta^{ab}_{\text{ghost}}(p^2) = \frac{i\delta^{ab}}{p^2 - \xi' M^2}, \tag{A.19}$$

depends on the unphysical gauge fixing parameter ξ', which not surprising since the ghost terms are not physical degrees of freedom. In unitary gauge ($\xi' \to \infty$) , the mass of the ghost fields become infinite and these degrees of freedom decouple from the theory.

The objective of this appendix is to standardize conventions and work out the Feynman rules for the spontaneously broken $SU(2)$-Lagrangian. These Feynman rules are now given.

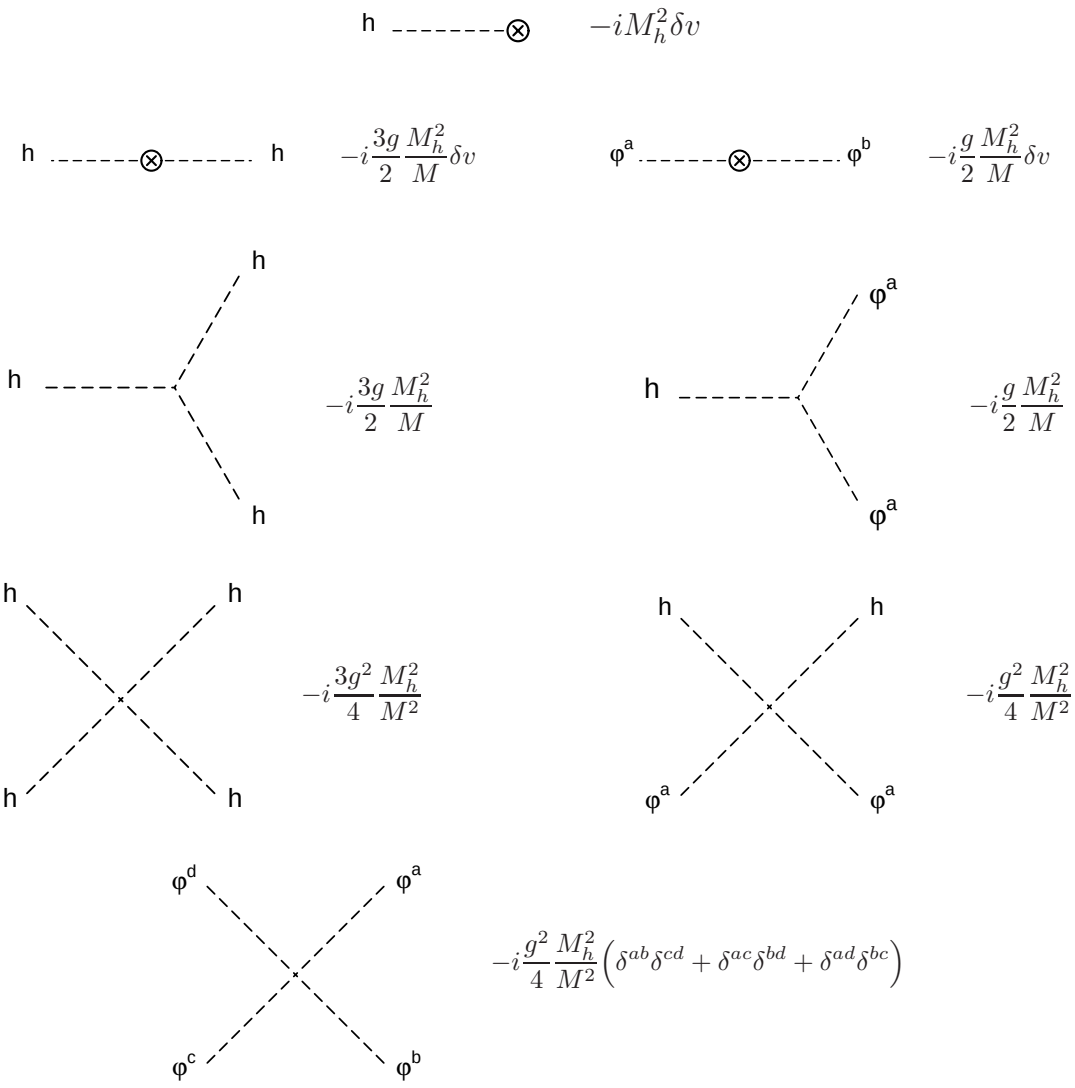

Figure A.1: Interactions involving the Higgs self couplings

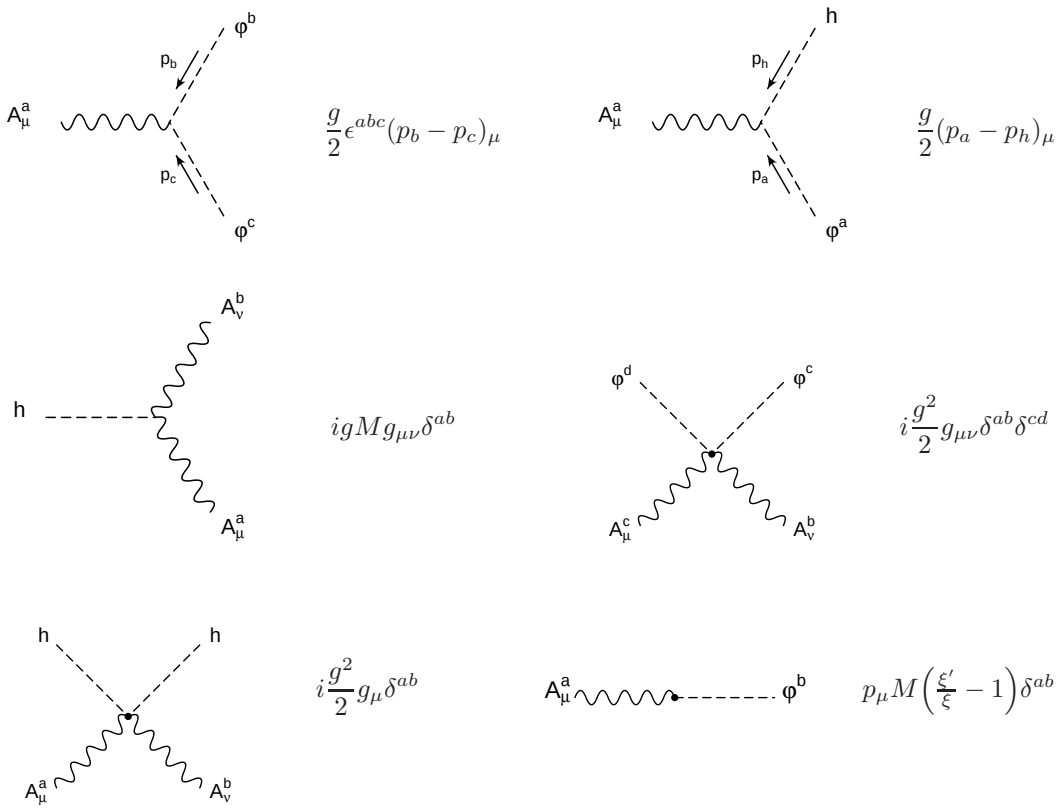

Figure A.2: Interactions involving the gauge fields and the Higgs scalar.

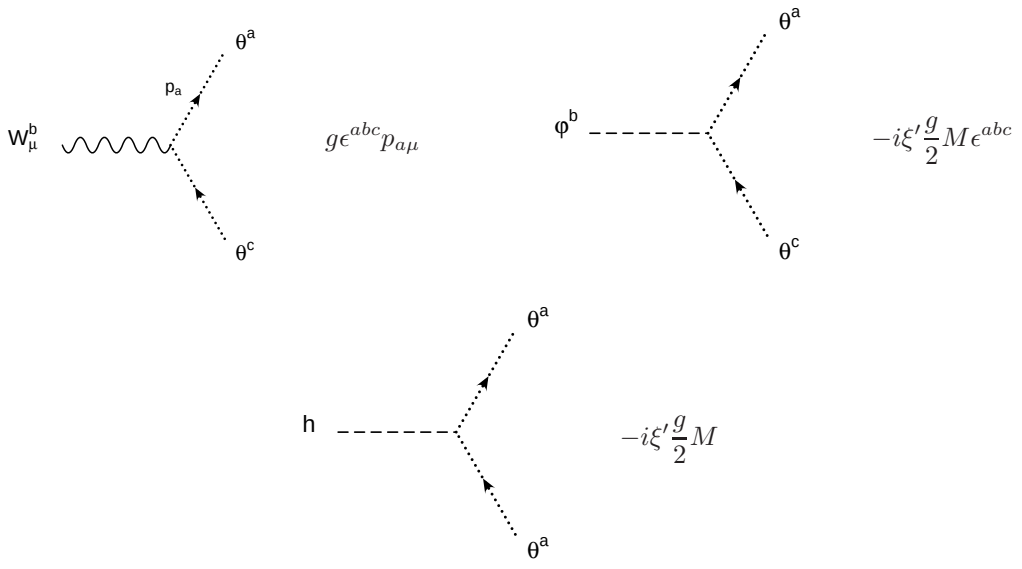

Figure A.3: Interactions involving ghost fields

Appendix B

Renormalization of the spontaneously broken $SU(2)$ theory

Calculations within the framework of a quantum field theory yield infinite corrections and so the theory must be renormalized. The renormalization of the spontaneously broken theory is quite involved and we will only summarize the one loop calculation, focusing only the parts of the theory needed for the calculation of the equivalence theorem factor $\mathcal{E}$ from Chap. 3. Additionally, in the calculation of S-matrix elements we will need to calculate the so called R-factors, that is the residue of the propagator for the various states which appear as final states. Finally, we will calculate an expression for the physical mass of the gauge and Higgs bosons. These calculations are done in R_ξ gauge in the modified minimal subtraction ($\overline{MS}$) scheme . We begin by introducing a wavefunction renormalization for each field in the toy theory,

$$\begin{aligned} A^a_\mu &\to Z_A A^a_\mu & \varphi^a &\to Z_\varphi \varphi^a \\ \Phi^i &\to Z_\Phi \Phi^i & h &\to Z_h h \\ \psi^i &\to Z_\psi \psi^i & \theta^a &\to Z_\theta \theta^a \\ \bar{\theta}^a &\to Z_{\bar{\theta}} \bar{\theta}^a \end{aligned} \tag{B.1}$$

The bare fields in Eq. (A.1) are replaced by these renormalized ones. Furthermore, we choose to renormalize the following parameters,

$$M^2 \to Z_{M^2} M^2 \qquad M_h^2 \to Z_{M_h^2} M_h^2 \qquad g \to Z_g g \tag{B.2}$$

Each term in the lagrangian in principle is renormalized by a different Z-factor; however, the underlying BRS symmetry relates seemingly unrelated terms in the lagrangian and so no other

Z-factors are needed to renormalize the theory. As a concrete example, one such Ward identity given in Eq. (3.75) takes the form after renormalization,

$$-i = k^2 \frac{Z_A}{Z_\xi \xi} G^{AA} + \frac{\sqrt{Z_A Z_{M^2} Z_\varphi} Z_{\xi'}}{Z_\xi} \frac{2\xi'}{\xi} M k^2 G^{A\varphi} + \frac{Z_\varphi Z_{M^2} Z_{\xi'}^2}{Z_\xi} \frac{\xi'^2}{\xi} M^2 G^{\varphi\varphi}. \tag{B.3}$$

The left hand side is finite, and since G^{AA}, $G^{A\varphi}$, and $G^{\varphi\varphi}$ are independent, each term on the right hands side must be separately finite. The proof of the Ward identity held for both the bare and the renormalized theory and so means that the coefficients involving the Z-factors are each finite. Of the three relationships among the Z-factors, only the following two are independent.

$$\begin{aligned} Z_A &= Z_\xi + \text{ finite} \\ Z_\varphi Z_{M^2} Z_{\xi'}^2 &= Z_\xi + \text{ finite} \end{aligned} \tag{B.4}$$

In the modified minimal scheme, $\overline{MS}$, the Z -factors do not have finite contributions and so the previous equations take the form

$$\begin{aligned} Z_A &= Z_\xi \\ Z_\varphi Z_{M^2} Z_{\xi'}^2 &= Z_\xi. \end{aligned} \tag{B.5}$$

These relations imply that the gauge fixing term is not renormalized,

$$\begin{aligned} \mathcal{L}_{\rm gf} &\rightarrow -\frac{Z_A}{2\xi Z_\xi} \left[(\partial_\mu A^{a\mu}) - \xi' M \varphi^a \frac{Z_{\xi'} \sqrt{Z_{M^2} Z_\varphi}}{\sqrt{Z_A}} \right]^2 \\ &= -\frac{1}{2\xi} \Big(\partial^\mu A_\mu^a - \xi' M \varphi^a \Big)^2 \end{aligned} \tag{B.6}$$

and so we will not need to calculate Z_ξ or $Z_{\xi'}$ for our one-loop calculation. The ghost and anti-ghost fields are in principle renormalized as well. Each vertex involving a ghost (anti-ghost) will pick up a factor of $\sqrt{Z_\theta}$ ($\sqrt{Z_{\bar\theta}}$) and each ghost (anti-ghost) propagator will pick up a factor $1/Z_\theta$ ($1/Z_{\bar\theta}$); however, the ghost fields are not physical and never appear as external states, and since each internal propagator is accompanied by two vertices, any such factors will always cancel. We will therefore not calculate the Z-factors for the ghost or anti-ghost fields.

With the exception of the gauge coupling, all of the Z-factors in Eqs. (B.1) and (B.2) can be calculated by considering the appropriate (1PI) two point function and for this we need to consider only the terms in the renormalized lagrangian that are at most quadratic in the fields. They are

$$\begin{aligned} \mathcal{L} &= -\frac{Z_A}{4} F_{\mu\nu} F^{\mu\nu} + Z_{M^2} Z_A \Big(1 + \frac{\delta v}{v} \Big)^2 \frac{M^2}{2} A^{a\mu} A_\mu^a - \frac{1}{2\xi} (\partial_\mu A^{a\mu})^2 \\ &\quad + \sqrt{Z_A Z_{M^2} Z_\varphi} \Big(1 + \frac{\delta v}{v} \Big) M A^{a\mu} \partial_\mu \varphi^a + \frac{\xi'}{\xi} M \varphi^a \partial_\mu A^{a\mu} \\ &\quad + \frac{Z_\varphi}{2} (\partial_\mu \varphi^a)^2 - \frac{\xi'^2}{\xi} \frac{M^2}{2} (\varphi^a)^2 - \frac{\delta v}{v} \frac{M_h^2}{2} Z_{M_h^2} Z_\varphi (\varphi^a)^2 \\ &\quad + \frac{Z_h}{2} (\partial_\mu h)^2 - Z_h Z_{M_h^2} \frac{M_h^2}{2} h^2 - \frac{3\delta v}{v} Z_{M_h^2} Z_h \frac{M_h^2}{2} h^2 \\ &\quad - M_h^2 \delta v Z_{M_h^2} \sqrt{Z_h} h + \cdots \end{aligned} \tag{B.7}$$

The ghost and anti-ghost have not been included since we do not need to calculate their Z-factors. The renormalized (1PI) proper two point functions are:

$$\begin{aligned}
\Gamma_T^{AA}(k^2) &= -k^2 Z_A + Z_{M^2} Z_A M^2 \Big(1+\frac{\delta v}{v}\Big)^2 + \Pi_T^{AA} \\
\Gamma_L^{AA}(k^2) &= -\frac{k^2}{\xi} + Z_{M^2} Z_A M^2 \Big(1+\frac{\delta v}{v}\Big)^2 + \Pi_L^{AA} \\
\Gamma^{A\varphi}(k^2) &= \frac{\xi'}{\xi} M - \sqrt{Z_{M^2} Z_\varphi Z_A} M \Big(1+\frac{\delta v}{v}\Big) + \Pi^{A\varphi} \\
\Gamma^{\varphi\varphi}(k^2) &= k^2 Z_\varphi - \frac{(\xi')^2}{\xi} M^2 - Z_{M_h^2} Z_\varphi M_h^2 \frac{\delta v}{v} - \Pi^{\varphi\varphi} \\
\Gamma^{hh}(k^2) &= k^2 Z_h - M_h^2 Z_{M_h^2} Z_h - 3 Z_{M_h^2} Z_h M_h^2 \frac{\delta v}{v} - \Pi^{hh}
\end{aligned} \tag{B.8}$$

where the Π's are are calculated by summing all one particle irreducible diagrams and are defined by the following conventions,

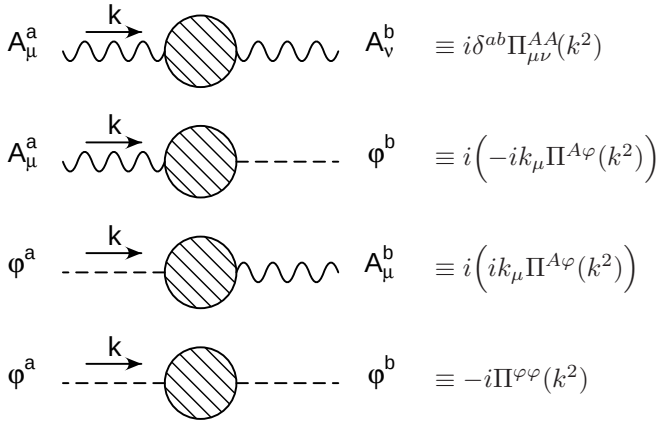

(B.9)

Since we will only work to one loop, the two point functions take a simpler form.

$$\begin{aligned}
\Gamma_T^{AA}(k^2) &= -k^2 + M^2 + \Pi_T^{AA} + 2M^2\frac{\delta v}{v} - k^2(Z_A - 1) + M^2(Z_{M^2}Z_A - 1) \\
\Gamma_L^{AA}(k^2) &= -\frac{k^2}{\xi} + M^2 + \Pi_L^{AA} + 2M^2\frac{\delta v}{v} + M^2(Z_{M^2}Z_A - 1) \\
\Gamma^{A\varphi}(k^2) &= M\Big(\frac{\xi'}{\xi} - 1\Big) + \Pi^{A\varphi} - M\frac{\delta v}{v} - M(\sqrt{Z_{M^2}Z_\varphi Z_A} - 1) \\
\Gamma^{\varphi\varphi}(k^2) &= k^2 - \frac{(\xi')^2}{\xi} M^2 - \Pi^{\varphi\varphi} - M_h^2\frac{\delta v}{v} + k^2(Z_\varphi - 1) \\
\Gamma^{hh}(k^2) &= k^2 - M_h^2 - \Pi^{hh} - 3M_h^2\frac{\delta v}{v} + k^2(Z_\varphi - 1) - M_h^2(Z_{M_h^2}Z_\varphi - 1)
\end{aligned} \tag{B.10}$$

We can calculate the Z-factors by considering each two point function in turn. All calculations are done with $\xi' = \xi$ so that the the A and φ do not mix at tree level.

The entire renormalization procedure is quite lengthy, and we will only summarize those aspects of the calculation that we will need in the main text. A more complete treatment of the calculations are given in [64] and various other places.

B.1 Calculation of δv

As demonstrated in Appendix A, there is a single linear term in the lagrangian involving h. The appearance of such a term indicates that we have considering field excitations around the wrong vacuum, and so we must adjust δv so that this term vanishes. The proper, renormalized, one point function for h is set to zero

$$\Gamma^h = -M_h^2 \delta v Z_{M_h^2} \sqrt{Z_h} + \Pi^h = 0 \tag{B.11}$$

Here Π^h is the sum of the one particle irreducible graphs with one external h leg. At one loop the tadpole graphs are shown in Fig. (B.1). The sum of these diagrams is denoted by $\Pi^{h(1)}$, where

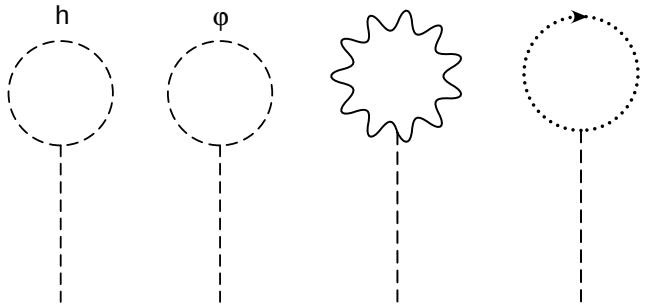

Figure B.1: The tadpole diagrams contribute to the one point function, Π^h, at one loop.

the superscript (1) is to remind us that we are considering only the one loop value of Π^h.

$$\begin{aligned}\Pi^{h(1)} &= \frac{g^2}{16\pi^2} M_h^2 \Big(\frac{2M}{g}\Big) \Bigg\{ \frac{1}{\epsilon}\left(\frac{9M^2}{4M_h^2} + \frac{3M_h^2}{8M^2} + \frac{3\xi}{8}\right) + \frac{3M^2}{4M_h^2} + \frac{3M_h^2}{8M^2} + \frac{3\xi}{8} \\ &\quad - \frac{9M^2}{4M_h^2}\log\frac{M^2}{\mu^2} - \frac{3M_h^2}{8M^2}\log\frac{M_h^2}{\mu^2} - \frac{3\xi}{8}\log\frac{\xi M^2}{\mu^2} \Bigg\}\end{aligned} \tag{B.12}$$

The value δv is adjusted so that $\Gamma^h = 0$ at one loop,

$$\frac{\delta v}{v} = \frac{1}{M_h^2}\frac{\Pi^{h(1)}}{v}. \tag{B.13}$$

Finally, using Eq. (B.11) together with $v = 2M/g$, we get

$$\begin{aligned}\frac{\delta v}{v} &= \frac{g^2}{16\pi^2} \Bigg\{ \frac{1}{\epsilon}\left(\frac{9M^2}{4M_h^2} + \frac{3M_h^2}{8M^2} + \frac{3\xi}{8}\right) + \frac{3M^2}{4M_h^2} + \frac{3M_h^2}{8M^2} + \frac{3\xi}{8} \\ &\quad - \frac{9M^2}{4M_h^2}\log\frac{M^2}{\mu^2} - \frac{3M_h^2}{8M^2}\log\frac{M_h^2}{\mu^2} - \frac{3\xi}{8}\log\frac{\xi M^2}{\mu^2} \Bigg\}.\end{aligned} \tag{B.14}$$

This expression for $\delta v/v$ is needed for the one loop calculation of the two point functions.

B.2 Calculation of the Z factors.

Calculating Γ^{AA} requires the computation of the diagrams in Figs. (B.2 - B.4). Fig. (B.2) involves only pure gauge diagrams, Fig. (B.3) involves massless (chiral) fermion and the scalar diagrams, and Fig. (B.4) involves the diagrams from the Higgs sector. The sum of all of these

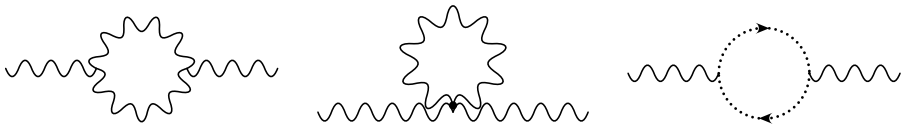

Figure B.2: Pure gauge and ghost diagrams contributing to Π^{AA}

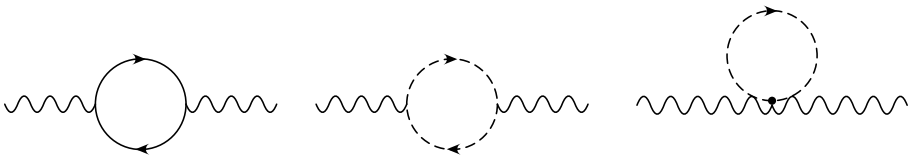

Figure B.3: Massless fermion and scalar diagrams contributing to Π^{AA}

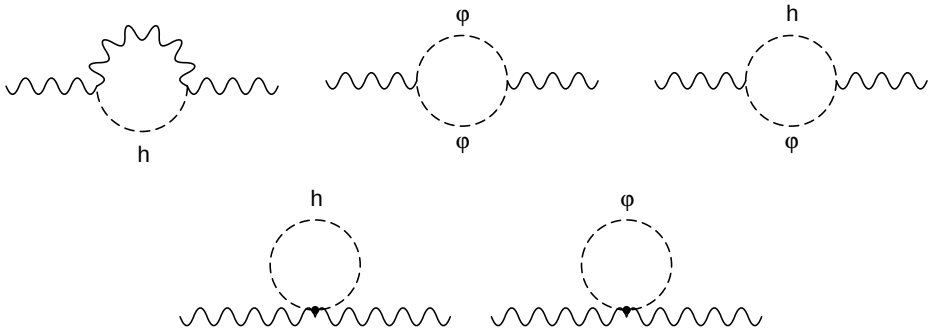

Figure B.4: The contributions from the h and φ to Π^{AA}.

diagrams gives Π_L^{AA} and Π_L^{AA} at one loop. Also, the term in the lagrangian proportional to $\frac{\delta v}{v}$ has been included explicitly in the two point function and is not considered a separate diagram. In order to render the expression finite, we choose the wavefunction and mass renormalization

for the gauge boson to be

$$\begin{aligned} Z_A &= 1+\frac{g^2}{16\pi^2}\frac{1}{\epsilon}\left[C_A\Big(\frac{13}{6}-\frac{\xi}{2}\Big)-\frac{1}{6}-\frac{2}{3}T_F n_F-\frac{1}{3}T_F n_S\right] \\ Z_{M^2} &= 1+\frac{g^2}{16\pi^2}\frac{1}{\epsilon}\Big(-\frac{59}{12}-\frac{9M^2}{2M_h^2}-\frac{3M_h^2}{4M^2}\Big). \end{aligned} \tag{B.15}$$

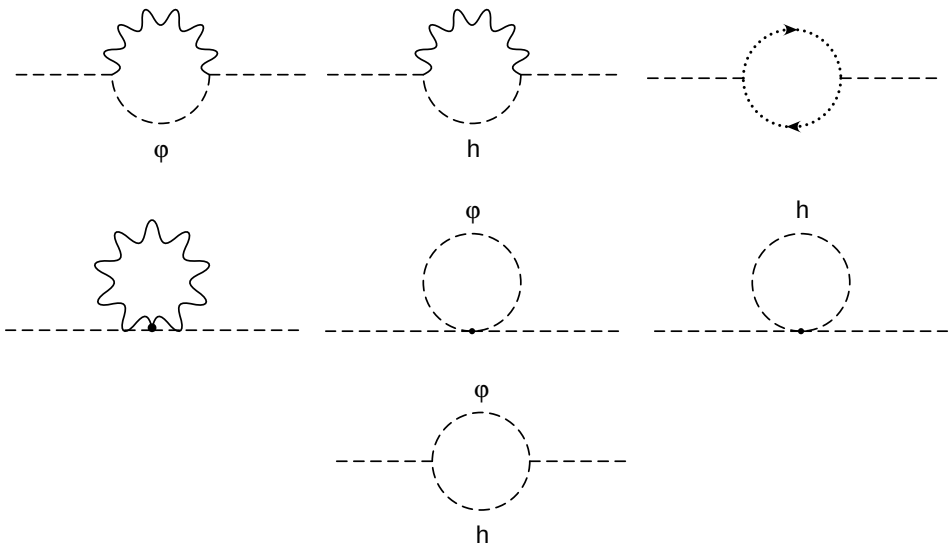

Figure B.5: Diagrams which contribute to $\Pi^{\varphi\varphi}$.

Calculating $\Gamma^{\varphi\varphi}$ requires the computation of the diagrams in Fig. (B.5). The sum of the diagrams gives $\Pi^{\varphi\varphi}$ and the remaining contribution comes from the term in the lagrangian proportional to $\delta v/v$. The following choice for the wavefunction renormalization renders $\Gamma^{\varphi\varphi}$ finite.

$$Z_\varphi = 1+\frac{g^2}{16\pi^2}\frac{1}{\epsilon}\left(\frac{9}{4}-\frac{3\xi}{4}\right) \tag{B.16}$$

There is no need for mass renormalization, as expected from Goldstone's theorem.

Calculating $\Gamma^{A\varphi}$ requires the computation of the diagrams in Fig. (B.5). The sum of the diagrams gives $\Pi^{W\varphi}$ at one loop and again there is a contribution from the $\delta v/v$ term. Furthermore, the constants Z_φ, Z_A and Z_{M^2} in the combination given in Eq. (B.10) eliminate all of the infinite terms and there is no need to introduce new renormalization constants. This provides a check of the calculation.

The final two point function we consider is Γ^{hh}, which requires the computation of the diagrams in Fig. (B.7). These diagrams contribute to Π^{hh} and there is a contribution from $\delta v/v$.

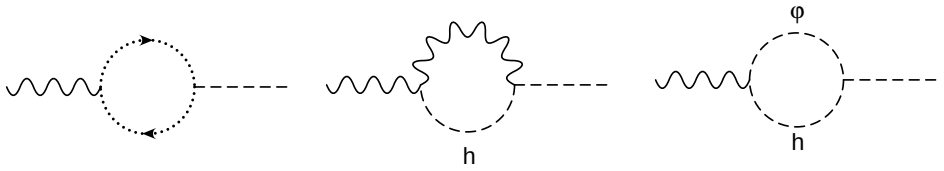

Figure B.6: Diagrams which contribute to $\Pi^{A\varphi}$.

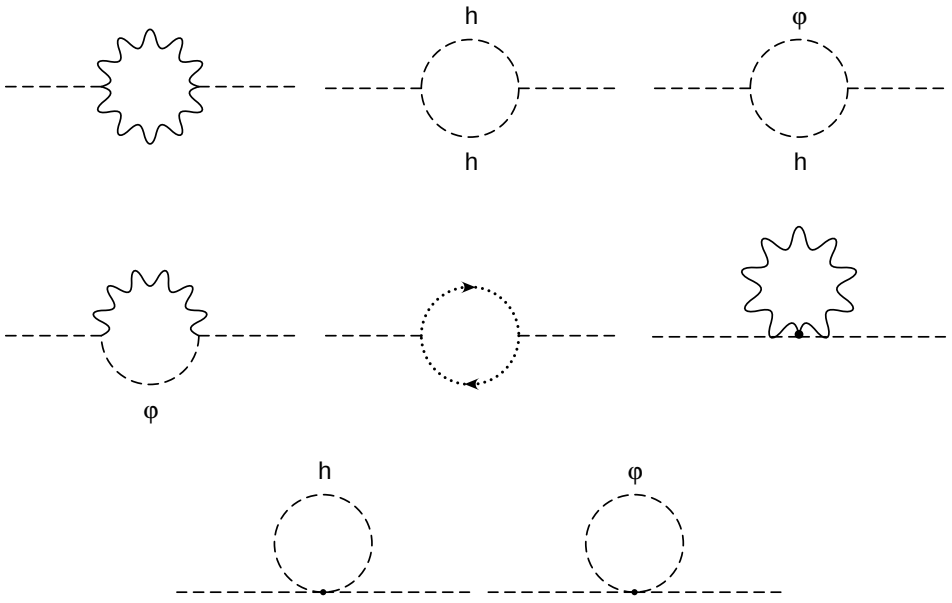

Figure B.7: Diagrams which contribute to Π^{hh}.

The following choice for the wavefunction renormalization renders $\Gamma^{\varphi\varphi}$ finite.

$$\begin{aligned} Z_h &= 1 + \frac{g^2}{16\pi^2}\frac{1}{\epsilon}\left(\frac{9}{4} - \frac{3\xi}{4}\right) \\ Z_{M_h^2} &= 1 + \frac{g^2}{16\pi^2}\frac{1}{\epsilon}\left(-\frac{9}{4} + \frac{3M_h^2}{4M^2}\right) \end{aligned} \tag{B.17}$$

The wavefunction renormalization for h turns out to be identical to the one for φ. This is not an accident. The $\overline{MS}$ scheme is mass-independent and so the wavefunction renormalization must be the same since the fields originally come from the same doublet.

The renormalization of the gauge coupling is well known and is calculated in many quantum field theory textbooks, for example [61].

$$Z_g = 1 + \frac{g^2}{16\pi^2}\frac{1}{\epsilon}\Big(-\frac{11}{6}C_A + \frac{1}{3}T_F n_F + \frac{1}{6}T_F(n_S + 1)\Big) \tag{B.18}$$

The extra $+1$ is due to the fact that there are n_S light scalar doublets and one broken doublet,

H, which give the same contribution. Furthermore, Z_g is gauge independent and thus gives a gauge invariant beta function.

These wavefunction and mass renormalization factors and the choice δv render the two point functions of Eq. (B.10) finite and now we can use these functions to calculate the physical mass and R-factors.

B.3 R factors

The two point function for two generic (scalar) fields can be written as

$$\begin{aligned}\int d^4x e^{ip\cdot(x-y)} \langle 0|\, T\phi(x)\phi(y)\,|0\rangle \\ = \frac{iR}{p^2 - m^2_{\rm phys} + i0^+} + \int_{\sim 4m^2}^{\infty} \frac{dM^2}{2\pi}\rho(M^2)\frac{i}{p^2 - M^2 + i0^+}\end{aligned} \tag{B.19}$$

where the first term is a simple pole at the physical mass, $m^2_{\rm phys}$, and the second contributes a branch cut starting at $p^2 = (2m)^2$. When calculating S matrix elements, the LSZ reduction formula requires the multiplication of the truncated Green's function with one factor of $\sqrt{R}$ for each external leg. We now turn to the calculation of these factors for the physical states.

The R factor for the massive gauge boson fields (A^a) is

$$\begin{aligned}
R_A &= 1 + \delta R_A^{(g)} + \delta R_A^{(H)} + \delta R_A^{(\psi)} + \delta R_A^{(\phi)} \\
\delta R_A^{(g)} + \delta R_A^{(H)} &= \frac{g^2}{16\pi^2}\Bigg[-\Big(\frac{25}{6} - \xi\Big)\log\frac{M^2}{\mu^2} - \frac{19}{18} + \frac{11\pi}{4\sqrt{3}} - \frac{z^2}{2} + \frac{z^4}{6} + \frac{\xi}{3} \\
&\quad + \Big(\frac{1}{3} + 2\xi\Big)\log\xi + \Big(1 - \frac{3z^2}{2} + \frac{3z^4}{4} - \frac{z^6}{6}\Big)\log z \\
&\quad + \Big(-6 + \frac{16z^2}{3} - \frac{13z^4}{6} + \frac{z^6}{3}\Big)\frac{z}{\sqrt{4-z^2}}\arctan\sqrt{\frac{2-z}{2+z}}\Bigg] \\
&\quad + \Big(-\frac{1}{3} + \frac{8\xi}{3} - \frac{16\xi^2}{3}\Big)\frac{1}{\sqrt{4\xi-1}}\arctan\sqrt{\frac{1}{4\xi-1}} \\
\delta R_A^{(\psi)} &= \frac{g^2}{16\pi^2}T_F n_F\Bigg[-\frac{2}{3\epsilon} + \frac{2}{3}\log\frac{M^2}{\mu^2} - \frac{10}{9} - \frac{i\pi}{3}\Bigg] \\
\delta R_A^{(\phi)} &= \frac{g^2}{16\pi^2}T_S n_S\Bigg[-\frac{1}{3\epsilon} + \frac{1}{3}\log\frac{M^2}{\mu^2} - \frac{8}{9} - \frac{i\pi}{3}\Bigg]
\end{aligned} \tag{B.20}$$

where $\delta R_A^{(g)}$ is the contribution from the pure gauge sector, including the ghost contribution, $\delta R_A^{(H)}$ is the contribution from the φ^a and h fields, and $\delta R_A^{(\psi)}, \delta R_A^{(\phi)}$ are the light fermions and scalar contributions, respectively. The last two contributions are gauge independent. The R

factor for the physical Higgs mode (h) is

$$\begin{aligned} R_A &= 1+\delta R_h \\ \delta R_h &= \frac{g^2}{16\pi^2}\Big[-\Big(\frac{9}{4}-\frac{3\xi}{4}\Big)\log\frac{M^2}{\mu^2}+\frac{9}{4}+\frac{9}{2z^2}+\frac{3z^2}{2}-\frac{\pi\sqrt{3}z^2}{4}-\frac{3\xi}{4} \\ &\quad +\frac{3}{4}(\xi-z^2)\log\xi-\frac{3z}{2}\sqrt{4\xi-z^2}\arctan\frac{z}{\sqrt{4\xi-z^2}} \\ &\quad +\left(-\frac{18}{z^4}-\frac{6}{z^2}+\frac{15}{2}-\frac{3z^2}{2}\right)\frac{z}{\sqrt{4-z^2}}\arctan\frac{z}{\sqrt{4-z^2}}\Big] \end{aligned} \tag{B.21}$$

The effective theory calculation we are considering requires only the calculation in t'Hooft Feynman gauge ($\xi=1$).

$$\begin{aligned} \delta R_A^{(g)}+\delta R_A^{(H)} &= \frac{g^2}{16\pi^2}\Big[-\frac{19}{6}\log\frac{M^2}{\mu^2}-\frac{13}{18}+\frac{9\pi}{4\sqrt{3}}-\frac{z^2}{2}+\frac{z^4}{6} \\ &\quad +\Big(1-\frac{3z^2}{2}+\frac{3z^4}{4}-\frac{z^6}{6}\Big)\log z \\ &\quad +\Big(-6+\frac{16z^2}{3}-\frac{13z^4}{6}+\frac{z^6}{3}\Big)\frac{z}{\sqrt{4-z^2}}\arctan\sqrt{\frac{2-z}{2+z}}\Big] \\ \delta R_h &= \frac{g^2}{16\pi^2}\Big[-\frac{3}{2}\log\frac{M^2}{\mu^2}+\frac{3}{2}+\frac{9}{2z^2}+\frac{3z^2}{2}-\frac{\pi\sqrt{3}z^2}{4}+\frac{3}{2}\log z \\ &\quad +\left(-\frac{18}{z^4}-\frac{6}{z^2}+\frac{3}{2}\right)\frac{z}{\sqrt{4-z^2}}\arctan\frac{z}{\sqrt{4-z^2}}\Big] \end{aligned} \tag{B.22}$$

In this gauge it is useful to calculate R_φ as well and this will be needed when calculating the equivalence theorem multiplication factor $\mathcal{E}$ as described in Chapter 3.

$$\begin{aligned} R_\varphi &= 1+\frac{g^2}{16\pi^2}\Big[-\frac{3}{2}\log\frac{M^2}{\mu^2}+\frac{7}{4}-\frac{\pi}{3\sqrt{3}}+\frac{z^4}{4}-\frac{z^2}{2} \\ &\quad +\left(-\frac{z^6}{4}+\frac{3z^4}{4}-\frac{3z^2}{4}-\frac{1}{4}\right)\log z \\ &\quad +\left(\frac{z^6}{2}-\frac{5z^4}{2}+\frac{7z^2}{2}-\frac{5}{2}\right)\frac{z}{\sqrt{4-z^2}}\arctan\sqrt{\frac{2-z}{2+z}}\Big] \end{aligned} \tag{B.23}$$

Appendix C

Parameter Integrals

The parameter integrals tablulated below arise from vertex and wavefunction graphs where the gauge boson has mass M, the external particle has mass m, and the internal particle has mass m'. They depend on the variables $w = m^2/M^2$ and $z = m'^2/M^2$. For any function $f(w, z)$ defined below, we define the corresponding function of a single argument by $f(z) \equiv f(z, z)$. In the standard model, where the only fermion with mass comparable to the gauge boson masses is the top quark, we need the integrals $f(z, z)$, $f(z, 0)$ and $f(0, z)$, with $z = m_t^2/M_W^2, m_t^2/M_Z^2, m_t^2/M_H^2$.

For $4z \geq 1$, the $f(z, z)$ results can be analytically continued using $\sqrt{1-4z} \to i\sqrt{4z-1}$ and $\tanh^{-1}(\sqrt{1-4z}) \to i \tan^{-1}(\sqrt{4z-1})$. In each integral, the factors of i cancel, and the function remains real. The $f(w, 0)$ formulæ are given by using $f(w + i0^+, 0)$ for $w \geq 1$. They have an imaginary part for large values of w.

C.1 Fermions

The gauge boson vertex graph leads to the integral

$$f_F\left(w = \frac{p^2}{M^2}, z = \frac{m_{int}^2}{M^2}\right) \quad = \quad 2\int_0^1 \mathrm{d}x \frac{1-x}{x} \log\left(\frac{1-x+zx-wx(1-x)}{1-x}\right) \tag{C.1}$$

For general w and z,

$$\begin{aligned} f_F(w,z) &= \frac{\pi^2}{3} + 2 + \frac{1-w-z}{w}\log z \\ &+ \frac{\sqrt{(1-z)^2 - 2(z+1)w + w^2}}{w}\left[\log\left(\frac{1-w+z+\sqrt{w^2-2(z+1)w+(z-1)^2}}{-1+w-z+\sqrt{w^2-2(z+1)w+(z-1)^2}}\right) + i\pi\right] \\ &-2\mathrm{Li}_2\left(\frac{2w}{1+w-z-\sqrt{(w-z+1)^2-4w}}\right) \\ &-2\mathrm{Li}_2\left(\frac{2w}{1+w-z+\sqrt{(w-z+1)^2-4w}}\right). \end{aligned} \tag{C.2}$$

Some useful special limits are

$$\begin{aligned} f_F(z) &= f_F(z,z) = 2 + \left(\frac{1}{z} - 2\right)\log(z) + \frac{1}{2}\log^2(z) \\ &+ \frac{2\sqrt{1-4z}}{z}\tanh^{-1}\sqrt{1-4z} - 2\left(\tanh^{-1}\sqrt{1-4z}\right)^2, \end{aligned} \tag{C.3}$$

$$f_F(0,z) = \frac{\pi^2}{3} + \frac{2z}{1-z}\log z - 2\,\mathrm{Li}_2(1-z), \tag{C.4}$$

and

$$f_F(w,0) = 2 + 2\frac{1-w}{w}\log(1-w) - 2\,\mathrm{Li}_2(w). \tag{C.5}$$

The function $f_F(z) = f_F(z,z)$ was used in Chapter 1.

Fermion wavefunction renormalization due to gauge boson exchange gives the coefficients A of $\not{p}$ and B of m. They lead to the parameter integrals a from A, b from $m^2\partial B/\partial p^2$, and c from $m^2\partial A/\partial p^2$.

$$\begin{aligned} a(w,z) &= -2\int_0^1 \mathrm{d}x(1-x)\log\left(\frac{1-x+zx-wx(1-x)}{1-x}\right) \\ b(w,z) &= \int_0^1 \mathrm{d}x\frac{4\sqrt{wz}\,x(1-x)}{1-x+zx-wx(1-x)} \\ c(w,z) &= \int_0^1 \mathrm{d}x\frac{2wx(1-x)^2}{1-x+zx-wx(1-x)} \end{aligned} \tag{C.6}$$

$$\begin{aligned} a(z,z) &= \frac{5}{2} - \frac{1}{z} - \frac{(1-2z)(1-4z)}{z^2\sqrt{1-4z}}\tanh^{-1}\sqrt{1-4z} \\ &\quad - \frac{1-4z+2z^2}{2z^2}\log z \\ a(0,z) &= -\frac{z}{(1-z)} - \frac{z^2}{(1-z)^2}\log z \\ a(w,0) &= \frac{3}{2} - \frac{1}{w} - \frac{(1-w)^2}{w^2}\log(1-w) \end{aligned} \tag{C.7}$$

$$\begin{aligned} b(z,z) &= -4 + \frac{4(3z-1)}{z\sqrt{1-4z}} \tanh^{-1}\sqrt{1-4z} \\ &\quad +2\left(1-\frac{1}{z}\right)\log z \\ b(0,z) &= 0 \\ b(w,0) &= 0 \end{aligned} \tag{C.8}$$

$$\begin{aligned} c(z,z) &= \frac{2}{z} - 3 + \frac{2(1-5z+5z^2)}{z^2\sqrt{1-4z}} \tanh^{-1}\sqrt{1-4z} \\ &\quad +\frac{1-3z+z^2}{z^2}\log z \\ c(0,z) &= 0 \\ c(w,0) &= \frac{2}{w} - 1 + \frac{2(1-w)}{w^2}\log(1-w) \end{aligned} \tag{C.9}$$

The function

$$h_F(z) = a(z,z) - 2b(z,z) + 2c(z,z) \tag{C.10}$$

was used in Chapter 1, and is the wavefunction correction in a vector-like theory.

The corresponding functions for radiative corrections due to a virtual scalar are

$$\begin{aligned} \tilde{a}(w,z) &= \frac{1}{2}a(w,z) \\ \tilde{b}(w,z) &= -\frac{1}{4}b(w,z) \\ \tilde{c}(w,z) &= \frac{1}{2}c(w,z) \end{aligned} \tag{C.11}$$

and

$$\tilde{h}_F(z) = \tilde{a}(z,z) - 2\tilde{b}(z,z) + 2\tilde{c}(z,z) \tag{C.12}$$

was used in Chapter 1.

C.2 Scalars

The gauge boson vertex graph for scalar particles leads to the integral

$$f_S\left(w=\frac{p^2}{M^2}, z=\frac{m_{int}^2}{M^2}\right) = \int_0^1 \mathrm{d}x \frac{(2-x)}{x}\log\frac{1-x+zx-wx(1-x)}{1-x} \tag{C.13}$$

For general w and z,

$$
\begin{aligned}
f_S(w,z) &= \frac{\pi^2}{3} + 1 + \frac{1-w-z}{2w}\log z \\
&+\frac{\sqrt{(1-z)^2-2(z+1)w+w^2}}{2w}\left[\log\left(\frac{1-w+z+\sqrt{w^2-2(z+1)w+(z-1)^2}}{-1+w-z+\sqrt{w^2-2(z+1)w+(z-1)^2}}\right)+i\pi\right] \\
&-2\mathrm{Li}_2\left(\frac{2w}{1+w-z-\sqrt{(1-z)^2-2(z+1)w+w^2}}\right) \\
&-2\mathrm{Li}_2\left(\frac{2w}{1+w-z+\sqrt{(1-z)^2-2(z+1)w+w^2}}\right)
\end{aligned}
$$

Some useful special cases are

$$
\begin{aligned}
f_S(z) &= f_S(z,z) = 1-\left(1-\frac{1}{2z}\right)\log(z)+\frac{1}{2}\log^2 z \\
&\quad +\frac{\sqrt{1-4z}}{z}\tanh^{-1}(\sqrt{1-4z}) - 2\left(\tanh^{-1}\sqrt{1-4z}\right)^2 \\
f_S(0,z) &= \frac{\pi^2}{3}+\frac{z}{1-z}\log z - 2\,\mathrm{Li}_2\,(1-z)\,, \text{ and} \\
f_S(w,0) &= 1+\frac{1-w}{w}\log(1-w) - 2\,\mathrm{Li}_2\,(w)\,.
\end{aligned} \tag{C.14}
$$

Scalar wavefunction renormalization due to gauge boson exchange gives the integral

$$
\begin{aligned}
h_S(w,z) &= \int_0^1 \mathrm{d}x\Bigg\{(3x^2-6x+4) \\
&\quad \times\log\left(\frac{1-x+zx-wx(1-x)}{1-x}\right) \\
&\quad -\frac{wx(1-x)(2-x)^2}{1-x+zx-wx(1-x)}\Bigg\},
\end{aligned} \tag{C.15}
$$

$$
\begin{aligned}
h_S(z) &= h_S(z,z) = \frac{3}{2}-\frac{1}{z}+\left[\frac{3}{2z}-\frac{1}{2z^2}\right]\log(z) \\
&\quad -\frac{\sqrt{1-4z}\,(1-z)}{z^2}\tanh^{-1}(\sqrt{1-4z}) \\
h_S(0,z) &= \frac{z(1-3z)}{2(1-z)^2}-\frac{z(2z^2-2z+1)}{(1-z)^3}\log z \\
h_S(w,0) &= -\frac{1}{2}-\frac{1}{w}+\left(2-\frac{1}{w^2}\right)\log(1-w).
\end{aligned} \tag{C.16}
$$

Scalar wavefunction renormalization due to scalar exchange gives:

$$
\tilde{h}_S(w,z) = = -\int_0^1 \mathrm{d}x\frac{zx^3}{1-x+zx-wx(1-x)} \tag{C.17}
$$

$$\begin{aligned}
\tilde{h}_S(z) = \tilde{h}_S(z,z) &= -\frac{1}{2} - \frac{1}{z} + \left[\frac{1}{2z} - \frac{1}{2z^2}\right]\log(z) \\
&\quad + \frac{3z-1}{z^2\sqrt{1-4z}}\tanh^{-1}(\sqrt{1-4z}) \\
\tilde{h}_S(0,z) &= \frac{z(2z^2-7z+11)}{6(1-z)^3} + \frac{z}{(1-z)^4}\log z \\
\tilde{h}_S(w,0) &= 0
\end{aligned} \tag{C.18}$$

Bibliography

[1] M. Ciafaloni, P. Ciafaloni and D. Comelli, Phys. Rev. Lett. **84**, 4810 (2000).

[2] P. Ciafaloni and D. Comelli, Phys. Lett. B **446**, 278 (1999); Phys. Lett. B **476**, 49 (2000).

[3] V. S. Fadin, L. N. Lipatov, A. D. Martin and M. Melles, Phys. Rev. D **61**, 094002 (2000).

[4] J. H. Kuhn, A. A. Penin and V. A. Smirnov, Eur. Phys. J. C **17**, 97 (2000).

[5] B. Feucht, J. H. Kuhn, A. A. Penin and V. A. Smirnov, Phys. Rev. Lett. **93**, 101802 (2004).

[6] B. Jantzen, J. H. Kuhn, A. A. Penin and V. A. Smirnov, Phys. Rev. D **72**, 051301 (2005) [Erratum-ibid. D **74**, 019901 (2006)].

[7] B. Jantzen, J. H. Kuhn, A. A. Penin and V. A. Smirnov, Nucl. Phys. B **731**, 188 (2005) [Erratum-ibid. B **752**, 327 (2006)].

[8] M. Beccaria, F. M. Renard and C. Verzegnassi, Phys. Rev. D **63**, 053013 (2001).

[9] A. Denner and S. Pozzorini, Eur. Phys. J. C **18**, 461 (2001).

[10] A. Denner and S. Pozzorini, Eur. Phys. J. C **21**, 63 (2001).

[11] M. Hori, H. Kawamura and J. Kodaira, Phys. Lett. B **491**, 275 (2000).

[12] W. Beenakker and A. Werthenbach, Nucl. Phys. B **630**, 3 (2002).

[13] A. Denner, M. Melles and S. Pozzorini, Nucl. Phys. B **662**, 299 (2003).

[14] S. Pozzorini, Nucl. Phys. B **692**, 135 (2004).

[15] B. Jantzen and V. A. Smirnov, Eur. Phys. J. C **47**, 671 (2006).

[16] A. H. . Mueller, *Perturbative Quantum Chromodynamics*, World Scientific, Singapore, 1989.

[17] C. W. Bauer, S. Fleming and M. E. Luke, Phys. Rev. D **63**, 014006 (2001).

[18] C. W. Bauer, S. Fleming, D. Pirjol and I. W. Stewart, Phys. Rev. D **63**, 114020 (2001); C. W. Bauer and I. W. Stewart, Phys. Lett. B **516**, 134 (2001); C. W. Bauer, D. Pirjol and I. W. Stewart, Phys. Rev. D **65**, 054022 (2002).

[19] C. W. Bauer, S. Fleming, D. Pirjol, I. Z. Rothstein and I. W. Stewart, Phys. Rev. D **66**, 014017 (2002) [arXiv:hep-ph/0202088].

[20] S. Fleming, A. H. Hoang, S. Mantry and I. W. Stewart, arXiv:hep-ph/0703207; arXiv:0711.2079 [hep-ph].

[21] J. y. Chiu, F. Golf, R. Kelley and A. V. Manohar, Phys. Rev. Lett. **100**, 021802 (2008) [arXiv:0709.2377 [hep-ph]].

[22] J. y. Chiu, F. Golf, R. Kelley and A. V. Manohar, Phys. Rev. D **77**, 053004 (2008) [arXiv:0712.0396 [hep-ph]].

[23] J. y. Chiu, R. Kelley and A. V. Manohar, Phys. Rev. D **78**, 073006 (2008) [arXiv:0806.1240 [hep-ph]].

[24] M. E. Luke, A. V. Manohar and I. Z. Rothstein, Phys. Rev. D **61**, 074025 (2000).

[25] J. C. Collins, Phys. Rev. D **22**, 1478 (1980).

[26] A. H. Mueller, Phys. Rev. D **20**, 2037 (1979).

[27] A. Sen, Phys. Rev. D **24**, 3281 (1981).

[28] A. V. Manohar, Phys. Rev. D **68**, 114019 (2003).

[29] A. V. Manohar, Phys. Rev. D **56**, 230 (1997).

[30] A. V. Manohar, arXiv:hep-ph/9606222.

[31] A. V. Manohar and I. W. Stewart, Phys. Rev. D **76**, 074002 (2007).

[32] C. W. Bauer and A. V. Manohar, Phys. Rev. D **70**, 034024 (2004).

[33] A. V. Manohar, Phys. Lett. B **633**, 729 (2006).

[34] M. Beneke and T. Feldmann, Nucl. Phys. B **685**, 249 (2004).

[35] V. A. Smirnov and E. R. Rakhmetov, Theor. Math. Phys. **120**, 870 (1999) [Teor. Mat. Fiz. **120**, 64 (1999)].

[36] S. Moch, J. A. M. Vermaseren and A. Vogt, Nucl. Phys. B **688**, 101 (2004).

[37] I. Z. Rothstein, Phys. Rev. D **70**, 054024 (2004) [arXiv:hep-ph/0301240].

[38] A. K. Leibovich, Z. Ligeti and M. B. Wise, Phys. Lett. B **564**, 231 (2003).

[39] A. V. Manohar and M. B. Wise, *Heavy Quark Physics*, Cambridge University Press (Cambridge, 2000).

[40] E. E. Jenkins and A. V. Manohar, Phys. Lett. B **255**, 558 (1991); Phys. Lett. B **281**, 336 (1992).

[41] A. H. Hoang and A. V. Manohar, Phys. Lett. B **483**, 94 (2000).

[42] C. W. Bauer, A. V. Manohar and M. B. Wise, Phys. Rev. Lett. **91**, 122001 (2003), C. W. Bauer, C. Lee, A. V. Manohar and M. B. Wise, Phys. Rev. D **70**, 034014 (2004), C. W. Bauer and M. D. Schwartz, Phys. Rev. Lett. **97**, 142001 (2006), M. Trott, Phys. Rev. D **75**, 054011 (2007).

[43] B. Jantzen, arXiv:0709.2311 [hep-ph].

[44] C. Lee and G. Sterman, Phys. Rev. D **75**, 014022 (2007) [arXiv:hep-ph/0611061].

[45] A. Idilbi and T. Mehen, Phys. Rev. D **75**, 114017 (2007) [arXiv:hep-ph/0702022].

[46] A. Idilbi and T. Mehen, Phys. Rev. D **76**, 094015 (2007) [arXiv:0707.1101 [hep-ph]].

[47] C. W. Bauer, M. P. Dorsten and M. P. Salem, Phys. Rev. D **69**, 114011 (2004) [arXiv:hep-ph/0312302].

[48] A. V. Manohar, Phys. Lett. B **633**, 729 (2006) [arXiv:hep-ph/0512173].

[49] J. M. Cornwall, D. N. Levin and G. Tiktopoulos, Phys. Rev. D **10**, 1145 (1974) [Erratum-ibid. D **11**, 972 (1975)].

[50] C. E. Vayonakis, Lett. Nuovo Cim. **17**, 383 (1976).

[51] B. W. Lee, C. Quigg and H. B. Thacker, Phys. Rev. D **16**, 1519 (1977).

[52] M. S. Chanowitz and M. K. Gaillard, Nucl. Phys. B **261**, 379 (1985).

[53] G. J. Gounaris, R. Kogerler and H. Neufeld, Phys. Rev. D **34**, 3257 (1986).

[54] J. Bagger and C. Schmidt, Phys. Rev. D **41**, 264 (1990).

[55] Y. P. Yao and C. P. Yuan, Phys. Rev. D **38**, 2237 (1988).

[56] M. Bohm, A. Denner and H. Joos, "Gauge theories of the strong and electroweak interaction," *Stuttgart, Germany: Teubner (2001) 784 p*

[57] L.D. Faddeev and V.N. Popov Phys. Lett. **25B**, 29 (1967)

[58] C. Becchi, A. Rouet and R. Stora, Annals Phys. **98**, 287 (1976).

[59] T. Kugo and I. Ojima, Prog. Theor. Phys. **60**, 1869 (1978). T. Kugo and I. Ojima, Prog. Theor. Phys. **61**, 294 (1979). T. Kugo and I. Ojima, Prog. Theor. Phys. **61**, 644 (1979).

[60] H. Lehmann, K. Symanzik and W. Zimmermann, Nuovo Cim. **1**, 205 (1955).

[61] M. E. Peskin and D. V. Schroeder, "An Introduction To Quantum Field Theory," *Reading, USA: Addison-Wesley (1995) 842 p*

[62] C. M. Arnesen, J. Kundu and I. W. Stewart, Phys. Rev. D **72**, 114002 (2005) [arXiv:hep-ph/0508214].

[63] C. W. Bauer, O. Cata and G. Ovanesyan, arXiv:0809.1099 [hep-ph].

[64] D. Y. Bardin and G. Passarino, *Oxford, UK: Clarendon (1999) 685 p*